Dissertation zur Erlangung
des Doktorgrades der Naturwissenschaften
an der Fakultät Statistik der
Technischen Universität Dortmund

März 2015

On modeling financial risk with tail copulas

STEFAN JÄSCHKE

technische universität
dortmund

Preface

I would like to express my gratitude to Professor Walter Krämer for supervising this thesis and for providing guidance and encouragement at any time. This work has been supported in part by the Collaborative Research Center Statistical Modeling of Nonlinear Dynamic Processes (SFB 823) of the German Research Foundation (DFG).

Next, I am grateful to Professor Karl Friedrich Siburg and Dr. Pavel Stoimenov for accompanying the initial stage of this work. Further, I would like to extend my sincere thanks to Dr. Axel Bücher and Junior Professor Dominik Wied for both the excellent collaborative work and their steady assistance during the entire phase of this thesis.

Special gratitude is owed to my brother Michael for discussing the topic with respect to its applicability and practical relevance in much detail. I am also thankful to Frank Daniel Fischer, Panos Karamanis and Stefan Stehling for useful discussions and comments. Further, a big thank you goes to Ulrich Mrozek for providing several hints with respect to the graphic implementation.

Finally, I am very much grateful to my beloved parents, Renate and Dieter, and my friends for their support and encouragement throughout the last years.

Contents

Introduction **1**

1 Modeling dependence of extreme events in energy markets using tail copulas **5**
1.1 Introduction . . . 5
1.2 Preliminaries . . . 6
1.3 Data . . . 9
1.4 Methodology and results . . . 11
1.4.1 Copula estimation . . . 11
1.4.2 Tail copula estimation . . . 14
1.5 Concluding remarks . . . 18

2 Estimation of risk measures in energy portfolios using modern copula techniques **19**
2.1 Introduction . . . 19
2.2 Preliminaries . . . 21
2.2.1 Copulas and tail dependence . . . 21
2.2.2 Nonparametric estimates . . . 22
2.3 Modeling marginal time series . . . 23
2.4 Rank-based goodness-of-fit tests . . . 28
2.4.1 Bootstrap procedures for copulas . . . 28
2.4.2 Multiplier bootstrap . . . 31
2.5 Empirical results . . . 33
2.5.1 Copula selection . . . 33
2.5.2 Tail copula fit . . . 36
2.6 Risk measures and backtesting . . . 39
2.7 Concluding remarks . . . 43

3 Nonparametric tests for constant tail dependence **45**
3.1 Introduction . . . 45
3.2 The concept of tail dependence and its nonparametric estimation . . . 47
3.3 Testing for constant tail dependence . . . 48
3.3.1 Setting and test statistics . . . 48
3.3.2 Asymptotic null distributions . . . 50
3.3.3 Asymptotics under fixed alternatives . . . 53
3.3.4 Testing for a break at a specific time point . . . 55
3.3.5 Choice of the parameter k . . . 56
3.3.6 Higher dimensions . . . 57
3.3.7 Testing for a break under non-stationarity of the marginals . . . 57
3.4 Evidence in finite samples . . . 59
3.4.1 Setup . . . 59

3.4.2 Results and discussion 62
3.5 Empirical applications 70
3.5.1 Energy sector 70
3.5.2 Financial markets 72
3.6 Conclusion and Outlook 76
3.7 Proof of the results in the main text 76
3.7.1 Proofs of additional results 84

A Commented code **87**
A.1 Goodness-of-fit tests 87
A.2 Simulation of copulas 93
A.3 Tests for constant tail dependence 95

List of Figures **100**

List of Tables **102**

Bibliography **108**

Introduction

The modeling and estimation of stochastic dependence in financial markets via copulas has become increasingly common in applications, see for example Embrechts et al. (2003). Although this development could also partly be observed in the closely intertwined energy and commodity sector, the practice of using copulas has still been in its infancy. There are essentially two ways of explaining the theory of copulas. From a probabilistic view, copulas are multivariate distribution functions whose one-dimensional margins are uniform on the interval $[0, 1]$. Alternatively, copulas are functions that join multivariate distribution functions to their one-dimensional marginal distribution functions, embodying all information about the dependence structure between the components of a random vector (see for instance Nelsen, 2006).

It is of particular interest, especially in risk management, to measure the amount of dependence in the upper-right or lower-left tail of a bivariate distribution, i.e., the dependence between extreme events of two random variables. Considering different directions to approach the tail we arrive at the concept of tail copulas (Schmidt and Stadtmüller, 2006). The latter approach being closely related to the theory of copulas allows for measuring tail dependence in a variety of scenarios. This includes the well-known tail dependence coefficients when following the *diagonal section* of a copula. For instance, the lower tail dependence coefficient can be interpreted as the limiting likelihood of a portfolio return falling below its Value-at-Risk, given that another portfolio return has fallen below its Value-at-Risk at the same level. Summing up, once a copula has been associated with a random vector, its tail dependence is also determined (Joe, 1997). As we will see at a later stage, the converse is not true; there are many copulas that result in the same tail copula. Formal definitions of the above concepts will be given in due course.

When estimating tail dependence, one could follow two principal routes. Within the traditional approach, a parametric copula family is initially fitted to the whole dataset characterizing the overall dependence structure and the tail behavior of that particular copula is extracted later. The second approach, a more direct one, relies on extreme-value techniques taking only a part of the dataset into account, hence being robust against changes in the center of the distribution. Here, the statistician has to choose the amount of data which could be considered as *being in the tail*. Similar to other applications in extreme-value theory, there is no perfect global answer to the question of where the tail begins (see for example Bücher, 2014). This thesis is based on the latter approach using empirical tail copulas and analyzes the shortcomings of the first one by testing the respective applicability on a variety of examples.

As a first example, which will be analyzed in much detail in the course of this thesis, Fig. 1 shows daily quotes in USD/barrel of the WTI Cushing Crude Oil Spot and the Bloomberg European Dated Brent from October 2, 2006 to October 1, 2010, collected from Bloomberg's Financial Information Services. At first sight, the development of the two crude oil grades seems to be almost identical, i.e., one could think of an almost perfect correlation. Among other topics, this thesis investigates the overall dependence structure

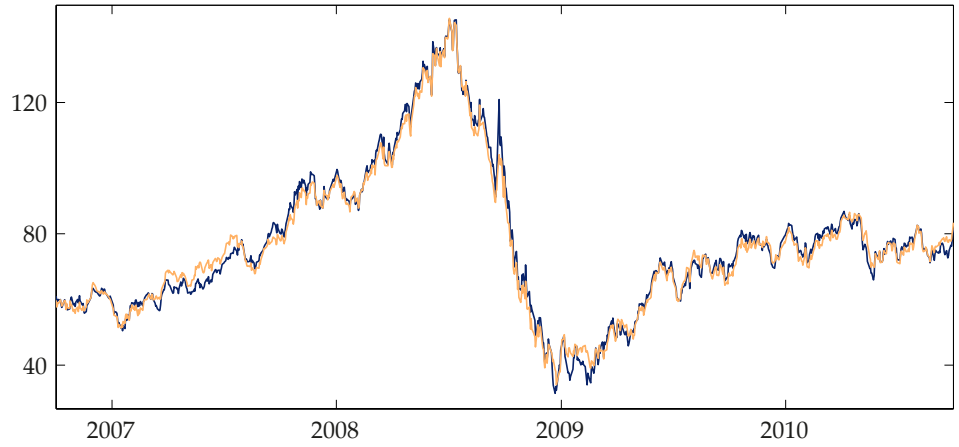

Fig. 1. Daily quotes in USD/barrel of the WTI Cushing Crude Oil Spot (blue) and the Bloomberg European Dated Brent (yellow) from October 2, 2006 to October 1, 2010.

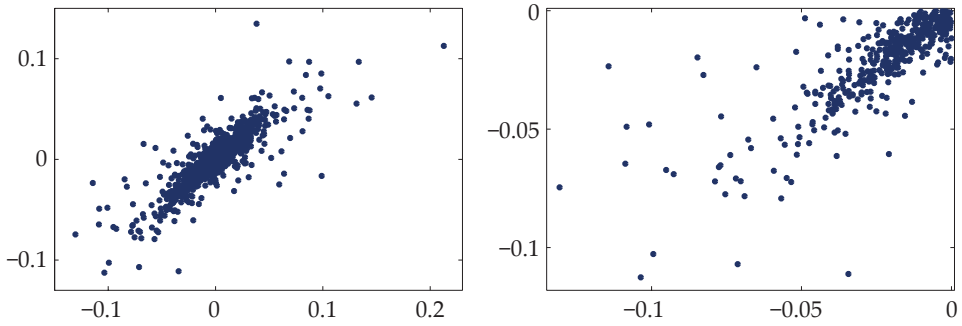

Fig. 2. Scatter plot of the WTI Cushing Crude Oil Spot (horizontal) and the Bloomberg European Dated Brent (vertical) log-returns from October 2, 2006 to October 1, 2010 (left) and enlarged third quadrant (right).

between the two oil grades and addresses the question whether the joint distribution has a (strong) tendency to generate extreme values simultaneously. In that case, a bivariate normal distribution with an arbitrary linear correlation coefficient would not be able to appropriately model the (tail) dependence. In this regard, see Embrechts et al. (2002) for common pitfalls and fallacies in risk management. A first view on the dependence can be gained from the scatter plots of the log-returns in Fig. 2. They reveal a strong co-movement between the two grades, which is not surprising at all, though a significant deviation from a comonotonic relationship (one random variable can be represented as an increasing function of the other) is evident.

So far, we have considered a static (time-independent) setting. However, there is an established empirical evidence that the dependence structure between financial returns, for instance measured by correlation (Krishnan et al., 2009), varies over time. Especially in times of crises, an increasing dependence is observable (sometimes referred to as *diversification meltdown*, see Campbell et al., 2008). Recently, nonparametric tests for constancy of the whole dependence structure have been developed (within the copula framework see Rémillard, 2010; Busetti and Harvey, 2011; Bücher and Ruppert, 2013; Bücher et al., 2014). The current thesis will follow this route of research and will present an approach to testing for constancy of the tail dependence using the concept of tail copulas. The newly developed tests allow for the verification of a constant tail dependence, which is

(implicitly) assumed by most former related empirical studies. Failing this, structural break-points might be revealed.

Contributing material This thesis is a cumulative one, comprising three peer-reviewed and published papers. The full bibliographic details are

(i) Jäschke, S., Siburg, K. F., and Stoimenov, P. A. (2012), *Modeling dependence of extreme events in energy markets using tail copulas*, Journal of Energy Markets, 5(4), 60–80,

(ii) Jäschke, S. (2014), *Estimation of risk measures in energy portfolios using modern copula techniques*, Computational Statistics and Data Analysis, 76, 359–376, CFEnetwork: The Annals of Computational and Financial Econometrics 2nd Issue,

(iii) Bücher, A., Jäschke, S., and Wied, D. (2015), *Nonparametric tests for constant tail dependence with an application to energy and finance*, Journal of Econometrics, 187(1), 154–168.

The first article (Chapter 1) studies, for the first time in the literature, the dependence of extreme events in energy markets and has been the starting point for the further research presented here. The particular dataset covers daily quotes of the generic one-month-ahead futures Light Sweet Crude Oil and Henry Hub Natural Gas traded on the New York Mercantile Exchange between July 2, 2007 and July 2, 2010. After a careful modeling of the marginals, it is shown that adopting general copula inference techniques (applying a goodness-of-fit test for copulas to the whole support of the bivariate distribution) can be very misleading for modeling the joint tail behavior of the log-returns of the crude oil and natural gas futures. Moreover, we emphasize the advantage of tail copulas over the single tail dependence coefficients allowing to account for different extreme outcomes. The nonparametric estimation of the tail copulas is carried out by calculation of the lower and upper empirical tail copulas according to Schmidt and Stadtmüller (2006). For this purpose, the optimal threshold *separating* the tail from the center of the joint distribution is found via a plateau-finding algorithm.

The objective of the second article (Chapter 2) is the modeling of stochastic tail dependence in energy and commodity markets. This is particularly relevant as a thorough understanding of energy portfolio risk requires an adequate assessment of the probability that extreme movements occur together. The dataset consists of the WTI Cushing Crude Oil Spot and the Bloomberg European Dated Brent log-returns from October 2, 2006 to October 1, 2010 (see Figs. 1 and 2). To obtain an adequate respective data generation process, several single equation models accounting for autocorrelation and volatility clustering are applied. The essential part of the article is the application of the newly introduced partial derivatives multiplier bootstrap goodness-of-fit test for tail copulas (Bücher and Dette, 2013) to the filtered dataset (more precisely, the standardized residuals calculated from the preceding time series models). The findings are then compared to a traditional copula fit as briefly described above. In this regard, the newly introduced Copula Information Criterion is applied (Grønneberg and Hjort, 2014). Finally, the article provides a wide and comprehensive backtesting framework for the risk measures Value-at-Risk and Expected Shortfall. As suspected, the best tail copula model slightly outperforms the traditional copula fit. This backtesting approach, derived from the (tail) copula techniques described above, has not yet been addressed before in the literature.

The third article (Chapter 3) develops asymptotic tests for detecting structural breaks in the tail dependence of multivariate time series. In particular, to obtain asymptotic properties, a new limit result for the sequential empirical tail copula process is derived.

Moreover, we perform an elaborated simulation study that investigates the finite sample properties of the proposed testing procedures. In the observed behavior, the tests are slightly conservative combined with reasonable power properties. The study further reveals that the asymptotic behavior of the estimator based on time series residuals is the same as the one based on independent and identically distributed observations. The developed tests allow for verifying the implicit assumption of constant tail dependence between the log-returns from Fig. 2. Indeed, it is shown that this assumption cannot be rejected. A second application investigates the constancy of the tail dependence between the Dow Jones Industrial Average and the Nasdaq Composite time series around Black Monday on 19th of October 1987. Here, the question is addressed whether Black Monday constitutes a significant break in the dependence structure. Whereas our tests for a break-point on Black Monday do not yield entirely unambiguous results, an overall model with *some* unspecified break-point can be accepted.

Remarks As this cumulative thesis consists of three self-contained articles, some parts within the respective preliminary sections may coincide. Furthermore, as an alternative to providing references at the end of each article, all of them are combined and sorted alphabetically at the end of this thesis. Whenever necessary, the bibliographic details have been updated. To achieve a consistent layout some parts of the published papers have been adjusted. This includes the common usage of American English and the standardization of notation across all articles where possible.

In the first article, all figures have been replaced by recreated colored versions and respective legends have been added. Moreover, instead of the published p-values, the standard errors of the estimated parameters in the univariate models (1.15) and (1.16) are provided, see Table 1.1. The latter does not imply a loss of information as each of the two quantities can be calculated once the other one is known.

The third published article contains an online supplement. All additional tables and figures contained therein have been integrated into the main part of this thesis. The proofs are now deferred to Section 3.7. In addition, whereas the finite sample study in the published version only reports the simulated rejection probabilities for the level of significance $\alpha = 5\%$, Section 3.4.2 presents the calculated target values for all three levels of significance $\alpha \in \{1\%, 5\%, 10\%\}$.

Appendix A lists selected source code and algorithms used for obtaining the results presented in this thesis. The commented code is written in a way that should make it possible for the interested reader to apply it without further instructions. With respect to the nonlisted parts, all algorithms and methods are described in detail in the following articles which should be sufficient for any efforts to reproduce the data.

Chapter 1

Modeling dependence of extreme events in energy markets using tail copulas

Abstract

This paper studies, for the first time, the dependence of extreme events in energy markets. Based on a large dataset comprising daily quotes of crude oil and natural gas futures, we estimate and model large co-movements of commodity returns. To detect the presence of tail dependence we apply a new method based on the concept of tail copulas, which accounts for different scenarios of joint extreme outcomes. Moreover, we show that the common practice of fitting copulas to the data cannot capture the dynamics in the tail of the joint distribution. It is therefore unsuitable for risk management purposes.

1.1 Introduction

As energy and commodity markets have become more volatile and increasingly interconnected in recent years, the ability to capture the joint dynamics of commodity prices has become indispensable for managing energy risk. In contrast to the vast literature on modeling dependence between stock returns, there is a relative paucity of related research for the energy market. Alexander (2004) shows that the log-returns of futures on crude oil and natural gas exhibit asymmetric behavior and strong, nonlinear dependence – a far cry from the assumption that their joint distribution is bivariate normal. The same problem is studied in Grégoire et al. (2008). They model the daily log-returns individually as time series, and account for the dependence between them by fitting various families of copulas to the error terms. In order to select the best copula, the authors perform a range of goodness-of-fit tests, which again show that the dependence between crude oil and natural gas log-returns cannot be characterized by the Gaussian copula. Accioly and Aiube (2008) study the dependence of oil and gasoline prices. After adjusting generalized autoregressive conditional heteroskedasticity (GARCH) models to filter the linear and the nonlinear time dependence in the series of returns they fit various copulas to the residuals of these models. Dividing the sample in two periods, it is shown that the dependence is well represented by the t-copula and the Plackett copula, respectively.

The departure from normality in a multivariate setting poses an additional problem from the perspective of risk management, whose primary concern is the occurrence of extreme events. In the univariate case, non-normality is associated to the skewness and leptokurtosis phenomena (more briefly, the fat-tail problem). In the multivariate case,

the fat-tail problem can be attributed not only to the marginal distributions but also to the probability of large co-movements of the individual returns, i.e., tail dependence. Consequently, a thorough understanding of energy portfolio risk requires an adequate assessment of the probability that large price movements in energy markets occur together.

The latest statistical standard to describe the amount of extremal dependence is represented by the concept of tail dependence. To the best of our knowledge, however, the problem of modeling and estimating tail dependence between returns of energy commodities has not yet been addressed in the literature. The present paper opens this line of research by analyzing a large dataset comprising daily quotes of the Light Sweet Crude Oil Futures and the Henry Hub Natural Gas Futures traded on the NYMEX (New York Mercantile Exchange). From a methodological point of view, the main tool is the theory of copulas, which allows the separate specification of the marginal distributions and the dependence structure.

The purpose of the paper is twofold: First, to provide an applicable model which estimates adequately the likelihood of joint extreme events in energy markets. Second, to illustrate the pitfalls of fitting copulas to data for risk management purposes. Undoubtedly, copulas represent the current standard for modeling stochastic dependence. However, we argue that a general goodness-of-fit test for copulas does not necessarily provide a good model for tail dependence. The reason is that the procedure is based on minimizing the distance between observed and model values over the whole support of the distribution and therefore cannot capture the joint dynamics in the tail of the underlying distribution. Thus, to some extent, the paper is also meant as an educative warning against adopting general copula inference techniques for modeling dependence of extreme events.

In order to overcome this difficulty, we apply the concept of tail copulas. A tail copula is a function of the underlying copula, which describes the dependence structure in the tail of multivariate distributions, but works more generally than the simple tail dependence coefficient, which is just the value of the tail copula at the point $(1, 1)$. Therefore, tail copulas enable the modeling of tail dependence of arbitrary form and, thus, account for all possible scenarios of joint extreme outcomes.

The paper is organized as follows. In the next section we briefly review some fundamental properties of copulas and introduce the closely related concept of tail copulas and tail dependence. Section 1.3 describes the data. To account for serial dependence in the data we estimate numerous univariate GARCH and asymmetric power ARCH (APARCH) models with various distributions for the error term. Section 1.4 presents our methodology and the empirical results. In a first step we fit different families of copulas to the residuals of the individual time series. Then, we estimate nonparametrically (Schmidt and Stadtmüller, 2006) the lower and upper tail copulas and show that the joint distribution of the log-returns of the crude oil and natural gas futures are both lower and upper tail dependent, a fact which can not be detected by fitting a copula to the whole dataset. The final Section 1.5 summarizes and provides an outlook for further research.

1.2 Preliminaries

The theory of copulas dates back to Sklar (1959), but its application to statistical modeling is far more recent. A copula is a function that embodies all the information about the dependence structure between the components of a random vector. From a probabilistic point of view, it is a multivariate distribution function with uniformly distributed

margins on the interval $[0,1]$. For notational convenience, all further definitions and results are provided for the bivariate case only. In the following, we consider a random vector (X,Y) with continuous marginal distribution functions $F(x) := \mathbb{P}[X \leq x]$ and $G(y) := \mathbb{P}[Y \leq y]$, $x, y \in \mathbb{R}$, respectively. By Sklar's theorem, there exists a unique copula C, called the copula of X and Y, such that

$$\mathbb{P}[X \leq x, Y \leq y] = C(F(x), G(y)), \tag{1.1}$$

for all $x, y \in \mathbb{R}$. Conversely, if C is a copula and F, G are distribution functions, then the function defined via (1.1) is a bivariate distribution function with margins F, G. It follows that copulas can be interpreted as dependence functions since they separate the marginal distributions from the dependence structure. In fact, the copula of X and Y is the joint distribution function of the probability integral transformations $U := F(X)$ and $V := G(Y)$, which are uniform on $[0,1]$. It follows that

$$C(u,v) = \mathbb{P}[U \leq u, V \leq v] = \mathbb{P}[X \leq F^-(u), Y \leq G^-(v)], \tag{1.2}$$

for all $u, v \in [0,1]$, where F^- and G^- denote the generalized inverses of F and G, respectively, i.e., $F^-(u) = \inf\{x \in \mathbb{R} | F(x) \geq u\}$, for all $u \in [0,1]$ (analogously for G).

Let $\bar{F}(x) := 1 - F(x) = \mathbb{P}[X > x]$ and $\bar{G}(y) := 1 - G(y) = \mathbb{P}[Y > y]$ denote the corresponding survival functions of X and Y. Define a function $\bar{C}$ by

$$\bar{C}(u,v) = u + v - 1 + C(1-u, 1-v), \tag{1.3}$$

for all $u, v \in [0,1]$. Then, for all $x, y \in \mathbb{R}$, we have

$$\mathbb{P}[X > x, Y > y] = \bar{C}(\bar{F}(x), \bar{G}(y)). \tag{1.4}$$

The function $\bar{C}$ is a copula itself and is called the survival copula of X and Y. In view of (1.4), the survival copula links the joint survival function to its univariate margins in a manner completely analogous to the one in which the copula connects the joint distribution function to its margins. Hence, for all $u, v \in [0,1]$, we have

$$\begin{aligned} \bar{C}(u,v) &= \mathbb{P}[U > 1-u, V > 1-v] \\ &= \mathbb{P}[X > F^-(1-u), Y > G^-(1-v)]. \end{aligned} \tag{1.5}$$

For further details regarding the theory of copulas we refer the reader to Nelsen (2006).

As the focus of this paper is to characterize and measure extremal dependence, the remainder of this section is devoted to the concept of tail dependence, which concentrates on the upper and lower quadrant tails of the joint distribution. The standard way to determine whether X and Y are tail dependent is to look at the so-called lower and upper tail dependence coefficients, denoted by λ_L and λ_U, respectively. λ_L is the limit (if it exists) of the conditional probability that X is less than or equal to the u-th quantile of F, given that Y is less than or equal to the u-th quantile of G as u approaches 0, i.e.,

$$\lambda_L := \lim_{u \searrow 0} \mathbb{P}[X \leq F^-(u) \mid Y \leq G^-(u)]. \tag{1.6}$$

Similarly, λ_U is the limit (if it exists) of the conditional probability that X is greater than the u-th quantile of F, given that Y is greater than the u-th quantile of G as u approaches 1, i.e.,

$$\lambda_U := \lim_{u \nearrow 1} \mathbb{P}[X > F^-(u) \mid Y > G^-(u)]. \tag{1.7}$$

The random vector (X, Y) is said to have lower (upper) tail dependence if $\lambda_L(\lambda_U) \in (0, 1]$, and no lower (upper) tail dependence if $\lambda_L(\lambda_U) = 0$.

The following identities show that the tail dependence coefficients are nonparametric and depend only on the copula C of X and Y. In particular, we have (see Nelsen, 2006)

$$\lambda_L = \lim_{u \searrow 0} \frac{C(u,u)}{u} \tag{1.8}$$

and

$$\lambda_U = \lim_{u \nearrow 1} \frac{1 - 2u + C(u,u)}{1-u} = \lim_{u \searrow 0} \frac{\bar{C}(u,u)}{u}, \tag{1.9}$$

where $\bar{C}$ is the survival copula of X and Y defined in (1.3). Since copulas are invariant under strictly increasing transformations of the random variables, it follows that λ_L and λ_U exhibit the same invariance property.

From a practitioner's point of view, tail dependence can be interpreted as the limiting likelihood of an asset/portfolio return falling below its Value-at-Risk at a certain level, given that another asset/portfolio return has fallen below its Value-at-Risk at the same level. However, like any scalar measure of dependence, λ_L and λ_U suffer from a certain loss of information concerning the joint behavior in the tails of the distribution. In the context of tail dependence, the immediate analogues of copulas, which describe the entire dependence structure, is given by tail copulas; see Schmidt and Stadtmüller (2006) for further details on tail copulas. The lower tail copula Λ_L associated with X and Y is a function of their copula C and is defined by

$$\Lambda_L(x,y) := \lim_{t \searrow 0} \frac{C(tx,ty)}{t}, \tag{1.10}$$

if the above limit exists for all $(x, y) \in \mathbb{E} = [0, \infty]^2 \setminus \{(\infty, \infty)\}$. The upper tail copula Λ_U associated with X and Y is a function of their survival copula $\bar{C}$ and is defined by

$$\Lambda_U(x,y) := \lim_{t \searrow 0} \frac{\bar{C}(tx,ty)}{t}, \tag{1.11}$$

if the above limit exists for all $(x, y) \in \mathbb{E}$.

The probabilistic interpretation of Λ_L and Λ_U is provided by the following relationships:

$$\Lambda_L(x,y) = y \lim_{t \searrow 0} \mathbb{P}[X \le F^-(tx) \mid Y \le G^-(ty)], \tag{1.12}$$

$$\Lambda_U(x,y) = y \lim_{t \searrow 0} \mathbb{P}[X > F^-(1-tx) \mid Y > G^-(1-ty)]. \tag{1.13}$$

It is easy to show that the tail dependence coefficients are a special case of the respective tail copulas. More precisely, we have

$$\lambda_L = \Lambda_L(1,1) \quad \text{and} \quad \lambda_U = \Lambda_U(1,1). \tag{1.14}$$

As pointed out in Schmidt and Stadtmüller (2006), another reason to embed the tail dependence coefficients in the framework of tail copulas is to facilitate their estimation, which is a nontrivial task, especially for nonstandard distributions.

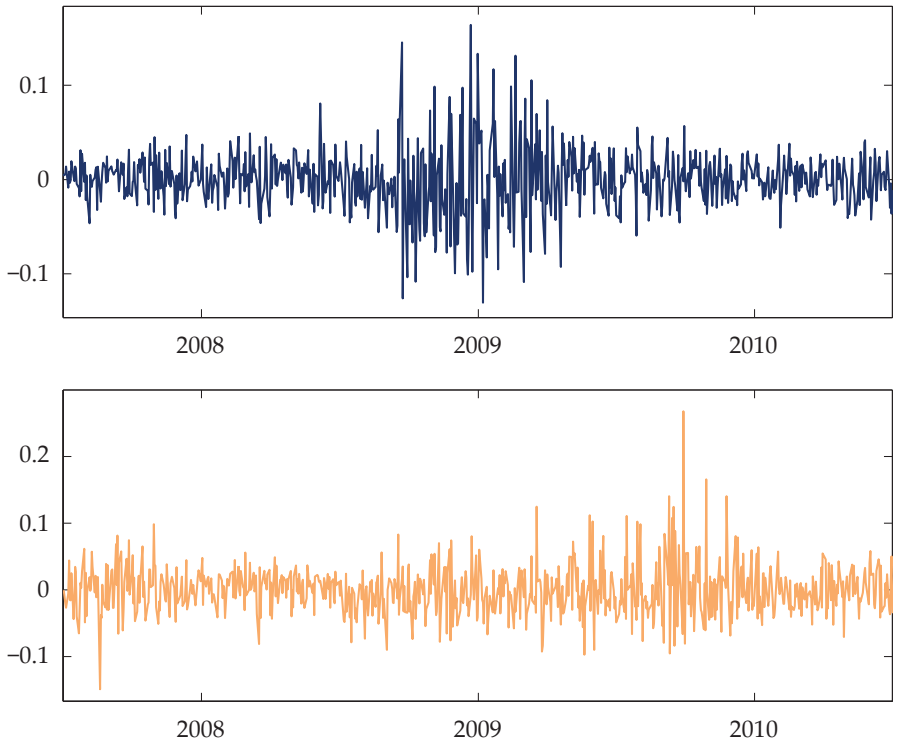

Fig. 1.1. Log-returns of the one-month-ahead futures on crude oil (top) and natural gas (bottom) between July 2, 2007 and July 2, 2010.

1.3 Data

Our empirical investigation focuses on the dependence between crude oil and natural gas log-returns. The dataset covers daily quotes of the Light Sweet Crude Oil Futures and the Henry Hub Natural Gas Futures traded on the NYMEX (New York Mercantile Exchange) between July 2, 2007 and July 2, 2010. Both futures contracts are generic one-month-ahead futures. The quotes are collected from Bloomberg's Financial Information Services.

The daily log-returns for both series are plotted in Fig. 1.1. In order to estimate and model the dependence between the two commodities, it is necessary to consider dependence within the individual time series. To detect the presence of heteroscedasticity we perform standard Box-Pierce and Ljung-Box tests on the squared log-returns for three different lags (lag 1, lag 5 and lag 10). For crude oil, both tests are significant at the 1% level for all lags. Applied to the natural gas data, the same is true for lag 5 and lag 10, while the null hypothesis that none of the autocorrelation coefficients up to a certain lag are different from zero cannot be rejected for lag 1 (p-value equals 0.18).

These findings show that the assumption of an independent and identically distributed sample is unrealistic and therefore one has to account for heteroscedasticity in the marginal series. For this purpose, we employ GARCH(p,q) and APARCH(p,q)-models, $p,q \in \{1,\dots,6\}$, with various distributions for the error term, including the normal, the generalized error, their skewed variants and the skewed Student's t-distribution. The 360 models under test are evaluated by simultaneously considering three selection criteria: statistical significance of the model parameters (p-value < 0.05), lack of autocorrelation in the squared standardized residuals of both series for different lags (p-value > 0.05)

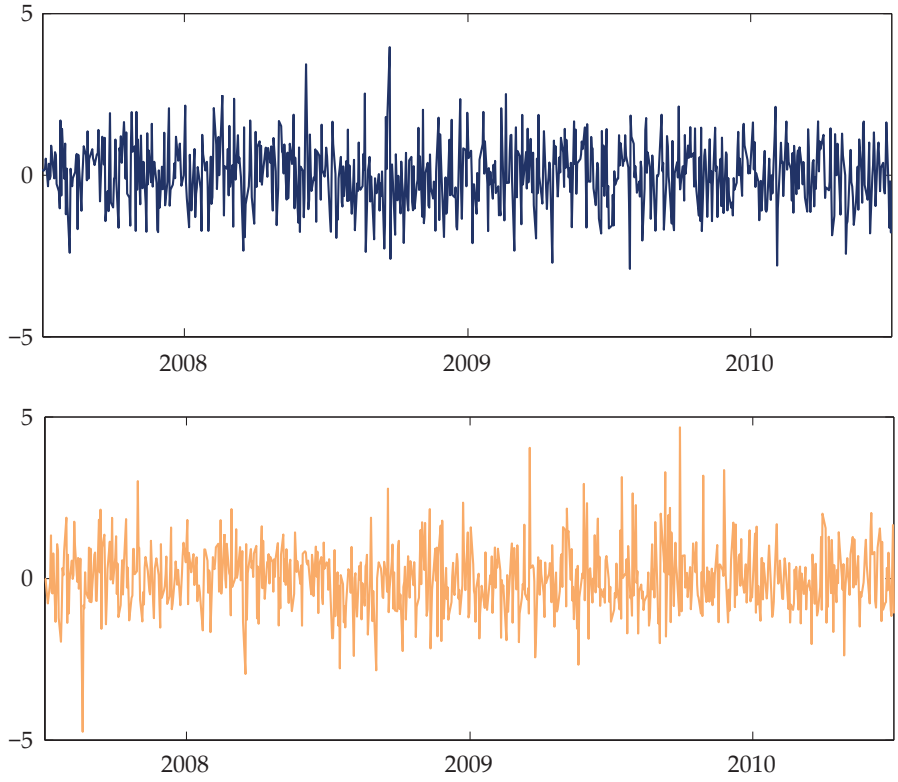

Fig. 1.2. Standardized residuals of the individual time series models (1.15) and (1.16) for the daily log-returns of the crude oil (top) and natural gas (bottom) futures.

and different information criteria (the Akaike information criterion, the Bayesian information criterion, the Schwarz information criterion and the Hannan-Quinn information criterion).

It turns out that the APARCH$(1,1)$-model with skewed normal distribution describes most adequately the data generating process for the log-returns O_t, $t = 1, \ldots, T$, of the crude oil futures:

$$\begin{aligned} O_t &= 2.639 \times 10^{-5} + \sigma_t X_t, \\ \sigma_t^2 &= 1.193 \times 10^{-5} \\ &\quad + 9.542 \times 10^{-2}(|\sigma_{t-1} X_{t-1}| - 2.384 \times 10^{-1} \sigma_{t-1} X_{t-1})^2 \\ &\quad + 8.880 \times 10^{-1} \sigma_{t-1}^2. \end{aligned} \tag{1.15}$$

Thus, the standardized residuals $X_1, X_2, \ldots, X_T$, which are plotted in the upper panel of Fig. 1.2, can be viewed as a random sample from a skewed normal distribution with skewness parameter $\xi = 0.986$; see Azzalini and Dalla Valle (1996) for details on the skewed normal distribution.

With respect to the log-returns N_t, $t = 1, \ldots, T$, of the natural gas futures, the following GARCH(1,1)-model with skewed Student's t-distribution

$$\begin{aligned} N_t &= -4.842 \times 10^{-4} + \sigma_t Y_t, \\ \sigma_t^2 &= 2.648 \times 10^{-5} + 5.106 \times 10^{-2} \sigma_{t-1}^2 Y_{t-1}^2 \\ &\quad + 9.283 \times 10^{-1} \sigma_{t-1}^2 \end{aligned} \tag{1.16}$$

provides the best fit to the data. Analogously, we conclude that the standardized residuals $Y_1, Y_2, \ldots, Y_T$, which are plotted in the lower panel of Fig. 1.2, are randomly drawn from a skewed Student's t-distribution with skewness parameter $\xi = 1.113$ and $\nu = 8.094$ degrees of freedom. For the definition and properties of the skewed Student's t-distribution we refer to Azzalini and Capitano (2003).

Applying now the Box-Pierce and Ljung-Box tests to the squared standardized residuals of both series for lag 1, lag 5 and lag 10, provides completely different test results than initially obtained. None of the tests detects the presence of auto correlation at the 5% level. In fact, apart from the test results for the crude oil futures at lag 1 (p-value equals 0.06), the p-values exceed 0.4. Further, standard errors based on the asymptotic distribution of the maximum likelihood estimates are shown in Table 1.1.

Table 1.1. Maximum likelihood estimates together with their corresponding standard errors for the crude oil APARCH(1,1)-model with skewed normal distribution and the natural gas GARCH(1,1)-model including the skewed Student's t-distribution.

Parameter	Crude oil log-returns		Natural gas log-returns	
	Estimate	std. error	Estimate	std. error
Variance equation				
ω	0.0000	0.0000	0.0000	0.0000
α_1	0.0954	0.0253	0.0511	0.0158
γ_1	0.2384	0.1657	–	–
β_1	0.8880	0.0317	0.9283	0.0204
Distribution				
ξ	0.9856	0.0559	1.1134	0.0611
ν	–	–	8.0938	2.0669

1.4 Methodology and results

1.4.1 Copula estimation

Having specified adequate models for the daily log-returns of the crude oil and natural gas futures, O_t and N_t, we now address the problem of modeling their dependence. For this purpose, we employ the theory of copulas, briefly introduced in Section 1.2. The main advantage of copulas is that they allow the separate specification of the marginal distributions and the dependence structure.

As shown in the preceding section, (O_t, N_t), $t = 1, \ldots, T$, certainly does not constitute an i.i.d. sample. Therefore, in order to estimate their copula, we consider the sample (X_t, Y_t) of the standardized residuals of the individual time-series models (1.15) and (1.16). The next step is to transform each pair of observation into its rank based representation (u_t, v_t), calculated by

$$u_t = \frac{\text{rank}(X_t)}{T+1} \quad \text{and} \quad v_t = \frac{\text{rank}(Y_t)}{T+1}. \tag{1.17}$$

Figure 1.3 shows a scatter plot of the 758 pairs (u_t, v_t). It reveals a certain tendency of u_t and v_t, and thus of X_t and Y_t to vary together, regardless of their marginal distributions.

To confirm this judgement, we first estimate the two most common rank correlation coefficients, Spearman's rho and Kendall's tau, which depend solely on the underlying copula via

$$\rho(C) = -3 + 12 \int_0^1 \int_0^1 C(u, v)\, d(u, v), \tag{1.18}$$

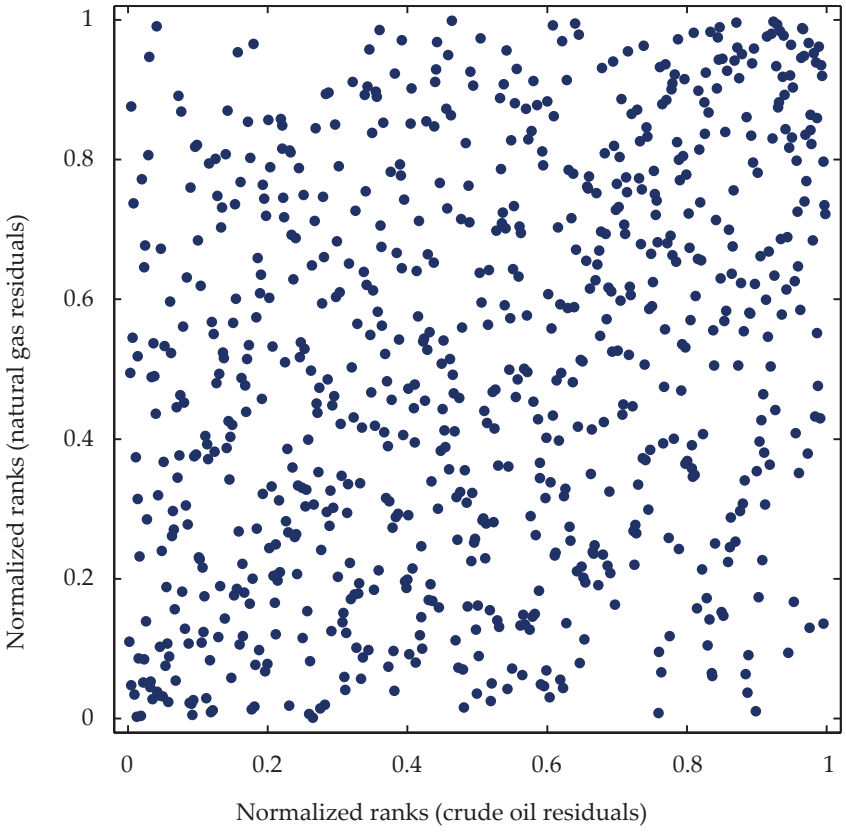

Fig. 1.3. Scatter plot of the ranks of the standardized residuals u_t and v_t.

$$\tau(C) = -1 + 4\int_0^1\int_0^1 C(u,v)c(u,v)\,d(u,v), \tag{1.19}$$

where $c(u,v) = \partial^2 C(u,v)/\partial u\partial v$ is the density of C (assuming it exists). For the empirical measures $\hat{\rho}_T$ and $\hat{\tau}_T$ (Genest and Favre, 2007) we find that $\hat{\rho}_T = 0.314$ and $\hat{\tau}_T = 0.214$, which are both significantly different from zero (p-value < 0.001). For details about the test statistics and their asymptotic distributions we refer to Genest and Favre (2007). These preliminary results are in accordance with the ones reported in Grégoire et al. (2008), who perform the same tests on their dataset.

Note that, as any scalar measure of dependence, ρ and τ cannot describe the whole dependence structure of the joint distribution. Therefore, having concluded that the log-returns of the crude oil and natural gas futures are positively dependent, we now address the problem of estimating their copula. For this purpose we first compute the empirical copula C_T (Deheuvels, 1979) and the empirical survival copula $\bar{C}_T$, defined by

$$C_T(u,v) = \frac{1}{T}\sum_{t=1}^{T} \mathbb{1}(u_t \le u, v_t \le v) \tag{1.20}$$

and

$$\bar{C}_T(u,v) = \frac{1}{T}\sum_{t=1}^{T} \mathbb{1}(u_t > u, v_t > v), \tag{1.21}$$

where $\mathbb{1}$ denotes the indicator function.

Table 1.2. Test results for the goodness-of-fit test of different copula models in ascending order (p-value).

Copula	p-value	$\hat{\theta}_T$-value
Independence	0.000	
Pareto	0.000	0.545
Frank	0.027	2.001
Gaussian	0.289	0.330
t ($\nu = 9$)	0.311	0.330
Gumbel	0.712	1.272

In order to find an appropriate copula model, we consider different parametric families of copulas commonly used in economics and finance. Beside the independence copula $C(u, v) = uv$, we fit two elliptical copulas, Gaussian and t, and three Archimedean copulas, Pareto, Frank and Gumbel. Each of these families is completely characterized by a single parameter, θ, with exception of the t-copula, which, in addition, requires the specification of its degree of freedom ν. For each copula family, we estimate the unknown parameter θ by inversion of Kendall's tau (Genest and Rémillard, 2008). More precisely, the estimate $\hat{\theta}_T$ is computed by substituting $\hat{\tau}_T$ for τ in Eq. (1.19), and then solving the equation to obtain $\hat{\theta}_T$, which gives us the best copula fit $C_{\hat{\theta}_T}$ within the respective copula family. The inversion approach utilizes the fact that, for the considered copula families, θ is a monotone function of τ, which, for example, for the Gaussian and the t-copula is given by $\theta = \sin(\tau\pi/2)$.

Finally, to select the optimal copula model, we apply a goodness-of-fit test, based on the Cramér-von Mises statistic

$$S_T = \sum_{t=1}^{T} \left\{ C_T(u_t, v_t) - C_{\hat{\theta}_T}(u_t, v_t) \right\}^2. \tag{1.22}$$

A review and comparison of goodness-of-fit procedures is given by Genest et al. (2009). This statistic measures how close the fitted copula $C_{\hat{\theta}_T}$ is from the empirical copula C_T. Since the distribution of S_T depends on the unknown value of $\hat{\theta}_T$ under the null hypothesis that the true copula C is from the respective copula family, we compute the p-values of the test using the parametric bootstrap procedure described by Genest and Rémillard (2008).

The test results together with the estimates $\hat{\theta}_T$ are summarized in Table 1.2. They clearly show that the log-returns of crude oil and natural gas are not independent. Furthermore, the Pareto copula and, to a great extent, the Frank copula seem inappropriate to model the dependence structure. As to the specific form of the dependence, no definite conclusion can be drawn. The null hypothesis cannot be rejected for any of the other three candidates. In particular, even the Gaussian copula could be an applicable alternative, which of course does not imply that the joint distribution is bivariate normal. Using the highest p-value as a criterion to select the model with the best fit to the data, we conclude that the Gumbel copula, with $\hat{\theta}_T = 1.272$, describes best the dependence between crude oil and natural gas.

Finally, we point out, that our results differ substantially from those of Grégoire et al. (2008), who find, for example, that for the Gumbel copula the null hypothesis can be rejected on the basis of the same test procedure. In fact, in view of the extremely low p-values, not exceeding 0.03, none of the six copula models considered in Grégoire et al. (2008) provides an adequate description of the dependence between crude oil and natural gas log-returns.

1.4.2 Tail copula estimation

We now address the question whether the joint distribution of the log-returns of the crude oil and natural gas futures has a tendency to generate extreme values simultaneously and is, in this sense, a dangerous distribution for risk managers. The scatter plot in Fig. 1.3 reveals a pronounced concentration of data points in both tails of the distribution. As concluded above, however, the overall dependence structure is well represented by the Gumbel copula, which exhibits no lower tail dependence since, in view of Eq. (1.8), its lower tail dependence coefficient λ_L is 0. Thus, for modeling extremal dependence in the lower tail of the distribution, the Gumbel copula is no better choice than the independence copula.

We point out that this seeming contradiction suggests neither that the variables are tail independent, nor that the selected copula is unsuitable to model the overall dependence. It rather shows that a general goodness-of-fit test for copulas does not necessarily provide an appropriate model for tail dependence, simply because the procedure is based on minimizing the distance between observed and model values over the whole support of the distribution. In fact, one of the main aims of this paper is to illustrate the lack of effectiveness of fitting copulas to the data in capturing the dependence in the tail of the underlying distribution.

In order to assess the risk of joint extreme events, we apply the theory of tail copulas, briefly introduced in Section 1.2. For the estimation of the tail copulas, we use the lower and upper empirical tail copulas, denoted by $\hat{\Lambda}_L$ and $\hat{\Lambda}_U$, respectively. These nonparametric estimators, introduced and studied by Schmidt and Stadtmüller (2006), are defined by

$$\begin{aligned}\hat{\Lambda}_L(x,y) &:= \frac{T}{k} C_T\left(\frac{kx}{T}, \frac{ky}{T}\right) \\ &\approx \frac{1}{k}\sum_{t=1}^{T} \mathbb{1}\left(u_t \leq \frac{kx}{T+1}, v_t \leq \frac{ky}{T+1}\right)\end{aligned} \tag{1.23}$$

and

$$\begin{aligned}\hat{\Lambda}_U(x,y) &:= \frac{T}{k} \bar{C}_T\left(\frac{kx}{T}, \frac{ky}{T}\right) \\ &\approx \frac{1}{k}\sum_{t=1}^{T} \mathbb{1}\left(u_t > \frac{T-kx}{T+1}, v_t > \frac{T-ky}{T+1}\right)\end{aligned} \tag{1.24}$$

with some parameter $k \in \{1, \ldots, T\}$ to be chosen by the statistician. Under the assumptions that $k = k(T) \to \infty$ and $k/T \to 0$ for $T \to \infty$, Schmidt and Stadtmüller (2006) establishes weak convergence and strong consistency for $\hat{\Lambda}_L$ and $\hat{\Lambda}_U$. The paper also describes a method of choosing the optimal threshold k via a simple plateau-finding algorithm. Implementing this procedure, we calculate the empirical tail copulas for the log-returns of the crude oil and natural gas futures. These are visualized in Figs. 1.4 and 1.5.

Schmidt and Stadtmüller (2006) develop a consistent nonparametric estimator for the lower and upper tail dependence coefficients, given by

$$\hat{\lambda}_L := \hat{\Lambda}_L(1,1) \quad \text{and} \quad \hat{\lambda}_U := \hat{\Lambda}_U(1,1), \tag{1.25}$$

respectively. The estimators $\hat{\lambda}_L$ and $\hat{\lambda}_U$, based on the empirical counterparts of the identities given in (1.14), emphasize that tail copulas are an intuitive generalization of the tail

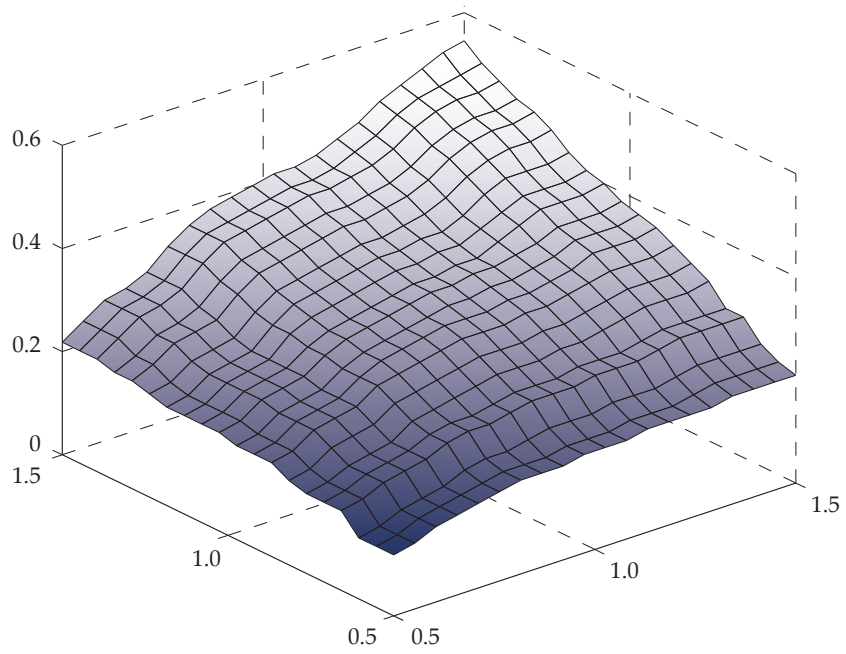

Fig. 1.4. Empirical lower tail copula $\hat{\Lambda}_L$ of the log-returns of the crude oil and natural gas futures.

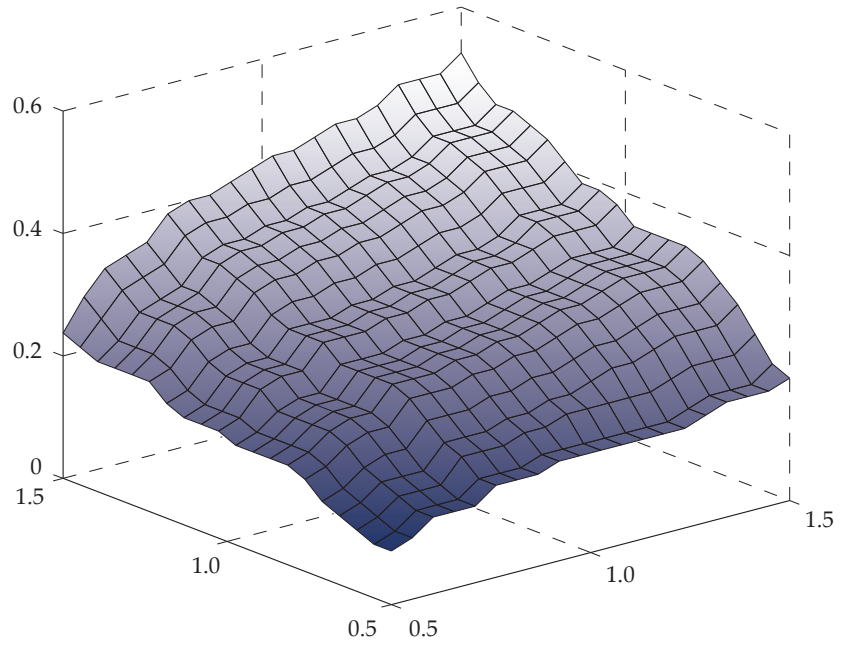

Fig. 1.5. Empirical upper tail copula $\hat{\Lambda}_U$ of the log-returns of the crude oil and natural gas futures.

Table 1.3. Tail dependence coefficients of the copulas considered for the goodness-of-fit test presented in Table 1.2.

Copula	$\hat{\lambda}_L(\hat{\theta}_T)$	$\hat{\lambda}_U(\hat{\theta}_T)$
Independence	0.000	0.000
Pareto	0.280	0.000
Frank	0.000	0.000
Gaussian	0.000	0.000
t ($\nu = 2.7$)	0.249	0.249
Gumbel	0.000	0.276
Empirical	0.318	0.281

dependence coefficients via a function describing the complete dependence structure in the tail of a distribution. Therefore, tail copulas constitute a powerful tool for modeling tail dependence of arbitrary form. Moreover, as pointed out in Schmidt and Stadtmüller (2006), tail copulas also provide a convenient method for the, otherwise, nontrivial task of estimating λ_L and λ_U.

For our dataset, we find $\hat{\lambda}_L = 0.318$ and $\hat{\lambda}_U = 0.281$, which implies that the log-returns of the crude oil and natural gas futures exhibit tail dependence. Our estimates clearly demonstrate that the Gumbel copula, with $\hat{\theta}_T = 1.272$, which, according to the goodness-of-fit test conducted in Section 1.4.1 provides the best fit to the data, does not describe adequately the risk of extreme events in the lower tail of the distribution. This raises the question of the optimal copula choice from a risk management perspective.

One possibility to deal with this problem is to select the copula, whose tail dependence coefficients are closest to their empirical counterparts. Table 1.3 lists the tail dependence coefficients of the copulas considered for the goodness-of-fit test. Note that the t-copula here has the same value of $\hat{\theta}_T$, but less degrees of freedom ν than the fitted one in Table 1.2 since the lower ν, the higher the tail dependence coefficients. Our choice $\nu = 2.7$ is dictated by the fact that for smaller degrees of freedom the null hypothesis of the goodness-of-fit test conducted in Section 1.4.1 must be rejected at the 5% level of significance.

It turns out that λ_L of the Pareto copula, with $\hat{\theta}_T = 0.545$, is closest to our estimate $\hat{\lambda}_L$, although according to the goodness-of-fit test results, presented in Table 1.2, the Pareto copula clearly fails to capture the overall dependence structure of the crude oil and natural gas returns. With respect to the upper tail of the distribution, the situation changes completely. Here the Gumbel copula, $\hat{\theta}_T = 1.272$, which exhibits the highest p-value of the goodness-of-fit test, remains the best model, since its $\lambda_U = 0.281$ almost coincides with the value of $\hat{\lambda}_U$.

At this point, we emphasize again that λ_L and λ_U, as scalar measures of tail dependence, cannot characterize the entire dependence structure in the tails of the distribution. For example, two tail copulas with the same value at $(1,1)$, corresponding to λ_L or λ_U, respectively, could differ substantially at other points in their domain. Thus, they could incorporate different levels of risk, although judging from the tail dependence coefficients alone, they would seem equally dangerous. In order to account for all possible scenarios of joint extreme outcomes one should utilize more information from the tail copula than simply its value at the point $(1,1)$.

From Table 1.3, it is evident that, beside the Pareto and Gumbel copulas, the only alternative for modeling tail dependence between the log-returns of crude oil and natural gas is the t-copula since all other copula models exhibit no tail dependence. Figures 1.6 and 1.7 visualize the values of the respective tail copulas and their empirical counterparts along the circle passing through the point $(1,1)$. Thus, the (empirical) tail dependence

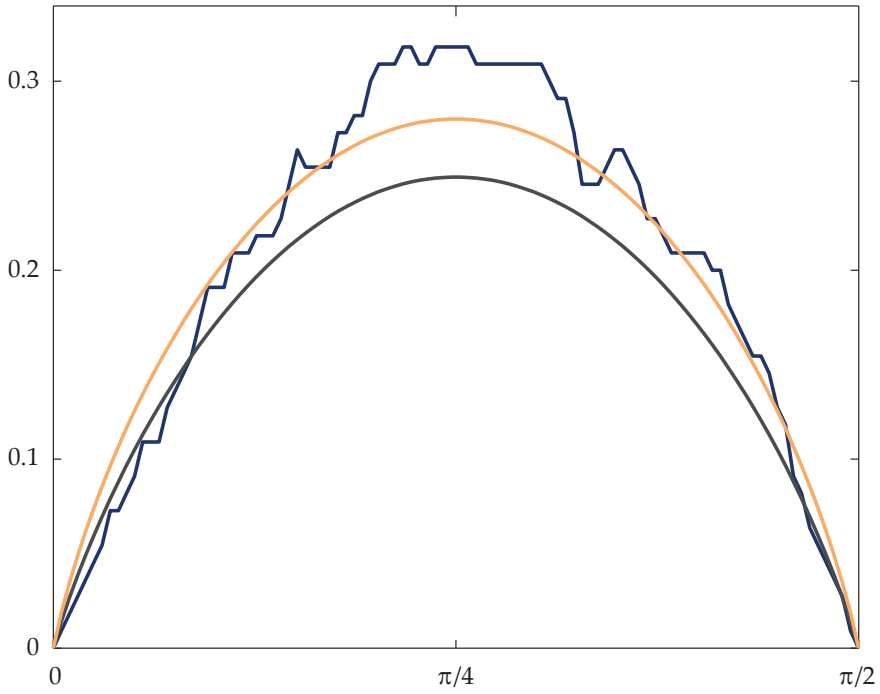

Fig. 1.6. Parametrization of the circle around the origin through the point $(1,1)$ in the first quadrant with values of the empirical lower tail copula $\hat{\Lambda}_L$ (blue line) as well as the lower tail copulas of the Pareto copula, $\hat{\theta}_T = 0.545$ (yellow line), and the t-copula, $\hat{\theta}_T = 0.330$, $\nu = 2.7$ (dark grey).

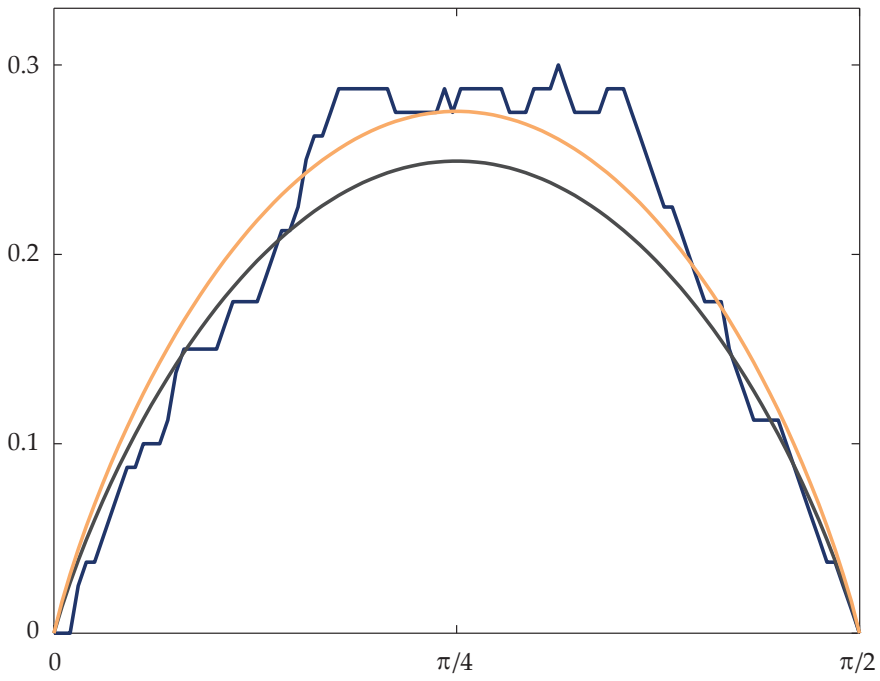

Fig. 1.7. Parametrization of the circle around the origin through the point $(1,1)$ in the first quadrant with values of the empirical upper tail copula $\hat{\Lambda}_U$ (blue line) as well as the upper tail copulas of the Gumbel copula, $\hat{\theta}_T = 1.272$ (yellow line), and the t-copula, $\hat{\theta}_T = 0.330$, $\nu = 2.7$ (dark grey).

coefficients are the values of the functions at $\pi/4$. Instead of comparing the plotted functions at a single point in their domain, we propose a least squares approach and calculate the Cramér-von Mises statistic for the empirical tail copula and the tail copula of each of the fitted copulas. This approach has the advantage of taking into account simultaneously different scenarios of extreme co-movements of the two variables. We find that the Pareto and Gumbel copulas remain the best models for lower and upper tail dependence, respectively.

1.5 Concluding remarks

This paper studies, for the first time, the dependence of extreme events in energy markets from both theoretical and empirical perspectives. Using daily quotes of the Light Sweet Crude Oil Futures and the Henry Hub Natural Gas Futures traded on the NYMEX between July 2, 2007 and July 2, 2010 we estimate and model both the overall dependence and the tail dependence of crude oil and natural gas log-returns. The main results which can be drawn from our empirical investigation can be summarized as follows.

According to the conducted goodness-of-fit test, the Gumbel copula describes best the overall dependence structure, but is unable to generate the joint occurrence of large drops in the analyzed commodity returns. However, applying the nonparametric technique for estimation of the tail copula introduced in Schmidt and Stadtmüller (2006), we detect the presence of such extreme events. These results suggest that a good model for the overall dependence between commodity returns can be a very bad model for their tail dependence. In fact, we see that using the copula which provides the best fit to the data can be very misleading for risk management which requires an adequate assessment of the probability that large price movements occur together.

With respect to the applicability of our results, it must be said that although the Pareto and Gumbel copulas describe well the lower and upper tail dependence in the data, respectively, they perform very badly in the other tail of the joint distribution. Among the considered copula families, the only copula which delivers satisfactory results as a general and, at the same time, as a tail dependence model is the t-copula.

An implicit assumption of our analysis is that the (tail) dependence between crude oil and natural gas log-returns is constant over time. Further research might analyze models with time-varying copulas to predict more accurately the probability of joint extreme movements in commodity returns. Finally, we point out that the use of our results for risk pricing and risk management depends on the effectiveness of different types of information on the tail dependence structure in bounding risk measures.

Chapter 2

Estimation of risk measures in energy portfolios using modern copula techniques

Abstract

The dependence structure between WTI and Brent crude oil spot log-returns is analyzed using modern copula techniques. In a first step, to account for autocorrelation and volatility clustering in the marginals, several single equation models are applied. Second, to select both copulas and tail copulas characterizing the joint dynamics between the time series, newly introduced bootstrap-based goodness-of-fit tests are implemented and evaluated. Based on each approach, a comprehensive backtesting is performed by simulating and comparing the risk measures Value-at-Risk and Expected Shortfall with observed values.

2.1 Introduction

The modeling of stochastic dependence in energy and commodity markets via copulas has become increasingly common in applications. Especially crude oil, which plays a major role in commodity investments, has been related to other markets (see, for instance Reboredo (2012); Wu et al. (2012); Aloui et al. (2013) for foreign exchange rate markets or Wen et al. (2012) for the stock market). When staying within the energy sector Grégoire et al. (2008) analyze the dependence structure of log-returns of futures on crude oil and natural gas, Accioly and Aiube (2008) study the co-movement of crude oil and gasoline prices, while Reboredo (2011) focuses on the dependence structure between crude oil benchmark prices. Using weekly data the article examines whether crude oil markets are rather globalized or regionalized. Having estimated each log-return time series individually, the author accounts for the dependence between the different crude oil grades by fitting various copula families to the error terms. The unknown parameters of the copula functions are obtained via maximum likelihood, whereas the decision which model performs best relies on an adjusted information criterion and a pseudo-likelihood ratio test. Additionally and directly linked to the estimated copula parameters, coefficients for upper and lower tail dependence are provided.

According to Jäschke et al. (2012) a general goodness-of-fit test for copulas does not necessarily provide a good model of tail dependence, as most of these procedures take the whole support of the distribution into account and therefore, adopting copula inference techniques for modeling joint extreme events can be very misleading for risk management purposes. Using the concept of tail copulas accounts for all possible scenarios of

joint extreme outcomes and thus decouples the decision to select an appropriate model describing the overall dependence from the analysis of the joint dynamics in the tail of the underlying distribution.

The present paper follows this route and extends the current state of knowledge within a couple of areas. First and foremost, we apply the partial derivatives multiplier bootstrap goodness-of-fit test for tail copulas (Bücher and Dette, 2013) to the log-returns of two crude oil grades. To compare the findings with a traditional copula fit we present both the best model characterizing the overall dependence structure using a bootstrap-based goodness-of-fit test for copulas and the newly introduced Copula Information Criterion (Grønneberg and Hjort, 2014). Moreover, from a risk management perspective it is indispensable to capture the joint behavior of certain assets within energy portfolios. Following Jäschke et al. (2012), a thorough understanding of energy portfolio risk requires an adequate assessment of the probability that large negative movements occur together, i.e., lower tail dependence. Therefore, the present paper introduces a wide and comprehensive backtesting framework for two of the most commonly applied risk measures, namely Value-at-Risk and Expected Shortfall.

Although the problem of modeling and assessing risk measures in energy portfolios using copulas is not completely new (see Liu, 2011; Lu et al., 2011; Wu et al., 2012), the backtesting approach derived from the techniques described above, to the best of our knowledge, has not yet been addressed before. The paper's claim to cover a topic of broad applicability and high practical relevance is backed by extensive guidelines from a practitioner's point of view as well as detailed comments concerning the empirical implementation.

The present analysis uses a large dataset of daily quotes of the WTI Cushing Crude Oil Spot and the Bloomberg European Dated Brent. WTI quotes are commonly used as a reference spot price for U.S. crude oil whereas the price for Brent serves as a benchmark for European crude oil. Both oil grades belong to the class of light and sweet crude oils, i.e., they are characterized by their low density and their low sulphur content. Although Brent is not as light or as sweet as WTI, it is still high-grade for subsequent processing and thus, both crude oils are not completely, but to a great extent, generally treated as interchangeable.

Due to these differences in quality, WTI futures were usually traded at a small premium to Brent futures. From early on in 2011 the development of the spread between the two futures has attracted the attention of energy and finance markets. Analysts and investors have become quite uncertain how to play the WTI-Brent anomaly. In fact, Brent did not only trade over WTI, but also the spread of the futures widened notably, which is reason enough to analyze the dependence structure between the two crude oil grades from a probabilistic point of view.

Historically, market participants often have not only assumed a physical interchangeability but accordingly a portfolio-interchangeability. Thus one could have thought of an almost perfect correlation between the two oil grades. After all, in view of the WTI-Brent anomaly, risk management needs to address the following two points. First, if a portfolio contains only one of the two varieties, it is really important to precisely consider and simulate the kind one is holding. Second, in the context of risk optimization with fixed expected returns it can be analyzed, whether or not it makes sense to hold both types simultaneously and thus diversifying the portfolio. However, should one keep both, a dedicated analysis of dependence is crucial since apparently structures have changed significantly and a simple correlation approach may mislead.

The paper is organized as follows: Section 2.2 briefly introduces the well-known copula framework and reviews the closely related concept of tail copulas with their corre-

sponding nonparametric estimates. Section 2.3 models the individual time series of both crude oil grades, accounting for serial dependence in the data. Section 2.4 describes the applied rank-based goodness-of-fit tests for copulas and tail copulas, respectively. Section 2.5 provides instruction on how to put the described theory into practice. Section 2.6 backtests the findings using the example of risk measures. Finally, Section 2.7 summarizes the results and the used methods.

2.2 Preliminaries

2.2.1 Copulas and tail dependence

The theory of copulas investigates the dependence structure of multivariate distribution functions. As this article focuses on co-movements between the WTI and Brent crude oil futures, we state all further definitions and results for the bivariate case only. From a probabilistic perspective, a copula is a joint distribution function with uniformly distributed margins on the interval $[0,1]$. To begin with, we consider a random vector (X,Y) with continuous marginal distribution functions $F(x) := \mathbb{P}[X \leq x]$ and $G(y) := \mathbb{P}[Y \leq y]$, $x, y \in \mathbb{R}$, respectively. The theoretical foundation for the application of copulas is provided by Sklar's theorem (Sklar, 1959), according to which there exists a unique copula C, called the copula of X and Y, such that

$$\mathbb{P}[X \leq x, Y \leq y] = C(F(x), G(y)), \tag{2.1}$$

for all $x, y \in \mathbb{R}$. Conversely, if C is a copula and F and G are distribution functions, then the function defined by Eq. (2.1) is a bivariate distribution function with margins F and G, respectively. It can be shown that

$$C(u,v) = \mathbb{P}[U \leq u, V \leq v] = \mathbb{P}[X \leq F^{-}(u), Y \leq G^{-}(v)], \tag{2.2}$$

for all $u, v \in [0,1]$, where F^{-} and G^{-} denote the quasi-inverses of F and G, respectively, i.e.,

$$F^{-}(u) = \inf\{x \in \mathbb{R} \mid F(x) \geq u\}, \tag{2.3}$$

for all $u \in [0,1]$ (analogously for G). Summing up, copulas allow for a stepwise modeling of the joint distribution whose dependence structure is independent of the respective marginal distributions. Further details can be found in Nelsen (2006).

Having set the copula framework, we are now able to introduce the concept of tail copulas that provides a generalized approach to model dependencies of extreme events. Following Schmidt and Stadtmüller (2006), the lower tail copula Λ_L associated with X and Y is a function of their copula C and is defined by

$$\Lambda_L(x,y) := \lim_{t \searrow 0} \frac{C(tx,ty)}{t}, \tag{2.4}$$

if the above limit exists for all $(x,y) \in \mathbb{E} := [0,\infty]^2 \setminus \{(\infty,\infty)\}$. Considered analytically, Λ_L describes the directional derivative of the copula C along the vector $(x,y) \in \mathbb{E}$ at the point $(0,0)$. According to Schmidt and Stadtmüller (2006), the lower tail copula admits the homogeneous structure among its components, i.e.,

$$\Lambda_L(sx,sy) = s\Lambda_L(x,y), \quad s \geq 0, \tag{2.5}$$

for all $(x,y) \in \mathbb{E}$. Regarding this property, we conclude that evaluating the lower tail copula on the unit circle in the first quadrant contains all information about the directional

derivatives of the copula C at the origin. Once these values are calculated the missing ones can be obtained by linear continuation according to Eq. (2.5). Moreover, in the following we assume that the lower tail copula is nonzero in some point $(x_0, y_0) \in \mathbb{E}$ and thus nonzero everywhere on $\mathbb{E}$ (Schmidt and Stadtmüller, 2006, Theorem 1).

The next part allows for embedding the well-known concept of tail dependence (see among others Joe, 1997; Frahm et al., 2005) into the framework of tail copulas. More precisely, two random variables X and Y are called lower tail dependent if the limit

$$\lambda_L := \Lambda_L(1,1) = \lim_{u \searrow 0} \mathbb{P}[X \leq F^-(u) \mid Y \leq G^-(u)] \tag{2.6}$$

exists and lies in the interval $(0,1]$. In case $\lambda_L = 0$, X and Y exhibit no lower tail dependence. Regarding the scope of this article, tail dependence can be viewed as the limiting likelihood of a commodity return falling below its Value-at-Risk at a certain level, given that another commodity return has fallen below its Value-at-Risk at the same level. As pointed out in Jäschke et al. (2012), the so-called lower tail dependence coefficient λ_L is not able to thoroughly capture the joint behavior in the lower tail of the distribution. Nevertheless, it is widely used as a simple and intuitive scalar measure for dependence between extreme losses of commodity returns.

2.2.2 Nonparametric estimates

In preparation for the rank-based goodness-of-fit tests in Section 2.4 we introduce nonparametric estimators for the copula C and the lower tail copula Λ_L, respectively. For this purpose we consider a sample $(X_1, Y_1), \ldots, (X_T, Y_T)$ from a pair (X, Y) of continuous random variables. Then the normalized rank-based representation (u_t, v_t) of the sample data (X_t, Y_t), $t = 1, \ldots, T$, is defined by

$$u_t = \frac{\text{rank}(X_t)}{T+1} \quad \text{and} \quad v_t = \frac{\text{rank}(Y_t)}{T+1}. \tag{2.7}$$

Assuming a time-independent dependence structure, the empirical copula C_T (see Deheuvels, 1979) is given by

$$C_T(u,v) = \frac{1}{T} \sum_{t=1}^{T} \mathbb{1}(u_t \leq u, v_t \leq v), \tag{2.8}$$

where $\mathbb{1}(A)$ denotes the indicator function of a set A. As argued in Genest and Favre (2007), the empirical Copula C_T is the best sample-based nonparametric representation of the copula C, which itself characterizes the dependence structure of the random vector (X, Y). Moreover, for any given pair (u, v), $C_T(u, v)$ serves as a consistent rank-based estimator of $C(u, v)$ that is asymptotically normally distributed with mean $C(u, v)$ (see Segers, 2012a).

To be able to adequately assess the risk of joint extreme losses, we now introduce the lower empirical tail copula $\hat{\Lambda}_L$ according to Schmidt and Stadtmüller (2006). This nonparametric estimator is defined by

$$\begin{aligned} \hat{\Lambda}_L(x,y) &:= \frac{T}{k} C_T\left(\frac{kx}{T}, \frac{ky}{T}\right) \\ &\approx \frac{1}{k} \sum_{t=1}^{T} \mathbb{1}\left(u_t \leq \frac{kx}{T+1}, v_t \leq \frac{ky}{T+1}\right) \end{aligned} \tag{2.9}$$

with some parameter $k \in \{1, \dots, T\}$ to be chosen by the statistician. As proven in Schmidt and Stadtmüller (2006), the estimator $\hat{\Lambda}_L$ exhibits weak convergence and strong consistency provided that $k = k(T) \to \infty$ and $k/T \to 0$ for $T \to \infty$ (and other regularity conditions, quod vide Huang, 1992). From an analytical perspective the lower empirical tail copula $\hat{\Lambda}_L$ can be viewed as the slope of the secant of the empirical copula $\widehat{C}_T$ containing the points $(0,0)$ and $(kx/T, ky/T)$ for $x^2 + y^2 = 1$, $x, y > 0$. Note that nonparametric estimation of several variants of Λ_L has been addressed in Drees and Huang (1998); Einmahl et al. (2006); de Haan and Ferreira (2006); Bücher and Dette (2013) for i.i.d. samples.

At the same time, the lower empirical tail copula yields a convenient method for the nontrivial task of estimating the lower tail dependence coefficient λ_L (see Schmidt and Stadtmüller, 2006). To be precise,

$$\hat{\lambda}_L := \hat{\Lambda}_L(1,1), \tag{2.10}$$

which again illustrates that the lower tail copula is an intuitive generalization of the lower tail dependence coefficient.

2.3 Modeling marginal time series

Since the copula is a function of the marginal distributions, an adequate modeling of the individual time series is crucial for estimating the dependence structure between two commodities. Recently, several empirical studies have analyzed the modeling of univariate time series for crude oil spot and futures prices considering different data frequencies (see among others Kang et al., 2009; Mohammadi and Su, 2010; Chang et al., 2010). For the purpose of the present study it is preferable to use daily returns over weekly returns to investigate joint extreme events, as weekly returns tend to smoothen returns especially in the tails of the distribution whose structure we are trying to capture here. Consequently, our dataset covers daily closing quotes of the WTI Cushing Crude Oil Spot and the Bloomberg European Dated Brent from October 2, 2006 to October 1, 2010, collected from Bloomberg's Financial Information Services.

First, to test the time series for weak stationarity we perform unit root tests on the logarithmic spot prices. Following the strategy proposed in Perron (1988), the realized Augmented Dickey-Fuller tests indicate that the null hypothesis of a unit root cannot be rejected for both WTI Crude Oil and European Brent. In a second step we apply the test to the first differences of the log time series. Here, the null hypothesis of non-stationarity can clearly be rejected at the 0.1% level. Taking the latter into account, we assume the log time series of both crude oil commodities to be integrated of order one. Accordingly, the following investigation focuses on the log-returns $r_t = \log(P_t) - \log(P_{t-1})$. Figure 2.1 shows the log-returns for both series.

To check for temporal dependence within the individual time series, we apply standard Ljung-Box tests to the observed and squared observed log-returns for three different lags (lag 1, lag 5 and lag 10). While for both series, in the case of squared observations, the null hypothesis that none of the autocorrelation coefficients up to the specified lag is different from zero can clearly be rejected at the 0.1% level of significance, the p-values for the nonsquared observations are given by $(0.239, 0.017, 0.004)$ for the WTI log-returns and $(0.167, 0.121, 0.052)$ for the Brent log-returns, respectively. Furthermore, applying the Lagrange multiplier test proposed by Engle (1982) rejects the null hypothesis of no ARCH effects for all lags at the 0.1% level.

Summing up, the findings show that the assumption of an i.i.d. sample is unrealistic. Thus, to account for autocorrelation and volatility clustering in the marginal

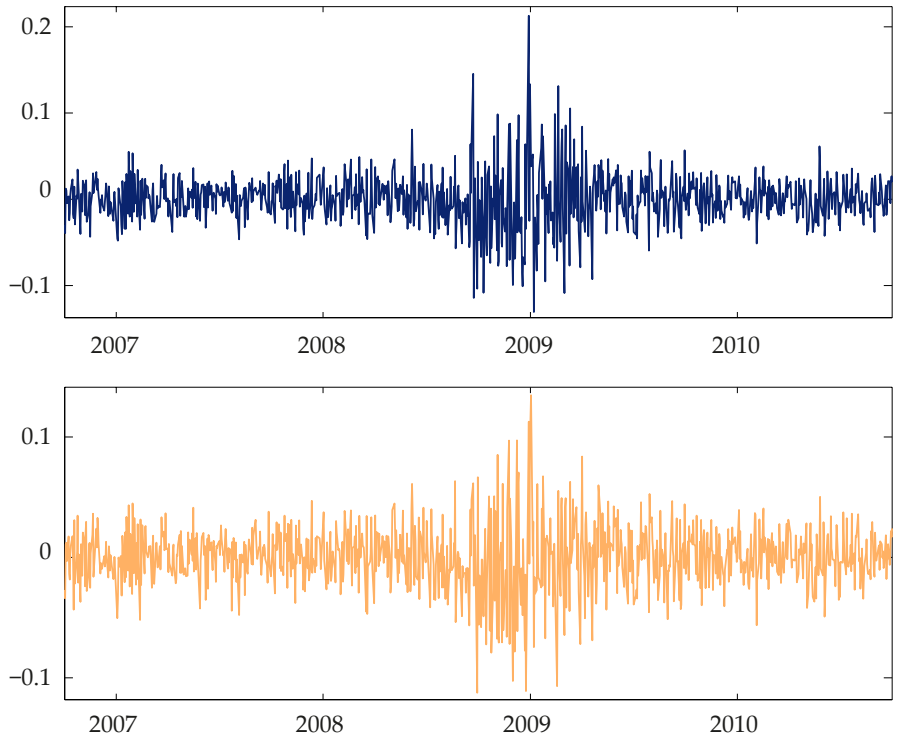

Fig. 2.1. Log-returns of the WTI Cushing Crude Oil Spot (top) and the Bloomberg European Dated Brent (bottom) from October 2, 2006 to October 1, 2010.

series we employ ARMA(a,b)-processes, $a,b \in \{0,1\}$, for modeling the conditional mean equation in combination with GARCH(p,q), APARCH(p,q), GJRGARCH(p,q) and EGARCH(p,q)-models, where $p,q \in \{1,2,3\}$. Additionally, following Liu (2011), we introduce exogenous variables into the conditional mean equation to explain the log-return time series. As energy prices are highly affected by imbalances of supply and demand, a representative indicator for this balance is given by the change in the energy inventory. Consequently, the applied model uses weekly U.S. stock data of commercial crude oil which is released by the Department of Energy. While Liu (2011) fits weekly published figures of the energy inventory data are fitted to daily granularity using piece-wise linear interpolation, we assume that the market is merely influenced on a single trading day, i.e., the weekly publication date. For details see Kemp (2010) and Fattouh (2010). Besides, the modeling allows various distributions for the error term, specifically the normal, the generalized error, the Student's t-distribution and their skewed extensions.

For illustration, we next consider the ARMA(a,b)-EGARCH(p,q)-model from Nelson (1991) with underlying fundamental factors:

$$r_t = \mu + \delta\mu_t + \sum_{i=1}^{a} \theta_i r_{t-i} + \varepsilon_t + \sum_{j=1}^{b} \psi_j \varepsilon_{t-j}, \tag{2.11}$$

where

$$\begin{aligned} &\mu, \delta \in \mathbb{R}, \quad a,b \in \mathbb{N}, \\ &\theta_i \in \mathbb{R}, \quad i = 1,\dots,a, \quad \psi_j \in \mathbb{R}, \quad j = 1,\dots,b \end{aligned}$$

and μ_t denotes the log-returns of the U.S. crude oil stock. The conditional variance process of the innovations $\varepsilon_t = \sigma_t z_t$ is given by

$$\begin{aligned}\log\left(\sigma_t^2\right) = \omega &+ \sum_{i=1}^{p} \alpha_i z_{t-i} + \gamma_i(|z_{t-i}| - E(|z_{t-i}|)) \\ &+ \sum_{j=1}^{q} \beta_j \log\left(\sigma_{t-j}^2\right),\end{aligned} \tag{2.12}$$

where

$$\begin{aligned}&p, q \in \mathbb{N}, \quad \omega \in \mathbb{R}, \\ &\alpha_i, \gamma_i \in \mathbb{R}, \quad i = 1, \ldots, p, \quad \beta_j \in \mathbb{R}, \quad j = 1, \ldots, q\end{aligned}$$

and $E(|z_t|)$ denotes the unconditional expected value of the absolute standardized innovations $|z_t|$.

The selection of an appropriate model requires criteria which are a priori specified. To be precise, all estimated parameters should be significant at the 1% level. Furthermore, standard Box-Pierce and Ljung-Box tests on the standardized and squared standardized residuals for three different lags (lag 1, lag 5 and lag 10) should indicate that the null hypothesis – none of the autocorrelation coefficients up to the certain lag is different from zero – cannot be rejected at the 10% level. The same threshold should be valid when applying Engle's Lagrange multiplier test for all lags up to and including lag 10. In addition we consider the information criteria AIC, BIC, SIC and HQIC as well as the corresponding QQ-plot of the standardized residuals. The modeling is carried out using the functionality of Ghalanos (2011).

Fulfilling all these criteria the ARMA(0,0)-EGARCH(2,3)-model with the explanatory variable and the skewed generalized error distribution adequately describes the data generating process W_t, $t = 1, \ldots, T$, of the daily WTI spot log-returns:

$$\begin{aligned}W_t &= 2.596 \times 10^{-4} - 3.216 \times 10^{-1}\mu_t \\ &\quad + \sigma_t X_t, \\ \log\left(\sigma_t^2\right) &= -3.438 \times 10^{-1} - 1.260 \times 10^{-1} X_{t-1} \\ &\quad - 1.267 \times 10^{-1} X_{t-2} \\ &\quad + 2.458 \times 10^{-1}(|X_{t-1}| - 7.961 \times 10^{-1}) \\ &\quad + 2.243 \times 10^{-1}(|X_{t-2}| - 7.961 \times 10^{-1}) \\ &\quad - 6.701 \times 10^{-1} \log\left(\sigma_{t-1}^2\right) + 9.745 \times 10^{-1} \log\left(\sigma_{t-2}^2\right) \\ &\quad + 6.494 \times 10^{-1} \log\left(\sigma_{t-3}^2\right).\end{aligned} \tag{2.13}$$

Consequently, the standardized residuals $X_1, \ldots, X_T$ can be viewed as a random sample from a skewed generalized error distribution with skewness parameter $\xi = 0.958$ and shape parameter $\nu = 1.960$; for details on the skewed generalized error distribution see Würtz et al. (2006).

At the same time, the ARMA(1,1)-EGARCH(2,3)-model including the explanatory variable and the skewed generalized error distribution provides the best fit to the daily

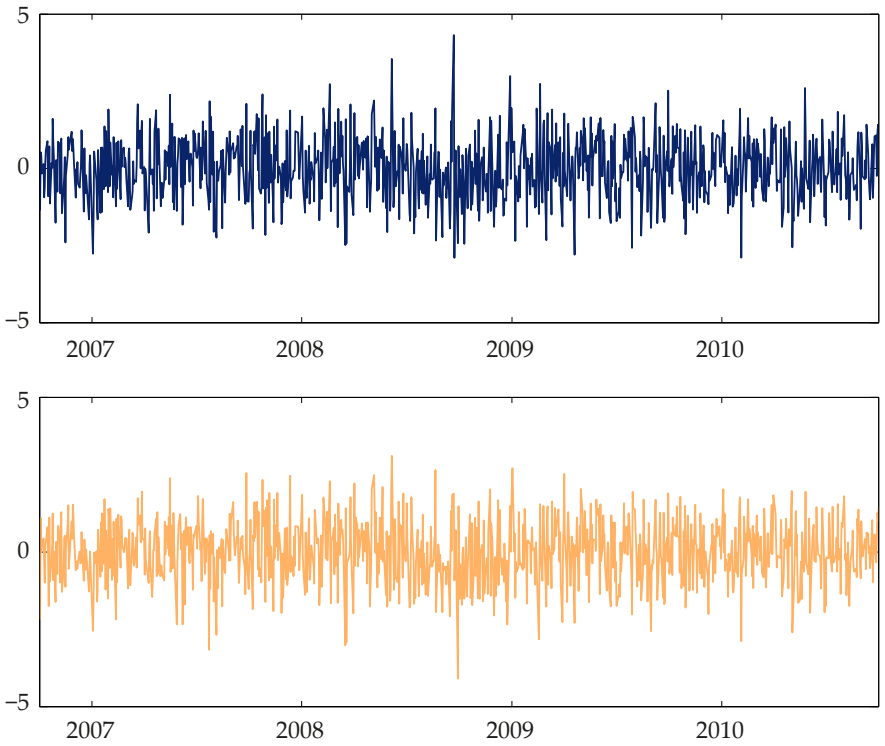

Fig. 2.2. Standardized residuals of both WTI Cushing Crude Oil Spot (top) and Bloomberg European Dated Brent (bottom) log-return time series.

Brent spot log-returns B_t, $t = 1, \ldots, T$:

$$\begin{aligned} B_t &= 3.064 \times 10^{-4} - 2.315 \times 10^{-1}\mu_t \\ &\quad - 7.893 \times 10^{-1} B_{t-1} \\ &\quad + \sigma_t Y_t + 7.641 \times 10^{-1}\sigma_{t-1}Y_{t-1}, \\ \log\left(\sigma_t^2\right) &= -2.803 \times 10^{-1} - 1.026 \times 10^{-1} Y_{t-1} \\ &\quad - 1.076 \times 10^{-1} Y_{t-2} \\ &\quad + 1.343 \times 10^{-1}(|Y_{t-1}| - 7.920 \times 10^{-1}) \\ &\quad + 8.270 \times 10^{-2}(|Y_{t-2}| - 7.920 \times 10^{-1}) \\ &\quad - 7.586 \times 10^{-1} \log\left(\sigma_{t-1}^2\right) + 9.098 \times 10^{-1} \log\left(\sigma_{t-2}^2\right) \\ &\quad + 8.117 \times 10^{-1} \log\left(\sigma_{t-3}^2\right). \end{aligned} \tag{2.14}$$

Therefore, we conclude that the standardized residuals $Y_1, \ldots, Y_T$ are randomly drawn from a skewed generalized error distribution with skewness parameter $\xi = 0.921$ and shape parameter $\nu = 1.873$. Figure 2.2 exhibits the standardized residuals which provide the basis for the following investigations for both WTI and Brent log-return time series. The corresponding QQ-plots are shown in Fig. 2.3. Although a few outliers do not fit the straight line, it seems safe to conclude that the respective residuals follow the specified distributions. To further validate the latter we apply the well-known Kolmogorov-Smirnov, Cramér-von Mises and Anderson-Darling goodness-of-fit tests. Here, the null hypotheses of the correct specification of the respective distribution function cannot be rejected at the 5% level of significance. More precisely, the p-values of the three tests are

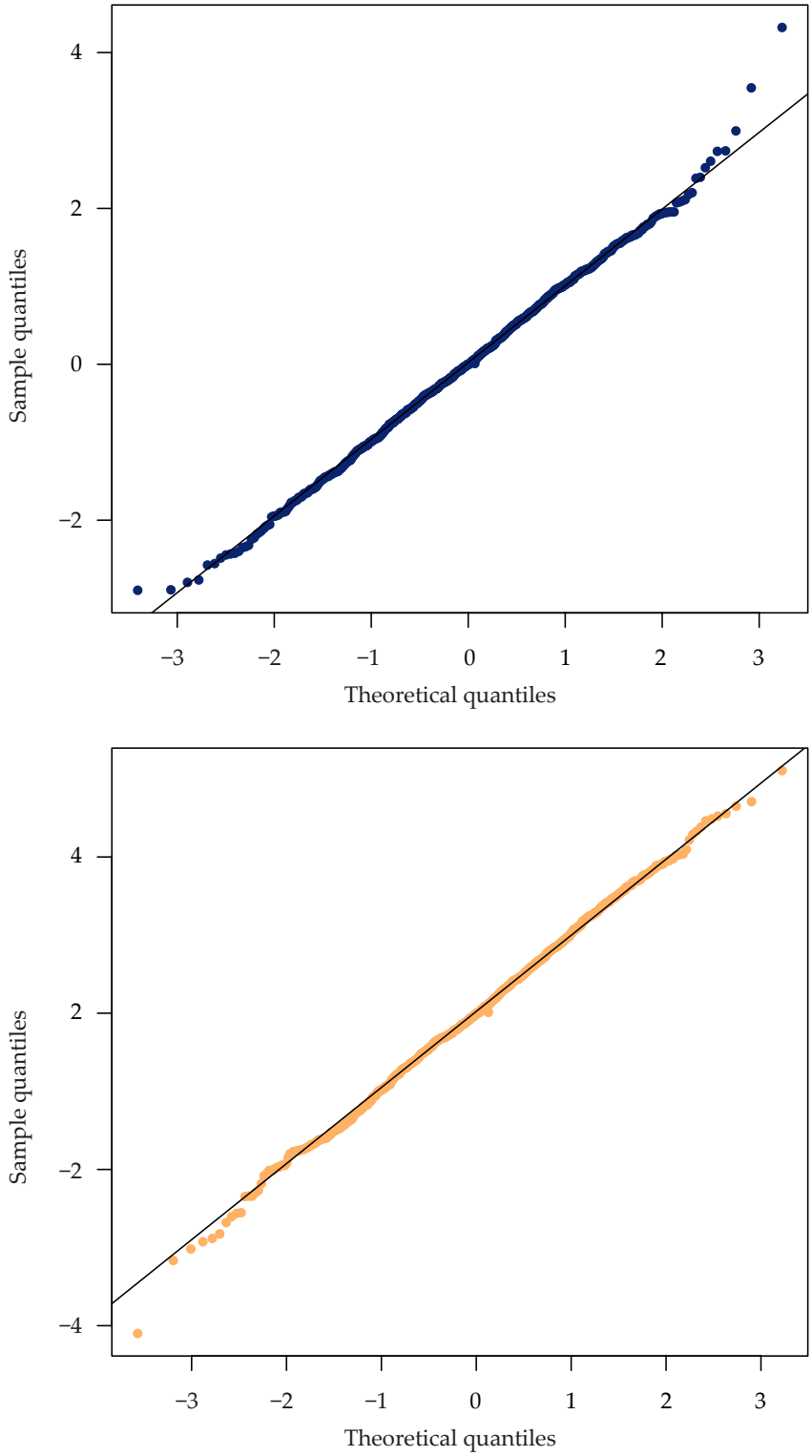

Fig. 2.3. QQ-plots of standardized residuals for the WTI Cushing Crude Oil Spot (top) and the Bloomberg European Dated Brent (bottom).

Table 2.1. Mean values and maximum likelihood estimates together with their corresponding standard errors for the WTI ARMA(0,0)-EGARCH(2,3)-model and the Brent ARMA(1,1)-EGARCH(2,3)-model both including the explanatory variable and the skewed generalized error distribution. All estimates are significant at the 1% level.

Parameter	WTI log-returns		Brent log-returns	
	Estimate	std. error	Estimate	std. error
Mean equation				
μ	0.0003	0.0009	0.0003	0.0008
δ	−0.3216	0.1176	−0.2315	0.0213
θ_1	–	–	−0.7893	0.0035
ψ_1	–	–	0.7641	0.0020
Variance equation				
ω	−0.3438	0.0153	−0.2803	0.0875
α_1	−0.1260	0.0178	−0.1026	0.0237
α_2	−0.1267	0.0172	−0.1076	0.0239
γ_1	0.2458	0.0247	0.1343	0.0269
γ_2	0.2243	0.0216	0.0827	0.0290
β_1	−0.6701	0.0022	−0.7586	0.0880
β_2	0.9745	0.0005	0.9098	0.0184
β_3	0.6494	0.0022	0.8117	0.0894
Distribution				
ξ	0.9580	0.0434	0.9213	0.0432
ν	1.9604	0.1455	1.8725	0.1334

given by $(0.982, 0.966, 0.934)$ for the WTI residuals and $(0.638, 0.667, 0.678)$ for the Brent residuals, respectively. Details on the parameter estimation are provided in Table 2.1.

2.4 Rank-based goodness-of-fit tests

Having modeled the individual time series, we are now able to investigate the dependence structure between the WTI and Brent crude oil log-returns. For this, we first apply a one-level bootstrap-based goodness-of-fit test for copulas (Genest and Rémillard, 2008) which takes the whole support of the joint distribution into account. In a second step we directly estimate the lower tail copula with a multiplier bootstrap along the lines of Bücher and Dette (2013). For an introduction to bootstrap-based goodness-of-fit tests see Stute et al. (1993). The next subsections show how to implement these procedures.

2.4.1 Bootstrap procedures for copulas

There are several rank-based tests of the appropriateness of copula families when modeling the dependence structure between two random variables. Following Genest and Rémillard (2008) we consider an open set $\mathcal{O} \subseteq \mathbb{R}$ and the parametric copula class

$$\mathcal{C} = \{C_\theta \mid \theta \in \mathcal{O}\}.$$

Hence, the test for the null hypothesis that C_θ belongs to a certain parametric class is given by

$$\mathcal{H}_0 \colon C_\theta \in \mathcal{C}, \quad \mathcal{H}_1 \colon C_\theta \notin \mathcal{C}. \tag{2.15}$$

The test statistic sums up the squared deviations between the empirical copula C_T and $C_{\hat{\theta}_T}$, vis.

$$S_T^* = \sum_{t=1}^{T} \left(C_T(u_t, v_t) - C_{\hat{\theta}_T}(u_t, v_t) \right)^2, \tag{2.16}$$

with (u_t, v_t) denoting the rank-based representation of the standardized residuals (X_t, Y_t) from Eq. (2.7).

To compute the optimal parameter estimate $\hat{\theta}_T$ for a given copula family we use a monotone relation between the parameter θ and Kendall's tau, one of the commonly applied rank-based correlation measures (Nelsen, 2006, Chapter 5). For example, in case of all nondegenerated elliptical copulas – in particular the Gaussian and the t-copula – the correlation parameter θ can be calculated by

$$\theta = \sin\left(\tau\pi/2\right). \tag{2.17}$$

For the t-copula we estimate the degrees of freedom ν by maximum likelihood, keeping the correlation parameter θ constant, i.e.,

$$\hat{\nu}_T = \arg\max_{\nu \in (2,\infty)} \sum_{t=1}^{T} \log\left(c_{\theta,\nu}^t(u_t, v_t) \right), \tag{2.18}$$

where $c_{\theta,\nu}^t$ denotes the density of a t-copula with correlation parameter θ and degrees of freedom ν. This method was chosen for its consistency with the other estimators as described above and also because it was found to give very similar estimates to the full maximum likelihood procedure (Demarta and McNeil, 2005). Evaluating the empirical equivalent of Kendall's tau yields $\hat{\tau}_T = 0.705$, and thus $\hat{\theta}_T = 0.895$ and $\hat{\nu}_T = 0.531$, respectively. For comparison only, we find Spearman's rho, another rank-based correlation measure, $\hat{\rho}_T = 0.878$, and Pearson's product-moment correlation coefficient $\hat{r}_T = 0.875$. See Genest and Favre (2007) for a detailed description of these quantities.

Figure 2.4 shows a scatter plot of the 1001 pairs (u_t, v_t) of standardized residuals. It reveals a strong tendency of u_t and v_t (and thus of X_t and Y_t) to vary together, without regarding their marginal distributions. This is not surprising as the log-returns originate from similar types of crude oil. More importantly, we notice that the dependence structure between the two commodities differs clearly from the Fréchet-Hoeffding upper bound, namely $C(u, v) = \min(u, v)$, which would indicate that Y is almost surely an increasing function of X. The latter fact suggests a small opportunity for diversification in the current framework, i.e., reducing the unsystematic risk by investing in a variety of assets.

The following one-level parametric bootstrap-based goodness-of-fit test yields approximated p-values assuming that the copula belongs to the selected parametric copula class. The algorithm (Genest and Rémillard, 2008) proceeds as follows:

1. transform the standardized residuals (X_t, Y_t), $t = 1, \ldots, T$, into their rank-based representation vectors (u_t, v_t), $t = 1, \ldots, T$;

2. evaluate the empirical copula C_T for all rank vectors (u_t, v_t), $t = 1, \ldots, T$:

$$C_T(u_t, v_t) = \frac{1}{T} \sum_{i=1}^{T} \mathbb{1}(u_i \leq u_t, v_i \leq v_t); \tag{2.19}$$

3. compute the optimal parameter estimate $\hat{\theta}_T$ by inversion of the empirical equivalent of Kendall's tau $\hat{\tau}_T$;

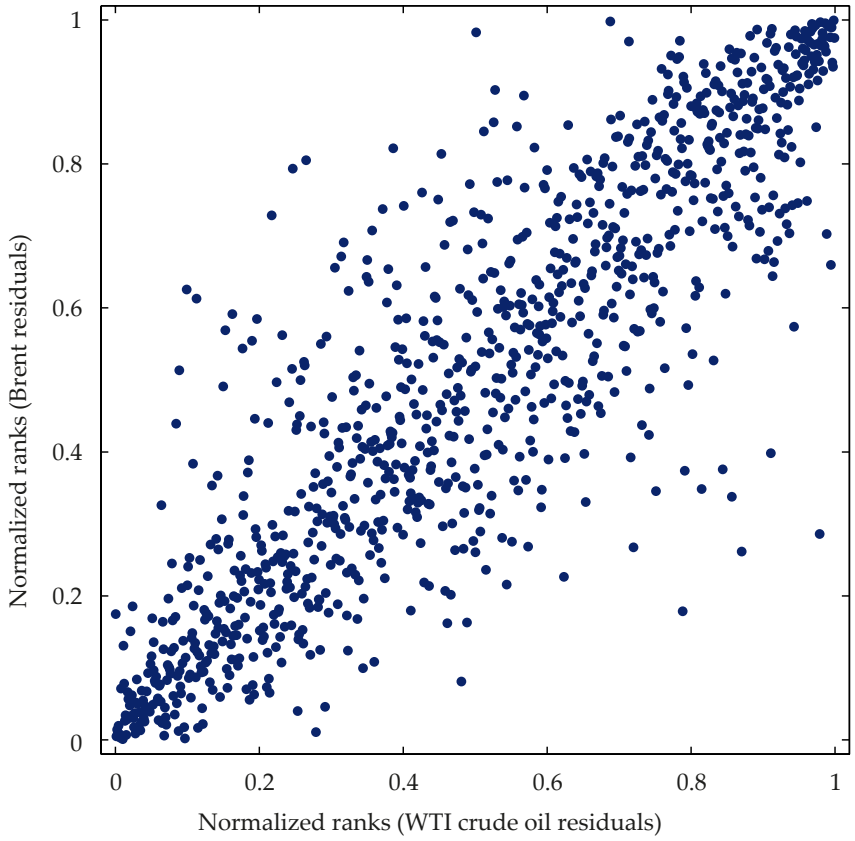

Fig. 2.4. Scatter plot of the rank-based representation of the standardized residuals.

4. calculate S_T^* according to (2.16);
5. choose $N \in \mathbb{N}$ sufficiently large and repeat the next steps for each $k \in \{1, \ldots, N\}$:
   (a) generate a random sample $(X_{k,t}, Y_{k,t})$, $t = 1, \ldots, T$, of the copula $C_{\hat{\theta}_T}$ and compute the corresponding rank vectors $(u_{k,t}, v_{k,t})$ for $t = 1, \ldots, T$;
   (b) evaluate the empirical copula for all simulated rank vectors $(u_{k,t}, v_{k,t})$, $t = 1, \ldots, T$:
   $$C_{k,T}(u_{k,t}, v_{k,t}) = \frac{1}{T} \sum_{i=1}^{T} \mathbb{1}(u_{k,i} \leq u_{k,t}, v_{k,i} \leq v_{k,t}); \tag{2.20}$$
   (c) use the same method as in Step 3 to construct a rank-based estimator $\hat{\theta}_{k,T}$ for θ;
   (d) compute
   $$S_{k,T} = \sum_{t=1}^{T} \left(C_{k,T}(u_{k,t}, v_{k,t}) - C_{\hat{\theta}_{k,T}}(u_{k,t}, v_{k,t}) \right)^2; \tag{2.21}$$
6. calculate
   $$\frac{1}{N} \sum_{k=1}^{N} \mathbb{1}\left(S_{k,T} > S_T^*\right) \tag{2.22}$$
   to obtain an approximated p-value of the goodness-of-fit test.

For an overview of goodness-of-fit tests for copulas see Genest et al. (2009).

2.4.2 Multiplier bootstrap

Initially, let $\hat{\Lambda}_L$ be the empirical lower tail copula of our dataset of standardized residuals (X_t, Y_t), $t = 1, \dots, T$, and Λ_L be an arbitrary lower tail copula. Following Bücher and Dette (2013) we introduce a distance ϱ between $\hat{\Lambda}_L$ and Λ_L by

$$\begin{aligned} \varrho(\hat{\Lambda}_L, \Lambda_L) &:= \int_0^{\pi/2} \left(\hat{\Lambda}_L(\cos\varphi, \sin\varphi) - \Lambda_L(\cos\varphi, \sin\varphi)\right)^2 d\varphi \\ &= \int_0^{\pi/2} \left(\hat{\Lambda}_L^{\swarrow}(\varphi) - \Lambda_L^{\swarrow}(\varphi)\right)^2 d\varphi, \end{aligned} \tag{2.23}$$

where

$$\hat{\Lambda}_L^{\swarrow}(\varphi) = \hat{\Lambda}_L(\cos\varphi, \sin\varphi), \quad \Lambda_L^{\swarrow}(\varphi) = \Lambda_L(\cos\varphi, \sin\varphi).$$

Analytically speaking, ϱ describes the squared distance between the empirical lower tail copula $\hat{\Lambda}_L$ and the arbitrary lower tail copula Λ_L, corresponding to the metric induced by the L^2-norm evaluated on the unit circle in the first quadrant. In the following this set is denoted by $K_+ = \{(\cos\varphi, \sin\varphi) \colon \varphi \in [0, \pi/2]\}$.

For the purpose of estimating the lower tail copula of the time series (X_t, Y_t), $t = 1, \dots, T$, we consider an open set $\mathcal{O} \subseteq \mathbb{R}$ and the one-parameter class $\mathcal{L} = \{\Lambda_L(\cdot;\theta) \mid \theta \in \mathcal{O}\}$. Then, the test for the hypothesis that Λ_L belongs to a certain parametric class is given by

$$\mathcal{H}_0 \colon \Lambda_L \in \mathcal{L}, \quad \mathcal{H}_1 \colon \Lambda_L \notin \mathcal{L}. \tag{2.24}$$

We estimate the optimal parameter θ by applying the minimum distance estimator

$$\hat{\theta}_T = \arg\min_{\theta \in \mathcal{O}} \varrho\left(\hat{\Lambda}_L, \Lambda_L(\cdot;\theta)\right), \tag{2.25}$$

where ϱ denotes the distance defined in (2.23) and $\hat{\Lambda}_L$ the empirical lower tail copula. The reference statistic of the test is given by

$$\begin{aligned} S_T^{*pdm} &:= k\varrho\left(\hat{\Lambda}_L, \Lambda_L(\cdot;\hat{\theta}_T)\right) \\ &= k \int_0^{\pi/2} \left(\hat{\Lambda}_L^{\swarrow}(\varphi) - \Lambda_L^{\swarrow}(\varphi;\hat{\theta}_T)\right)^2 d\varphi. \end{aligned} \tag{2.26}$$

To construct multiplier bootstrap critical values, we introduce i.i.d. nonnegative random variables ξ_t, independent of (X_t, Y_t), $t = 1, \dots, T$, with mean μ in $(0, \infty)$ and finite variance σ^2 which satisfy the regularity condition $\int_0^\infty \sqrt{\mathbb{P}(|\xi_t| > x)}dx < \infty$. A multiplier bootstrap analog of Eq. (2.9) can then be defined by

$$\hat{\Lambda}_L^{\xi}(x, y) := \frac{1}{k} \sum_{t=1}^{T} \frac{\xi_t}{\bar{\xi}_T} \mathbb{1}\left(u_t \leq \frac{kx}{T+1}, v_t \leq \frac{ky}{T+1}\right), \tag{2.27}$$

where $\bar{\xi}_T = T^{-1} \sum_{t=1}^{T} \xi_t$ denotes the mean of $\xi_1, \dots, \xi_T$. As proposed in Bücher and Dette (2013) we will use *Laplacian*$(0, 2)$ multipliers, more precisely, the discrete random variables ξ_t are i.i.d. with probability density function $\mathbb{P}(\xi = 0) = \mathbb{P}(\xi = 2) = 1/2$, which obviously fulfill the aforementioned conditions.

Having determined the multipliers, we are now able to formulate the process

$$\begin{aligned} \beta_T^{pdm}(x, y) &= \frac{\mu}{\sigma} \sqrt{k} \left(\hat{\Lambda}_L^{\xi}(x, y) - \hat{\Lambda}_L(x, y)\right) \\ &= \frac{\mu}{\sigma} \frac{1}{\sqrt{k}} \sum_{t=1}^{T} \left(\frac{\xi_t}{\bar{\xi}_T} - 1\right) \mathbb{1}\left(u_t \leq \frac{kx}{T+1}, v_t \leq \frac{ky}{T+1}\right), \end{aligned} \tag{2.28}$$

which will be part of the partial derivatives multiplier bootstrap (*pdm*-bootstrap) process. Furthermore, following Rémillard and Scaillet (2009), we compute consistent estimates for the partial derivatives of the lower tail copula as follows:

$$\widehat{\partial_x \Lambda_L}(x,y) := \begin{cases} \dfrac{\hat{\Lambda}_L(x+h,y) - \hat{\Lambda}_L(x-h,y)}{2h}, & h \leq x < \infty, \\ \dfrac{\hat{\Lambda}_L(x+2h,y) - \hat{\Lambda}_L(0,y)}{2h}, & x < h, \end{cases} \tag{2.29}$$

where $h \sim k^{-1/2}$ tends to 0 with increasing sample size. For $x = \infty$, we set $\widehat{\partial_x \Lambda_L}(\infty, y) = 0$. In the same vein, we define $\widehat{\partial_y \Lambda_L}(x,y)$. Summing up, this yields the process

$$\begin{aligned} \alpha_T^{pdm}(x,y) = \beta_T^{pdm}(x,y) \\ - \widehat{\partial_x \Lambda_L}(x,y)\beta_T(x,\infty) \\ - \widehat{\partial_y \Lambda_L}(x,y)\beta_T(\infty,y), \end{aligned} \tag{2.30}$$

which only depends on the standardized residuals of the log-return time series and the multipliers $\xi_1, \ldots, \xi_T$.

Finally, let $\delta_\theta(x,y) = \partial_\theta \Lambda_L(x,y;\theta)$ denote the partial derivative of the lower tail copula with respect to $\theta \in \mathcal{O}$. Given some regularity conditions it can be easily shown that this partial derivative function is also homogeneous. The *pdm*-bootstrap statistic is obtained as

$$S_T^{pdm} = \int_0^{\pi/2} \left(\alpha_T^{pdm\angle}(\varphi) - \delta_{\hat{\theta}_T}^{\angle}(\varphi) \int_0^{\pi/2} \gamma_{\hat{\theta}_T}(\varphi) \alpha_T^{pdm\angle}(\varphi) d\varphi \right)^2 d\varphi, \tag{2.31}$$

where

$$\gamma_{\hat{\theta}_T}(\varphi) = \hat{A}_{\hat{\theta}_T}^{-1} \delta_{\hat{\theta}_T}^{\angle}(\varphi), \quad \alpha_T^{pdm\angle}(\varphi) = \alpha_T^{pdm}(\cos\varphi, \sin\varphi)$$

and

$$\hat{A}_{\hat{\theta}_T} := \int_0^{\pi/2} \left(\delta_{\hat{\theta}_T}^{\angle}(\varphi) \right)^2 d\varphi, \quad \delta_{\hat{\theta}_T}^{\angle}(\varphi) = \delta_{\hat{\theta}_T}(\cos\varphi, \sin\varphi). \tag{2.32}$$

Note that we only consider one-parameter families of tail copulas and therefore Eq. (2.32) is also one-dimensional. For a detailed description of the required regularity conditions and a more theoretical view see Bücher and Dette (2013).

The following goodness-of-fit test based on the partial derivatives multiplier bootstrap (Bücher and Dette, 2013) yields approximated p-values assuming that the respective lower tail copula has a specific parametric form. The detailed algorithm proceeds as follows:

1. transform the standardized residuals (X_t, Y_t), $t = 1, \ldots, T$, into their rank-based representation vectors (u_t, v_t), $t = 1, \ldots, T$;
2. discretize the unit circle in the first quadrant K_+ and choose the parameter k in relation to the sample size T for calculating the empirical tail copula $\hat{\Lambda}_L^{\angle}(\varphi)$ according to (2.9);
3. for the purpose of evaluating the reference statistic (2.26) compute the optimal parameter estimate $\hat{\theta}_T$ by applying the minimum distance estimator (2.25);
4. to prepare for the next steps estimate the partial derivatives of the selected lower tail copula via (2.29) and approximate (2.32) using central difference quotients, if applicable;

5. choose $N \in \mathbb{N}$ sufficiently large and repeat the next steps for each $j \in \{1, \dots, N\}$:
   (a) generate a random sample $\xi_{j,1}, \dots, \xi_{j,T}$ of the random variables $\xi_1, \dots, \xi_T$ as described above;
   (b) compute the statistics $\alpha_{j,T}^{pdm} = \alpha_T^{pdm}(\xi_{j,1}, \dots, \xi_{j,T})$ for every $(x, y) \in K_+$ using the updated multiplier bootstrap analog of the empirical lower tail copula (2.27), the evaluated process β_T^{pdm} from Eq. (2.28) and the calculated partial derivatives from Step 4;
   (c) evaluate

$$S_{j,T}^{pdm} = \int \left(\alpha_{j,T}^{pdm\angle}(\varphi) - \delta_{\hat{\theta}_T}^{\angle}(\varphi) \int \gamma_{\hat{\theta}_T}(\varphi) \alpha_{j,T}^{pdm\angle}(\varphi) d\varphi \right)^2 d\varphi$$

   according to (2.31);

6. calculate

$$\frac{1}{N} \sum_{j=1}^{N} \mathbb{1} \left(S_{j,T}^{pdm} > S_T^{*pdm} \right) \tag{2.33}$$

   to obtain an approximated p-value of the goodness-of-fit test.

2.5 Empirical results

The following subsections provide guide on how to implement the methodology above. First, we apply the parametric bootstrap-based goodness-of-fit test to suitable classes of copulas. Having rejected certain copula models according to a predefined level of significance, we use a newly introduced information criterion for copulas to find the best fit to the crude oil log-returns. In a second step a closed-form expression of the lower tail copula is derived and several possibly suitable one-parametric models are presented. The results of the goodness-of-fit test based on the partial derivatives multiplier bootstrap finalize the tail copula fit.

2.5.1 Copula selection

The goodness-of-fit test from Section 2.4.1 requires a preselection of possible one-parametric copula classes. The structure of the scatter plot in Fig. 2.4 suggests to limit the range to symmetric copulas, i.e., $C(u, v) = C(v, u)$ for all (u, v) in $[0, 1]^2$. In addition to two elliptical copulas, Gaussian and t, we fit the widely used Plackett copula and three Archimedean copulas. Within the latter class we choose the Frank family and two relatively unknown strict copulas from (4.1.12) and (4.1.14) in Nelsen (2006), Table 4.1, with corresponding functions given by

$$C_\theta(u, v) = \left(1 + \left[(u^{-1} - 1)^\theta + (v^{-1} - 1)^\theta \right]^{1/\theta} \right)^{-1} \tag{2.34}$$

and

$$C_\theta(u, v) = \left(1 + \left[(u^{-1/\theta} - 1)^\theta + (v^{-1/\theta} - 1)^\theta \right]^{1/\theta} \right)^{-\theta}, \tag{2.35}$$

respectively, $\theta \in [1, \infty)$. Both copulas share the same limit case $C_\infty = \min(u, v)$, which is not Archimedean anymore.

Table 2.2. Test results ($N = 2000$ bootstrap iterations) for the goodness-of-fit of different copula models in ascending order (p-value).

Copula	p-value	$\hat{\theta}_T$-value
Frank	0.000	11.649
(4.1.14)	0.001	2.891
Plackett	0.012	47.150
Gaussian	0.052	0.895
(4.1.12)	0.065	2.261
t ($\hat{\nu}_T = 5.313$)	0.074	0.895

Table 2.3. Cross-validation Copula Information Criterion values for the remaining copula models in ascending order (CIC-value).

Copula	CIC-value	$\hat{\theta}$-value	$\ell_T(\hat{\theta})$-value
Gaussian	1454	0.877	729.75
(4.1.12)	1471	2.088	743.61
t ($\hat{\nu} = 5.101$)	1522	0.880	764.36

Table 2.2 summarizes the results (p-values) of the goodness-of-fit tests for the above mentioned copula classes together with their estimated optimal parameter $\hat{\theta}_T$. For the Plackett copula, where no explicit expression for the parameter θ is available, we apply penalized splines to approximate the function $\theta(\tau)$ using an appropriately chosen grid of θ values (Kojadinovic and Yan, 2010). Figure 2.5 presents scatter plots of $n = 1001$ sampling points from simulations for all copula families under consideration, $\hat{\theta}_T$ as listed in Table 2.2. From these scatter plots alone it is nearly impossible to draw definite conclusion about the goodness-of-fit.

The results of the parametric bootstrap procedure indicate that neither the Frank family nor the copula $(4.1.14)$, and to a great extent, the Plackett copula seem to be appropriate to model the dependence structure between the residuals of the crude oil log-returns. On the contrary, at a 5% level of significance, the null hypothesis cannot be rejected for any of the remaining three candidates. At this point we emphasize – as the actual investigation focuses on the behavior of joint extreme events – that it is fairly unlikely to achieve p-values higher than 10%, while, at the same time, not trimming or winsorizing the original data in order to mitigate the effects of (marginal) extreme outliers.

However, as the p-values are 'only' inverse measures of the strength of evidence against the null hypothesis $\mathcal{H}_0$, we need to select the most appropriate model from the remaining candidates. Following Grønneberg and Hjort (2014), we implement the generally applicable cross-validation Copula Information Criterion for the left three copula families. In contrast to the common used formula AIC $= 2\ell_{T,\max} - 2$, where $\ell_{T,\max}$ is defined as the maximizer of the pseudo likelihood $\ell_T(\theta) = \sum_{t=1}^{T} \log\left(c_\theta(u_t, v_t)\right)$, the cross-validation CIC corrects for finite-sample bias introduced by the rank-based nonparametric modeling of the marginals. For a more detailed view on the different model selection criteria see Claeskens and Hjort (2008).

Table 2.3 shows the maximum pseudo likelihood estimate together with its corresponding likelihood and the cross-validation Copula Information Criterion value. Using the maximal CIC-value as a criterion to select the model with the best fit to the data, we conclude that the t-copula, with correlation parameter $\hat{\theta}_T = 0.895$ and degrees of freedom $\hat{\nu}_T = 5.313$, best describes the dependence between the WTI and Brent crude oil log-returns. Note that in this case evaluating the frequently applied AIC formula would lead to the same decision. In addition, when leaving the symmetric setting, further re-

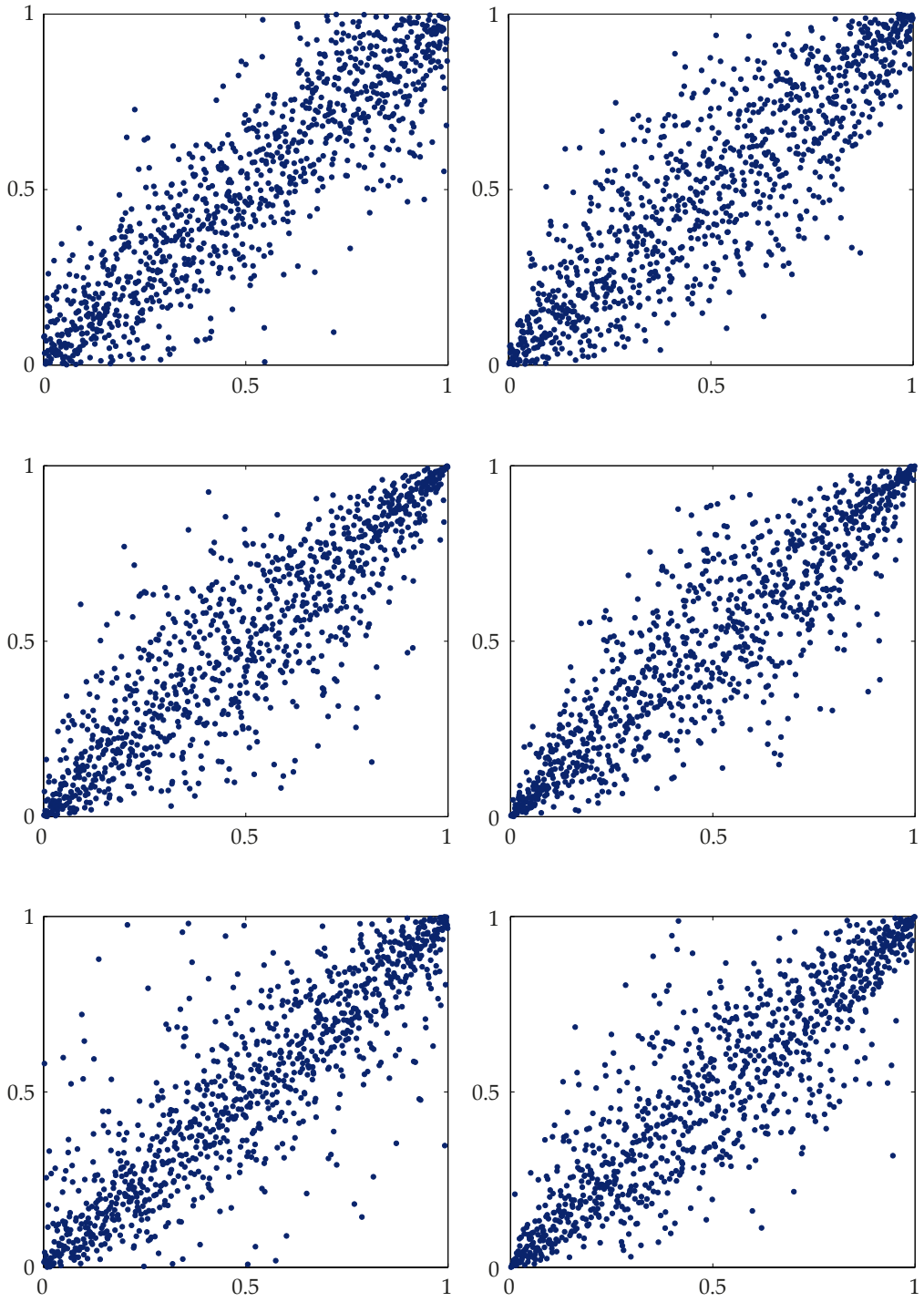

Fig. 2.5. Simulation of Frank copula (top left), copula (4.1.14) (center left), Plackett copula (bottom left), Gaussian copula (top right), copula (4.1.12) (center right) and t-copula (bottom right).

search might extend the present paper by analyzing a skewed version of the t-copula (Smith et al., 2012) which can capture asymmetric and extremal dependence at the same time.

2.5.2 Tail copula fit

Implementing the goodness-of-fit test for tail copulas described in Section 2.4.2 requires some background. In order to derive a closed-form expression of the lower tail copula (in contrast to the limit definition in Eq. (2.4)), let (U, V) be a random vector with uniformly distributed margins on the interval $[0, 1]$ and joint distribution

$$C_A(u, v) = \exp\left(\log(uv) A\left(\frac{\log(v)}{\log(uv)}\right)\right), \tag{2.36}$$

where $A\colon [0,1] \to [1/2, 1]$ is called Pickands dependence function. C_A can be identified with the class of extreme-value copulas which arise naturally as limits of copulas of componentwise maxima in independent random samples and provide a convenient framework for modeling the dependence structure between extreme events (see Gudendorf and Segers, 2010). Following Pickands (1981) the extreme-value copula $C_A(u, v)$ is a copula if and only if the function $A\colon [0,1] \to [1/2, 1]$ is a convex function which satisfies $\max(t, 1-t) \leq A(t) \leq 1$. Next, it can be shown that the joint distribution of the random vector $(1-U, 1-V)$ is given by the survival copula

$$\bar{C}_A(u, v) = u + v - 1 + C_A(1-u, 1-v). \tag{2.37}$$

From the homogeneous structure of the lower tail copula in Eq. (2.5) it is sufficient to consider the restriction of these functions to the unit simplex $\Delta_1 = \{(u, v) \in [0,1]^2 : u + v = 1\}$ (see Segers, 2012b). By substituting Eq. (2.37) in Eq. (2.4) and applying l'Hôpital's rule, a tedious but straightforward calculation yields

$$\Lambda_L(1-x, x) = \lim_{t \searrow 0} \frac{\bar{C}_A(t(1-x), tx)}{t} = 1 - A(x) \tag{2.38}$$

for the lower tail copula of the random vector $(1-U, 1-V)$. Finally, by renaming variables and the homogeneity property the entire lower tail copula can be obtained as $\Lambda_L(1-t, t) = 1 - A(t)$ with Pickands dependence function $A(t)$. The latter implies the existence of a one-to-one and onto relationship between lower tail copulas and Pickands dependence functions.

Consequently, the next part focuses on different classes of Pickands dependence functions. The structure of the empirical estimate $\hat{\Lambda}_L$, see Eq. (2.9), evaluated on the unit circle in the first quadrant and displayed in Fig. 2.6, suggests to limit the range to symmetric lower tail copulas. Below, we seek to cover a spectrum as wide as possible via

(i) the logistic or Gumbel model (Gumbel, 1960), defined by

$$\Lambda_L(1-t, t) = 1 - \left((1-t)^\theta + t^\theta\right)^{1/\theta}, \quad \theta \in [1, \infty),$$

which belongs, among others, to the survival copula of the well-known Gumbel-Hougaard copula,

(ii) the negative logistic or Galambos model (Galambos, 1975), given by

$$\Lambda_L(1-t, t) = \left((1-t)^{-\theta} + t^{-\theta}\right)^{-1/\theta}, \quad \theta \in (0, \infty),$$

that is the lower tail copula of, among others, the Clayton copula, the survival copula of the Galambos copula and the copula family (4.1.12),

(iii) the mixed model (Tawn, 1988), defined by

$$\Lambda_L(1-t,t) = \theta(1-t)t, \quad \theta \in [0,1],$$

which constitutes the complete class of quadratic functions for differentiable parametric models; in the case $\theta = 1$, Λ_L belongs, among others, to the copula family (4.1.14),

(iv) the Hüsler-Reiss model (Hüsler and Reiss, 1989), vis.

$$\begin{aligned}\Lambda_L(1-t,t) = 1 - (1-t)\Phi\left(\theta + \frac{1}{2\theta}\log\left(\frac{1-t}{t}\right)\right) \\ - t\Phi\left(\theta + \frac{1}{2\theta}\log\left(\frac{t}{1-t}\right)\right), \quad \theta \in (0,\infty),\end{aligned}$$

with Φ denoting the standard normal distribution function; Λ_L is, among others, the lower tail copula of the survival copula of the Hüsler-Reiss copula.

Note that the list does not contain the well-known class of t-extreme-value copulas C_A^t, (see Demarta and McNeil, 2005). Following their remarks the correspondent Pickands dependence function is not particularly convenient for practical application. Demarta and McNeil (2005) show empirically that for each fixed (θ, ν) in the t-model there exists a parameter θ from either the Gumbel or the Galambos model such that the resulting curves are indistinguishable.

Referring back to the applied copula models in Section 2.5.1 and digressing, the relationship between the lower tail copula of the t-copula and the t-extreme-value copula can be obtained as:

$$\begin{aligned}\Lambda_L^t(1-s,s) &= \log\left(C_A^t\left(e^{-(1-s)}, e^{-s}\right)\right) \\ &= 1 - A(s) \quad s \in [0,1].\end{aligned} \tag{2.39}$$

The latter can be proven (also in a general setting) by using the natural definition of extreme-value copulas (Gudendorf and Segers, 2010), applying the Taylor expansion and finally, considering the identity $\widehat{C} = C$ for radially symmetric copulas (Nelsen, 2006). Equation (2.39) shows that, in order to avoid the complexity of the univariate t-distribution, the lower tail copula of the t-copula can again be accurately approximated by the simpler Gumbel or Galambos models. Furthermore, neither the Frank copula nor the Plackett copula nor the Gaussian copula allow for lower tail dependence and thus $\Lambda_L(x,y) = 0$ for all $(x,y) \in \mathbb{E}$.

Care should be taken when implementing the derivatives multiplier bootstrap with respect to the different applied norms. Whereas the Pickands dependence functions are defined within the L^1-norm framework, the minimum distance estimator in Eq. (2.25) is formulated using the L^2-norm. Furthermore, the transformation of the radian coordinate $\varphi \in [0, \pi/2]$ to $t \in [0,1]$ can be obtained by $t = \tan(\varphi)/(1+\tan(\varphi))$. In the specific situation of estimating tail dependence, Frahm et al. (2005) use plots of the function $k \mapsto \mathrm{TDC}(k)$ to define a plateau-finding algorithm that provides a single data-adaptive choice of k. Here, we graphically search for a value k^* such that the tail dependence coefficient (TDC), as a function of k^*, is as constant as possible in a suitable neighborhood of k^*. In combination with appealing finite sample coverage probabilities in Bücher and

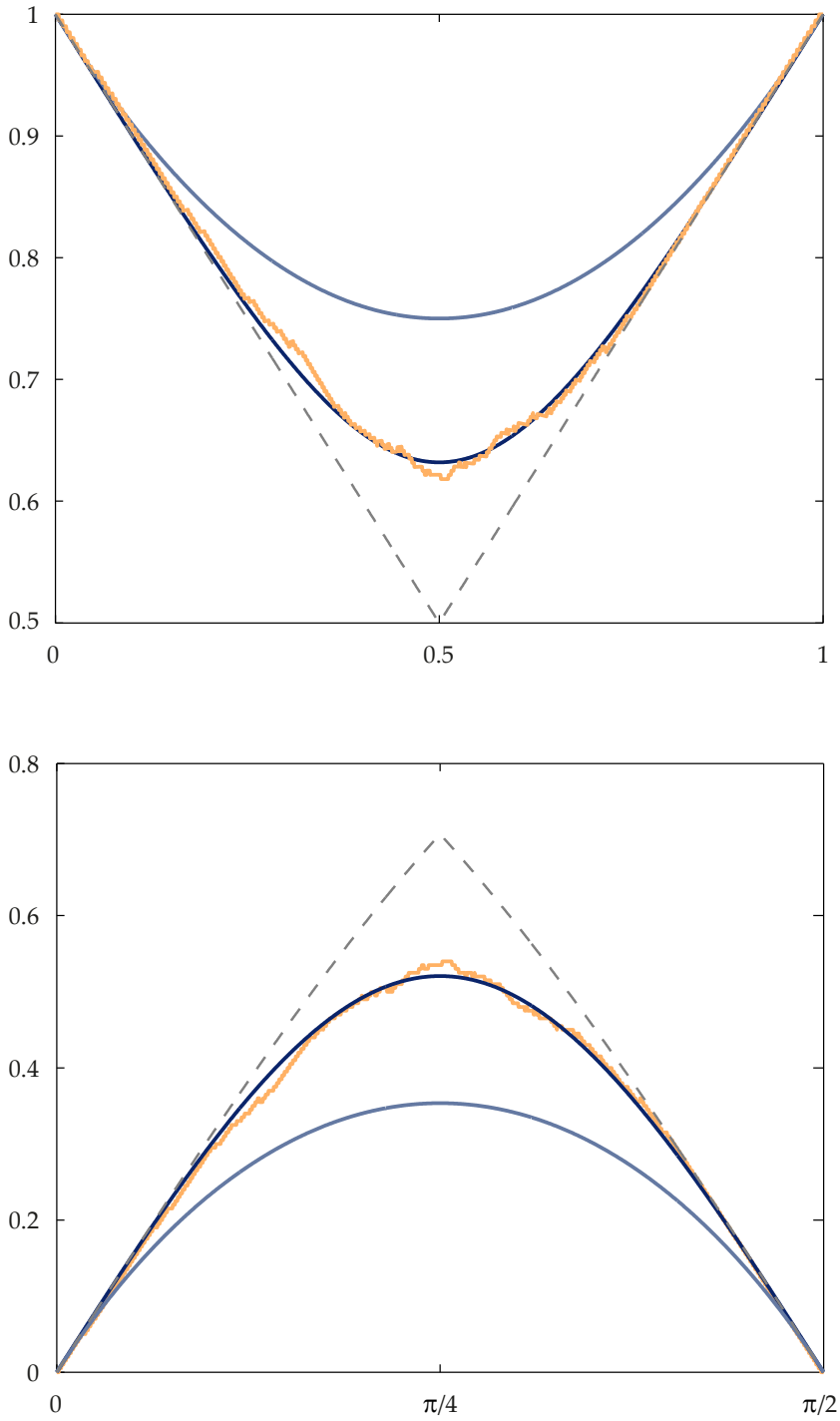

Fig. 2.6. Plot of the empirical lower tail copula $\hat{\Lambda}_L$ (yellow), Gumbel model (blue line), mixed model (light blue) and the overall range (grey dashed line) for both the Pickands framework (top) and the tail copula approach (bottom).

Table 2.4. Test results ($N = 10\,000$ bootstrap iterations) for the derivatives multiplier bootstrap of different lower tail copulas in ascending order (p-value).

Model	p-value	$\hat{\theta}_T$-value	$\hat{\lambda}_L(\hat{\theta}_T)$-value
Mixed	0.000	1.000	0.500
Hüsler-Reiss	0.146	0.343	0.732
Galambos	0.242	2.251	0.735
Gumbel	0.290	2.961	0.736

Dette (2013) we decide to take the value $k^* = 200$ for the subsequent analysis. The results of this computationally efficient goodness-of-fit test for tail copulas based on the partial derivatives multiplier bootstrap are summarized in Table 2.4. In addition to the p-value, the table lists the minimum distance estimator $\hat{\theta}_T$ and the estimated lower tail dependence coefficient $\hat{\lambda}_L(\hat{\theta}_T)$, which is obtained by evaluating the lower tail copula at the point $t = (1/2, 1/2)$ multiplied with the factor $\sqrt{2}$.

While the mixed model is definitely not appropriate for the joint behavior in the lower tails, the null hypothesis, at a 5% level of significance, cannot be rejected for any of the remaining three candidates. We decide to use the smallest distance between the empirical lower tail dependence coefficient $\hat{\lambda}_L = 0.757$ and the estimated lower tail dependence coefficient $\hat{\lambda}_L(\hat{\theta}_T)$ as criterion to select the model with the best fit to the data in the lower tails, which turns out to be the logistic or Gumbel model with $\hat{\theta}_T = 2.961$. Note that both the Hüsler-Reiss and the Galambos models also seem appropriate to model the structure of the lower tail dependence.

Although the lower tail copula of the t-copula can be accurately approximated with the Gumbel model, it is a far cry from saying that the joint dynamics in the lower tail of the t-copula ($\hat{\theta}_T = 0.895$, $\hat{\nu}_T = 5.313$) from Section 2.5.1 are identical to the corresponding behavior of the Gumbel model ($\hat{\theta}_T = 2.961$). This can be explained by the completely different ways of estimating the model parameters in both subsections. When comparing, for instance, the lower tail dependence coefficient we find $\hat{\lambda}_L = 0.575$ for the t-copula and $\hat{\lambda}_L = 0.736$ for the Gumbel model. Figure 2.6 shows the plot of the empirical lower tail copula $\hat{\Lambda}_L$, the selected Gumbel model, the unsuitable mixed model and the overall range for both the Pickands framework and the tail copula setting.

2.6 Risk measures and backtesting

With oil being an integral part of commodity portfolios the question arises how one can obtain an (additional) diversification effect by splitting an oil proportion of a portfolio to WTI and Brent crude oil (cf. Section 2.4.1, Page 15). Taking this into account and returning to the initial intention, having selected both the copula and tail copula model, we are now interested in the risk measurement of a portfolio consisting of an arbitrary convex combination of the WTI and Brent crude oil. For this purpose, we simulate the common risk parameters Value-at-Risk and Expected Shortfall. According to Jorion (2006) the Value-at-Risk summarizes the worst loss over a target horizon that will not be exceeded with a given level of confidence, or more formally, it describes the quantile of the projected distribution of gains or losses over the target horizon. If α is the selected level of confidence, the Value-at-Risk corresponds to the $1 - \alpha$ lower tail level. Extending this concept, the Expected Shortfall (also known as Conditional Value-at-Risk) for a given level of confidence α is defined as the expected loss, given the loss is larger or equal to the Value-at-Risk (Deutsch, 2009).

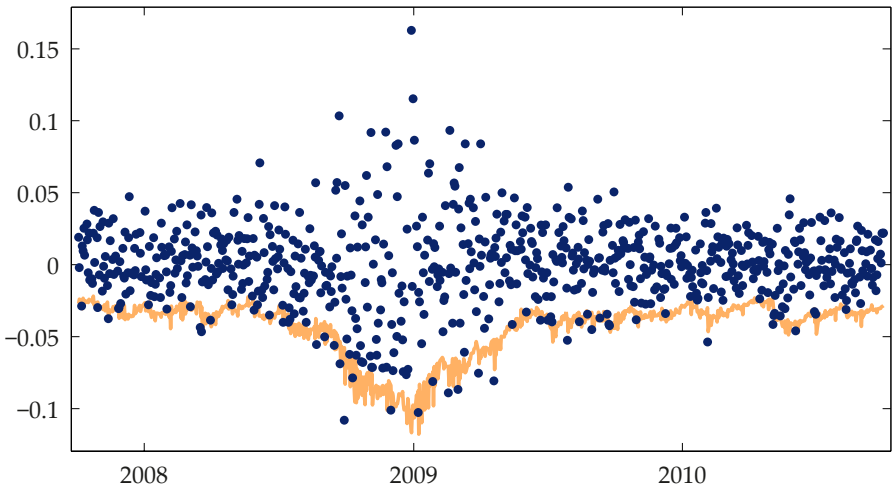

Fig. 2.7. In sample one day-ahead simulated portfolio ($\omega_1 = \omega_2 = 0.5$) Value-at-Risk for a given level of confidence $\alpha = 95\%$ for the Gumbel model (yellow) and the realized (observed) returns (blue).

Following Rank and Siegl (2002) we first generate n pairs (u, v) of observations of $U(0,1)$ distributed random variables U and V whose joint distribution function is either given by the t-copula ($\hat{\theta}_T = 0.895$, $\hat{\nu}_T = 5.313$) from Section 2.5.1 or the survival copula of the Gumbel copula ($\hat{\theta}_T = 2.961$) from Section 2.5.2. The simulation is carried out using the functionality of Kojadinovic (2010) and Yan (2007). To obtain the required marginal distributions we apply the inverse distribution functions, estimated in Section 2.3, to the sample (u, v). Accordingly, the n obtained pairs (x_i, y_i), $i = 1, \ldots, n$, form scenarios of possible logarithmic changes of the two crude oil grades, while at the same time having preserved the desired dependence structure.

For the purpose of simulating the Value-at-Risk we consider a simple linear portfolio position with weighting factors $\omega_1, \omega_2 \in [0,1]$ and $\omega_2 = 1 - \omega_1$. The change a_t of the (simulated) portfolio at time t is given by

$$a_t = \omega_1 W_t + \omega_2 B_t, \tag{2.40}$$

where the univariate WTI crude oil model W_t is described in Eq. (2.13) and the Brent analog B_t in Eq. (2.14), respectively. To sum up, the applied Monte Carlo method generates n scenarios for each day t and evaluates the present value change of a portfolio under each scenario. Finally, calculating the $1 - \alpha$ quantile yields the daily Value-at-Risk with level of confidence α. Note that within a nonrolling target horizon framework, and having once modeled the univariate time series, the only remaining task is to simulate the standardized residuals (x_i, y_i), $i = 1, \ldots, n$, and substitute these values into the corresponding model equation.

Figure 2.7 shows the in sample one day-ahead simulated portfolio ($\omega_1 = \omega_2 = 0.5$) Value-at-Risk for a given level of confidence $\alpha = 95\%$ for the estimated Gumbel model in combination with the realized (observed) returns (quod vide Palaro and Hotta, 2006). To be able to judge the effectiveness of the applied Value-at-Risk model, we compare the simulated (predicted) and empirical number of outliers, where the actual loss exceeds the Value-at-Risk (Rank and Siegl, 2002). Consequently, from a risk management point of view, this backtesting approach is easily comprehensible and allows for the required transparency. To benchmark the simulated Value-at-Risk with a fully deterministic approach we apply historical simulation. The freedom from model assumptions is one of

Table 2.5. Relative number (absolute number) of backtest outliers $1-\hat{\alpha}$ for the different applied Value-at-Risk simulations with level of confidence $1-\alpha$, weighted average error $|\hat{\alpha}-\alpha|$ and error ranking.

$1-\alpha$	ω_1	ω_2	t-copula	Gumbel	Historical
0.050	0.50	0.50	0.059 (44)	0.056 (42)	0.067 (50)
0.025	0.50	0.50	0.021 (16)	0.021 (16)	0.052 (39)
0.010	0.50	0.50	0.008 (06)	0.008 (06)	0.021 (16)
0.050	0.25	0.75	0.056 (42)	0.055 (41)	0.063 (47)
0.025	0.25	0.75	0.017 (13)	0.019 (14)	0.048 (36)
0.010	0.25	0.75	0.011 (08)	0.009 (07)	0.025 (19)
0.050	0.75	0.25	0.056 (42)	0.055 (41)	0.069 (52)
0.025	0.75	0.25	0.027 (20)	0.024 (18)	0.045 (34)
0.010	0.75	0.25	0.011 (08)	0.011 (08)	0.016 (12)
0.050	**Average**		0.007	0.005	0.016
0.025	**Average**		0.005	0.004	0.023
0.010	**Average**		0.001	0.001	0.011
Average	**Average**		0.003	0.002	0.015
	Ranking		2	1	3

the primary advantages of this method (Deutsch, 2009). Based on the given time series and the target horizon of $T = 250$ business days we compute 751 daily Value-at-Risk estimates for the confidence level vector α_i ($\alpha_1 = 95\%, \alpha_2 = 97.5\%, \alpha_3 = 99\%$). Note that the latter approach takes a rolling dataset of 250 (observed) values (for each one day-ahead estimated Value-at-Risk) into account whereas the Value-at-Risk simulations via copulas depend on the entire considered time horizon. Consequently, a comparison between the applied models is only of limited use.

Table 2.5 summarizes the results of the backtesting for the set of scenarios $w_{1,i}$ ($\omega_{1,1} = 0.50$, $\omega_{1,2} = 0.25$, $\omega_{1,3} = 0.75$) with a given level of confidence α. Following Rank and Siegl (2002) we define the prediction error as the absolute difference between the relative number of outliers $1-\hat{\alpha}$ and the predicted relative number $1-\alpha$. While the average over the portfolios uses equal weights, the average over the level of confidence α emphasizes the tails by a weighting scheme β_i ($\beta_1 = 1, \beta_2 = 2, \beta_3 = 5$). The Value-at-Risk simulation via copulas is carried out generating $n = 100\,000$ samples of pairs (u, v). As expected, the tail copula fit from Section 2.5.2 yields the best result, whereas both the t-copula and the survival copula of the Gumbel copula obviously outperform the historical simulation. The latter should be regarded with caution as outlined before. Furthermore, although the Gumbel model yields a slightly better result than the t-copula, both models seem to pass the backtesting stage.

To further verify the validity of the t-copula and the Gumbel model we apply the traffic light approach used by the supervising authorities when auditing banks' internal risk management models (Deutsch, 2009). For this, a confidence interval for the observed outliers has to be constructed. It is quite obvious to assume that the number of outliers follows a binomially distributed random variable with probability $p = 1-\alpha$ and number of trials n. Within this framework the probability of observing more than k outliers is

$$1 - \sum_{i=0}^{k} B_{n,p}(i) = \sum_{i=k+1}^{n} \binom{n}{i} p^i (1-p)^{n-i}. \tag{2.41}$$

This is equal to the probability of making a type-I-error (the rejection of a correct model) when the hypothesis is rejected if more than k outliers are observed. Based on this prob-

Table 2.6. Average relative error between the observed outliers and the Expected Shortfall for the different applied Expected Shortfall simulations with level of confidence $1-\alpha$, weighted averages and error ranking.

$1-\alpha$	ω_1	ω_2	t-copula	Gumbel	Historical
0.050	0.50	0.50	0.141	0.144	0.235
0.025	0.50	0.50	0.129	0.131	0.284
0.010	0.50	0.50	0.056	0.061	0.374
0.050	0.25	0.75	0.168	0.170	0.261
0.025	0.25	0.75	0.138	0.135	0.298
0.010	0.25	0.75	0.097	0.087	0.548
0.050	0.75	0.25	0.140	0.142	0.353
0.025	0.75	0.25	0.111	0.108	0.415
0.010	0.75	0.25	0.056	0.057	0.282
0.050	**Average**		0.150	0.152	0.283
0.025	**Average**		0.126	0.125	0.332
0.010	**Average**		0.070	0.068	0.401
Average	**Average**		0.094	0.093	0.369
	Ranking		2	1	3

ability the supervising authorities establish the boundaries for three different zones, i.e., a lower bound of the red zone (equals the upper bound of the yellow zone) for a type-I-error of less than 0.01% and a lower bound of the yellow zone (equals the upper bound of the green zone) for a type-I-error less than 5%. For $p = 1 - 0.95 = 0.05$ and $n = 751$ this translates into the following intervals as a function of realized outliers k

$$f(k) = \begin{cases} \text{green zone}, & k \leq 47, \\ \text{yellow zone}, & 48 \leq k \leq 61, \\ \text{red zone}, & k \geq 62. \end{cases} \tag{2.42}$$

Table 2.5 clearly shows that both models (for each type of portfolio weighting) are in the green zone and thus no adjustments are necessary. Completely analogous calculations yield the same results for the cases $\alpha = 0.025$ and $\alpha = 0.01$. The previous implementation being in line with reporting the unconditional coverage due to Kupiec (1995) we are now interested in the analysis of the conditional coverage (Christoffersen, 1998), namely testing the joint hypothesis that the Value-at-Risk model has the right frequency of *independent* outliers. Here as well, the p-values of the latter null hypothesis clearly exceed the 10% threshold.

Having assessed the Value-at-Risk for a given level of confidence α it is straightforward to estimate the corresponding Expected Shortfall, i.e., averaging the $(1-\alpha)$-quantile. Table 2.6 lists the average relative errors between the observed outliers and the Expected Shortfall based on the full backtesting period (751 days). Note that here the absolute values of the relative errors are taken into account. Finally, the concluding averages use the same weights as in the Value-at-Risk approach. As it can be seen from Table 2.6, the results are consistent with the previous Value-at-Risk measures. Here as well, the Gumbel model yields the overall best result having in mind that the t-copula results are very close. For the sake of completeness, the historical simulation shows the worst fit.

2.7 Concluding remarks

This paper studies the dependence structure of log-returns of two crude oil grades, namely the WTI Cushing Crude Oil Spot and the Bloomberg European Dated Brent, from a probabilistic point of view. The investigation focuses on lower tail dependence, i.e., on assessing the probability that large losses occur together. As a rough but not exhaustive indicator (see Jäschke et al., 2012), the lower tail dependence coefficient is estimated as the value of the empirical lower tail copula at the point $(1, 1)$ (Schmidt and Stadtmüller, 2006). The resulting estimate $\hat{\lambda}_L = 0.757$ reveals a relatively high level of lower tail dependence.

The empirical analysis can be summarized as follows: the overall dependence between the log-returns sample of the two crude oil grades can be adequately described by a t-copula. When directly modeling the joint dynamics in the lower tail via tail copulas the Gumbel model performs best. Here, for the first time in the literature, the partial derivatives multiplier goodness-of-fit test for tail copulas (Bücher and Dette, 2013) is applied to energy portfolios.

From a risk management perspective it is crucial to backtest the findings using commonly applied risk measures. Therefore, the present paper simulates the Value-at-Risk and Expected Shortfall for both models and compares the results for different portfolio weights and certain levels of confidence (Rank and Siegl, 2002). As suspected and confirmed by the backtesting the Gumbel model slightly outperforms the t-copula. Finally, the traffic light approach verifies the validity of both the Gumbel model and the t-copula.

The present article focuses on studying downside risk, mainly relevant for investors holding long positions. Further research might also examine upper tail dependence between the two crude oil grades, i.e., assessing the upside risk being inherited in short positions. Based on this, strategies of hedging and effective risk mitigation could be developed.

Chapter 3

Nonparametric tests for constant tail dependence with an application to energy and finance

Abstract

New tests for detecting structural breaks in the tail dependence of multivariate time series using the concept of tail copulas are presented. To obtain asymptotic properties, we derive a new limit result for the sequential empirical tail copula process. Moreover, consistency of both the tests and a break-point estimator are proven. We analyze the finite sample behavior of the tests by Monte Carlo simulations. Finally, and crucial from a risk management perspective, we apply the new findings to datasets from energy and financial markets.

3.1 Introduction

Modeling and estimating stochastic dependencies has attracted increasing attention over the last decades in various fields of applications, including mathematical finance, actuarial science or hydrology, among others. Of particular interest, especially in risk management, is a sensible quantitative description of the dependence between extreme events, commonly referred to as tail dependence; see for example Embrechts et al. (2003). A formal definition of this concept is given in Section 3.2.

In applications, tail dependence is often assessed by fitting a parametric copula family to the data and by subsequently extracting the tail behavior of that particular copula. Examples can be found in Breymann et al. (2003) and Malevergne and Sornette (2003), among others. Fitting the copula typically requires some sort of goodness-of-fit testing. Recent reviews on these methods are given by Genest et al. (2009) and Fermanian (2013). More robust methods to assess tail dependence are based on the assumption that the underlying copula is an extreme-value copula. The class of these copulas can be regarded as a nonparametric copula family indexed by a function on the unit simplex (Gudendorf and Segers, 2010). Since the copula is a rather general measure for stochastic dependence, the estimation techniques for both of the latter approaches are usually based on the entire available dataset (see, for instance, Genest et al. (1995); Chen and Fan (2006) for parametric families or Genest and Segers (2009) for extreme-value copulas). However, due to the fact that the center of a distribution does not contain any information about the tail behavior, these techniques might in general yield biased estimates for the tail dependence. We refer to Frahm et al. (2005) for a more elaborated discussion of this issue. In order to circumvent the problem and to obtain estimators that are robust with

respect to deviations in the center of the distribution, there are basically two important approaches: either one could extract the tail dependence from subsamples of block maximal data, for which extreme-value copulas provide a natural model (McNeil et al., 2005, Section 7.5.4), or one could rely on extreme-value techniques some of which are presented in Section 3.2. Applications of these procedures can be found in Breymann et al. (2003); Caillault and Guégan (2005); Jäschke et al. (2012); Jäschke (2014), among others.

Most of the aforementioned applications to time series data are based on the implicit assumption that the tail dependence remains constant over time. Whereas nonparametric testing for constancy of the whole dependence structure, as for instance measured by the copula, has recently drawn some attention in the literature (Rémillard, 2010; Busetti and Harvey, 2011; Krämer and van Kampen, 2011; Bücher and Ruppert, 2013; Bücher et al., 2014; Wied et al., 2014), there does not seem to exist a unified approach to testing for constancy of the tail dependence. It is the main purpose of the present paper to fill this gap. Our proposed testing procedures are genuine extreme-value methods depending only on the dependence between the tails of the data and are hence robust with respect to potential (non-)constancy of the dependence between the centers of the distributions. In particular, the presented tests do not rely on the assumption of a constant copula throughout the sample period.

Our procedures are based on new limit results for the sequential empirical tail copula process, formally defined in Section 3.3.1. We derive its asymptotic distribution under the null hypothesis and propose several variants to approximate the required critical values. When restricting to the case of testing for constancy of the simple tail dependence coefficient, the limiting process can be easily transformed into a Brownian bridge. In this case, the asymptotic critical values of the tests can be obtained by direct calculations or simulations. In the more complicated case of testing for constancy of the whole extremal dependence structure as measured by the tail copula, we propose a multiplier bootstrap procedure to obtain approximate asymptotic quantiles. The finite-sample performance of all proposals is assessed in a simulation study, which reveals accurate approximations of the nominal level and reasonable power properties.

We apply our methods to two real datasets. The first application revisits a recent investigation in Jäschke (2014) on the tail dependence between WTI and Brent crude oil spot log-returns, which is based on the implicit assumption that the tail dependence remains constant over time. Our testing procedures show that this assumption cannot be rejected. The second application concerns the tail dependence between the Dow Jones Industrial Average and the Nasdaq Composite time series around Black Monday on 19th of October 1987, it reveals a significant break in the tail dependence. However, our results do not show clear evidence for the hypothesis that this break takes place at the particular date of Black Monday.

The structure of the paper is as follows: in Section 3.2, we briefly summarize the concept of tail dependence and corresponding nonparametric estimation techniques. The new testing procedures for constancy of the tail dependence are introduced in Section 3.3. In particular, we derive the asymptotic distribution of the sequential empirical tail copula process, propose a multiplier bootstrap approximation of the latter and show consistency of various asymptotic tests. Additionally, we deal with the estimation of break-points in case the null hypothesis is rejected and make use of a data-adaptive process for the necessary parameter choice, common to inference methods in extreme-value theory. A comprehensive simulation study is presented in Section 3.4, followed by the two elaborate empirical applications in Section 3.5. All proofs are deferred to Section 3.7.

3.2 The concept of tail dependence and its nonparametric estimation

Let (X, Y) be a bivariate random vector with continuous marginal cumulative distribution functions (c.d.f.s) F and G. *Lower or upper tail dependence* concerns the tendency that extremely small or extremely large outcomes of X and Y occur simultaneously. Simple, widely used and intuitive scalar measures for these tendencies are provided by the well-established coefficients of tail dependence (TDC), defined as

$$\lambda_L = \lim_{t \searrow 0} \mathbb{P}\{F(X) \leq t \mid G(Y) \leq t\}, \qquad \lambda_U = \lim_{t \nearrow 1} \mathbb{P}\{F(X) \geq t \mid G(Y) \geq t\}, \tag{3.1}$$

see for instance Joe (1997); Frahm et al. (2005), among others.

It is well-known that the joint c.d.f. H of (X, Y) can be written in a unique way as

$$H(x, y) = C\{F(x), G(y)\}, \qquad x, y \in \mathbb{R}, \tag{3.2}$$

where the copula C is a c.d.f. on $[0, 1]^2$ with uniform marginals. Elementary calculations show that the conditional probabilities in (3.1) can be written as

$$\lambda_L = \lim_{t \searrow 0} \frac{C(t, t)}{t}, \qquad \lambda_U = \lim_{t \searrow 0} \frac{\bar{C}(t, t)}{t},$$

where $\bar{C}$ denotes the survival copula of (X, Y). Therefore, the coefficients of tail dependence can be regarded as directional derivatives of C or $\bar{C}$ at the origin with direction $(1, 1)$. Considering different directions, we arrive at the so-called tail copulas, defined for any $(x, y) \in \mathbb{E} = [0, \infty]^2 \setminus \{(\infty, \infty)\}$ by

$$\Lambda_L(x, y) = \lim_{t \searrow 0} \frac{C(xt, yt)}{t}, \qquad \Lambda_U(x, y) = \lim_{t \searrow 0} \frac{\bar{C}(xt, yt)}{t}, \tag{3.3}$$

see Schmidt and Stadtmüller (2006). Note that the upper tail copula of (X, Y) is the lower tail copula of $(-X, -Y)$, whence there is no conceptual difference between upper and lower tail dependence.

Several variants of tail copulas have been proposed in the literature on multivariate extreme-value theory. For instance, $L(x, y) = x + y - \Lambda_U(x, y)$ denotes the stable tail dependence function, see, e.g., de Haan and Ferreira (2006). The function $A(t) = 1 - \Lambda_U(1 - t, t)$, which is simply the restriction of L to the unit sphere with respect to the $\|\cdot\|_1$-norm, is called Pickands dependence function, see Pickands (1981). All these variants are one-to-one and are known to characterize the extremal dependence of X and Y, see de Haan and Ferreira (2006). In the present paper we restrict ourselves to the case of tail copulas.

Nonparametric estimation of L and Λ has been addressed in Huang (1992); Drees and Huang (1998); Einmahl et al. (2006); de Haan and Ferreira (2006); Bücher and Dette (2013); Einmahl et al. (2012) for i.i.d. samples $(X_i, Y_i)_{i \in \{1, \ldots, n\}}$. For instance, in the case of lower tail copulas, the considered estimators are slight variants, differing only up to a term of uniform order $O(1/k)$, of the function

$$(x, y) \mapsto \frac{1}{k} \sum_{i=1}^{n} \mathbb{1}\Big(R_i \leq kx, S_i \leq ky\Big) \tag{3.4}$$

where R_i (resp. S_i) denotes the rank of X_i (resp. Y_i) among $X_1, \ldots, X_n$ (resp. $Y_1, \ldots, Y_n$), and where $k = k_n \to \infty$ denotes an intermediate sequence to be chosen by the statistician. Under suitable assumptions on k_n and on the speed of convergence in (3.3) the estimators are known to be $\sqrt{k_n}$-consistent. Additionally, under certain smoothness conditions on Λ, the corresponding process $\sqrt{k_n}(\hat{\Lambda} - \Lambda)$ converges to a Gaussian limit process.

3.3 Testing for constant tail dependence

3.3.1 Setting and test statistics

Let $(X_i, Y_i)_{i\in\{1,\dots,n\}}$ be an independent sequence of bivariate random vectors with joint c.d.f. H_i and identical continuous marginal c.d.f.s F and G, respectively. According to Sklar's Theorem, see (3.2), we can decompose

$$H_i(x,y) = C_i\{F(x), G(y)\}, \qquad x,y \in \mathbb{R},$$

where $C_i(u,v) = \mathbb{P}(U_i \leq u, V_i \leq v)$ with $U_i = F(X_i)$ and $V_i = G(Y_i)$. We assume that the corresponding lower tail copulas

$$\Lambda_i(x,y) = \lim_{t\to\infty} tC_i(x/t, y/t) \tag{3.5}$$

exist for all $(x,y) \in \mathbb{E} = [0,\infty]^2 \setminus \{(\infty,\infty)\}$ and all $i = 1,\dots,n$.

At first sight, the assumption of serially independent time series may appear somewhat restrictive. However, the assumption does not seem to be too problematic because of the following argument. In Section 3.5, the role of (X_i, Y_i) will be played by the unobservable, serially independent innovations of common time series models such as AR or GARCH processes. We will apply the proposed tests to the observable, standardized residuals (obtained by univariate filtering) and consider these residuals as *marginally almost i.i.d.* Our extensive simulation study in Section 3.4 indicates that the additional estimation step does not influence the asymptotic behavior of our test statistics, i.e., the asymptotic distribution of the estimator based on residuals is the same as the one based on the unobservable, serially independent innovations. Note that this observation is supported by the results in Chen and Fan (2006); Rémillard (2010); Chan et al. (2009), where it is shown that the asymptotic distributions of both semi- and nonparametric estimators in copula models are not influenced by marginal filtering.

Also, the assumption of strict stationarity of the marginal distributions may appear restrictive. Note that, in the literature on testing for constant copulas, it can be considered as a common practice hitherto, see for instance Busetti and Harvey (2011); Rémillard (2010); Bücher and Ruppert (2013); Bücher et al. (2014). In Section 3.3.7, we adapt our methods to a more general setting that allows for potential breaks in the marginal distributions. Note that, as we are only interested in strict stationarity in the following (calculation of ranks, see (3.4), originating from different distributions is of doubtful validity), we drop the adjective strict.

Throughout this paper, it is our aim to develop tests for detecting breaks in the tail dependence, i.e., to test for

$$H_0^{\Lambda}: \text{ there exists } \Lambda > 0 \text{ such that } \Lambda_i \equiv \Lambda \text{ for all } i = 1,\dots,n$$

against alternatives involving the non-constancy of Λ_i. A special case of this null hypothesis is given by considering the conventional lower tail dependence coefficient $\lambda_i = \Lambda_i(1,1)$. The corresponding null hypothesis reads as

$$H_0^{\lambda}: \text{ there exists } \lambda > 0 \text{ such that } \lambda_i = \lambda \text{ for all } i = 1,\dots,n.$$

In order to motivate our test statistics, let us first recapitulate the *empirical tail copula* from Schmidt and Stadtmüller (2006) as the basic nonparametric estimator for Λ under

H_0^Λ, see also (3.4) and the corresponding citations. Replacing the unknown copula in (3.5) by the empirical copula $\hat{C}_n$, it is defined as

$$\hat{\Lambda}_n(x,y) = \frac{n}{k}\hat{C}_n\left(\frac{kx}{n}, \frac{ky}{n}\right) = \frac{1}{k}\sum_{i=1}^{n} \mathbb{1}\left(\hat{U}_i \le kx/n, \hat{V}_i \le ky/n\right), \tag{3.6}$$

where $(\hat{U}_i, \hat{V}_i)$ denote *pseudo-observations* from the copula C, defined by

$$\hat{U}_i = \frac{n}{n+1}F_n(X_i), \qquad \hat{V}_i = \frac{n}{n+1}G_n(Y_i),$$

with F_n and G_n denoting the marginal empirical c.d.f.s. Additionally, $k = k_n \to \infty$, $k = o(n)$ as $n \to \infty$, represents a sequence of parameters discussed in detail below. The ratio k/n can be interpreted as the fraction of data that one considers as *being in the tail* and thus taken into account to estimate the tail dependence in Equation (3.6). Under suitable regularity conditions some of which are given in the subsequent Section 3.3.2, it is known that $\hat{\Lambda}_n$ is $\sqrt{k}$-consistent for Λ and that the corresponding *empirical tail copula process* $(x,y) \mapsto \sqrt{k}\{\hat{\Lambda}_n(x,y) - \Lambda(x,y)\}$ converges weakly to a Gaussian limit process.

Now, in order to test for H_0^Λ, it is natural to consider a suitable sequential version of $\hat{\Lambda}_n$. We define

$$\hat{\Lambda}_n^\circ(s,x,y) = \frac{1}{k}\sum_{i=1}^{\lfloor ns \rfloor} \mathbb{1}\left(\hat{U}_i \le kx/n, \hat{V}_i \le ky/n\right)$$

as the sequential empirical tail copula. Under H_0^Λ, $\hat{\Lambda}_n^\circ$ should be regarded as an estimator for $\Lambda^\circ(s,x,y) = s\Lambda(x,y)$. Note that $\hat{\Lambda}_n^\circ(1,x,y) = \hat{\Lambda}_n(x,y)$. The crucial quantity for all test procedures in this paper is now given by the *sequential empirical tail copula process* $\{\mathbb{G}_n(s,x,y), s \in [0,1], (x,y) \in \mathbb{E}\}$ with

$$\mathbb{G}_n(s,x,y) = \sqrt{k}\left\{\hat{\Lambda}_n^\circ(s,x,y) - s\hat{\Lambda}_n^\circ(1,x,y)\right\}. \tag{3.7}$$

Note that, despite its name, the sequential empirical tail copula process is not completely sequential. More precisely, the unknown marginal distributions are estimated based on all the available marginal information, whereas only the quantity of interest, the dependence, is assessed sequentially.

Now, some simple calculations show that, for $s \in (0,1)$, $\mathbb{G}_n$ can be written as

$$\mathbb{G}_n(s,x,y) = \sqrt{k}\{s(1-s)\}\left\{\frac{1}{ks}\sum_{i=1}^{\lfloor ns \rfloor} \mathbb{1}\left(\hat{U}_i \le kx/n, \hat{V}_i \le ky/n\right) - \frac{1}{k(1-s)}\sum_{i=\lfloor ns \rfloor+1}^{n} \mathbb{1}\left(\hat{U}_i \le kx/n, \hat{V}_i \le ky/n\right)\right\}.$$

Since $ks \approx \lfloor ks \rfloor$, $ns \approx \lfloor ns \rfloor$ and $k/n \approx \lfloor ks \rfloor / \lfloor ns \rfloor$ for any $s \in (0,1)$, the two summands in the brackets on the right-hand side can be interpreted as (slightly adapted) empirical tail copulas of the subsamples $(X_1,Y_1),\ldots,(X_{\lfloor ns \rfloor}, Y_{\lfloor ns \rfloor})$ and $(X_{\lfloor ns \rfloor+1}, Y_{\lfloor ns \rfloor+1}),\ldots,(X_n,Y_n)$, respectively, with corresponding sequence of parameters $k' = \lfloor ks \rfloor$ and $k'' = \lfloor k(1-s) \rfloor$. Under H_0^Λ, one would expect that the difference between these two estimators converges to 0. Therefore, any statistic that can be interpreted as a distance between $\mathbb{G}_n$ and the function being constantly equal to 0 is a reasonable candidate for a test statistic for the null hypothesis. A simulation study similar to one presented in Section 3.4 showed that a Cramér-von Mises functional yields the best finite-sample performance, which is why

we restrict ourselves to this case in the subsequent presentation. Consequently, in case of the simple null hypothesis H_0^λ, we propose the test statistic

$$\mathcal{S}_n := \hat{\lambda}_n^{-1} \int_0^1 \{\mathbb{G}_n(s,1,1)\}^2 \, ds, \tag{3.8}$$

where $\hat{\lambda}_n = \hat{\Lambda}_n^\circ(1,1,1)$, and to reject the null hypothesis whenever $\mathcal{S}_n$ is larger than an appropriate critical value to be determined later on.

For the construction of a test for the null hypothesis H_0^Λ, we make use of the fact that, by homogeneity, the lower tail copula is uniquely determined by its values on the sphere $S(c) = \{\mathbf{x} \in [0,\infty)^2 : \|\mathbf{x}\| = c\}$, where $\|\cdot\|$ denotes an arbitrary fixed norm on $\mathbb{R}^2$ and where $c > 0$ is an arbitrary fixed constant. The most popular choice in bivariate extreme value theory is $c = 1$ together with the $\|\cdot\|_1$-norm resulting in the function $\Lambda_{||\cdot||_1} : [0,1] \to [0,1/2] : t \mapsto \Lambda_{||\cdot||_1}(t) = \Lambda(1-t,t)$. Note that $\Lambda_{||\cdot||_1}(t) = 1 - A(t)$ with the Pickands dependence function A, see, e.g., Segers (2012b).

In order to test for overall constancy of Λ_i it is sufficient to test for constancy of Λ_i on some sphere $S(c)$. In Section 3.3.5, we will propose a data-adaptive procedure for the choice of the parameter k, which will suggest to use a sphere that contains the point $(1,1)$. For that reason, we introduce the following test statistic

$$\mathcal{T}_n := \int_{[0,1]^2} \{\mathbb{G}_n(s,2-2t,2t)\}^2 \, d(s,t),$$

whose support corresponds to the $\|\cdot\|_1$-norm and $c = 2$, and let H_0^Λ again be rejected when $\mathcal{T}_n$ is larger than an appropriate critical value.

In order to determine the critical values, we will derive the asymptotic null distributions of the tests in the next subsection. For both statistics, they will rely on a limit result for the sequential empirical tail copula process.

3.3.2 Asymptotic null distributions

Let $\mathcal{B}_\infty([0,1] \times \mathbb{E})$ denote the space of all functions $f : [0,1] \times \mathbb{E} \to \mathbb{R}$ which are uniformly bounded on every compact subset of $[0,1] \times \mathbb{E}$ (here and throughout, we understand $\mathbb{E} = [0,\infty]^2 \setminus \{(\infty,\infty)\}$ as the one-point uncompactification of the compact set $[0,\infty]^2$), equipped with the metric

$$d(f,g) := \sum_{m=1}^\infty 2^{-m}(\|f-g\|_{S_m} \wedge 1),$$

where $a \wedge b = \min(a,b)$, where the sets S_m are defined as $S_m = [0,1] \times T_m$ with

$$T_m := [0,m]^2 \cup (\{\infty\} \times [0,m]) \cup ([0,m] \times \{\infty\})$$

and where $\|\cdot\|_S$ denotes the sup-norm on a set S. Note that convergence with respect to d is equivalent to uniform convergence on each S_m.

In the following we are going to show weak convergence of $\mathbb{G}_n$ as an element of the metric space $(\mathcal{B}_\infty([0,1] \times \mathbb{E}), d)$. Similar as in related references on the estimation of tail copulas (see Section 3.2), we have to impose several regularity conditions. First, we need a second order condition quantifying the speed of convergence in (3.5) uniformly in i and (x,y).

Assumption 3.1
We have $\Lambda_i \not\equiv 0$ and

$$\Lambda_i(x,y) - tC_i(x/t, y/t) = O(S(t)), \quad t \to \infty, \tag{3.9}$$

uniformly on $\{(x,y) \in [0,1]^2 : x+y=1\}$ (and hence uniformly on each T_m) and uniformly in $i \in \mathbb{N}$, where $S : [0,\infty) \to [0,\infty)$ denotes a function satisfying $\lim_{t\to\infty} S(t) = 0$.

Second, the following conditions have to be imposed on the sequence $k = k_n$.

Assumption 3.2
The nondecreasing sequence $k = k_n \to \infty$ satisfies the conditions

$$(a)\ k_n/n \downarrow 0, \qquad (b)\ \sqrt{k_n} S(n/k_n) = o(1),$$

as n tends to infinity.

Condition (a) is needed anyway to define a meaningful estimator. Condition (b) allows to control appearing bias terms in the nonsequential empirical tail copula process, see also Schmidt and Stadtmüller (2006) and Bücher and Dette (2013).

With these assumptions we can now state the main result of our paper.

Proposition 3.3
Suppose that Assumptions 3.1 and 3.2 hold. Then, under H_0^Λ,

$$\mathbb{G}_n \rightsquigarrow \mathbb{G}_\Lambda \quad \text{in } (\mathcal{B}_\infty([0,1]\times\mathbb{E}), d),$$

where $\mathbb{G}_\Lambda(s,x,y) = \mathbb{B}_\Lambda(s,x,y) - s\mathbb{B}_\Lambda(1,x,y)$. Here, $\mathbb{B}_\Lambda$ is a tight centered Gaussian process with continuous sample paths and with covariance structure

$$\mathbb{E}[\mathbb{B}_\Lambda(s_1,x_1,y_1)\mathbb{B}_\Lambda(s_2,x_2,y_2)] = (s_1 \wedge s_2)\Lambda(x_1 \wedge x_2, y_1 \wedge y_2).$$

As stated above, Assumption 3.2 (b) is needed to control bias terms occurring when estimating Λ by $\hat{\Lambda}_n$. As the process $\mathbb{G}_n$ does not involve the true tail copula Λ, the assertion of Proposition 3.3 actually holds if (b) is replaced by a quite technical, but less restrictive assumption, see Remark 3.16 in the appendix. However, as an application of the proposed test procedures in this paper will usually be followed by the application of estimation techniques relying on (b), we do not feel that imposing this condition is too restrictive.

Proposition 3.3 immediately yields the asymptotic null distributions of $\mathcal{S}_n$ and $\mathcal{T}_n$.

Corollary 3.4
Suppose that Assumptions 3.1 and 3.2 hold. Then, under H_0^Λ,

$$\mathcal{S}_n \rightsquigarrow \mathcal{S} := \int_0^1 \{B(s)\}^2 ds,$$

where B is a one-dimensional standard Brownian bridge, and

$$\mathcal{T}_n \rightsquigarrow \mathcal{T} := \int_{[0,1]^2} \{\mathbb{G}_\Lambda(s, 2-2t, 2t)\}^2 \, d(s,t),$$

where $\mathbb{G}_\Lambda$ is defined in Proposition 3.3.

Note that, in fact, the weak convergence of $\mathcal{S}_n$ can be derived under a relaxation of H_0^Λ, as it suffices that $\Lambda_i(x,y) \not\equiv 0$ exists and is constant in time in a neighborhood of $(1,1)$. This is, however, *a bit more* than assumed in H_0^λ.

Since the limiting distribution for $\mathcal{S}_n$ in Corollary 3.4 is pivotal, we directly obtain an asymptotic level α test for H_0^λ.

TDC-Test 1. Reject H_0^λ for $\mathcal{S}_n \geq q_{1-\alpha}^C$, where $q_{1-\alpha}^C$ denotes the $(1-\alpha)$-quantile of the Cramér-von Mises distribution, the latter being defined as the distribution of the random variable $\int_0^1 \{B(s)\}^2\, ds$.

In order to derive critical values for the test based on $\mathcal{T}_n$, some more effort is needed. Its limiting distribution in Corollary 3.4 is not pivotal and cannot be easily transformed to a distribution which is independent of Λ. Therefore, we propose an appropriate bootstrap approximation for $\mathbb{G}_\Lambda$ which will also allow for the definition of an alternative test for H_0^λ.

Let $B \in \mathbb{N}$ be a large integer and let $\xi_1^{(1)}, \ldots, \xi_n^{(1)}, \ldots, \xi_1^{(B)}, \ldots, \xi_n^{(B)}$ be an independent sequence of $n \times B$ i.i.d. random variables with mean 0 and variance 1 which are independent of the data $(X_1, Y_1), \ldots, (X_n, Y_n)$ and possess finite moments of any order. We will refer to $\xi_i^{(b)}$ as a multiplier. Similar in spirit as in Rémillard (2010); Bücher and Dette (2013) we define, for any $(s,x,y) \in [0,1] \times \mathbb{E}$ and $b \in \{1, \ldots, B\}$,

$$\mathbb{G}_{n,\xi^{(b)}}(s,x,y) = \mathbb{B}_{n,\xi^{(b)}}(s,x,y) - s\mathbb{B}_{n,\xi^{(b)}}(1,x,y), \tag{3.10}$$

where

$$\begin{aligned}\mathbb{B}_{n,\xi^{(b)}}(s,x,y) &:= \frac{1}{\sqrt{k}} \sum_{i=1}^{\lfloor ns \rfloor} \xi_i^{(b)} \left\{ \mathbb{1}\left(\hat{U}_i \leq kx/n, \hat{V}_i \leq ky/n\right) - \hat{C}_n(kx/n, ky/n) \right\} \\ &= \frac{1}{\sqrt{k}} \sum_{i=1}^{\lfloor ns \rfloor} \xi_i^{(b)} \left\{ \mathbb{1}\left(\hat{U}_i \leq kx/n, \hat{V}_i \leq ky/n\right) - k/n \times \hat{\Lambda}_n^\circ(1,x,y) \right\}.\end{aligned}$$

The following proposition essentially states that, for large n, $\mathbb{G}_{n,\xi^{(1)}}, \ldots, \mathbb{G}_{n,\xi^{(B)}}$ can be regarded as *almost* independent copies of $\mathbb{G}_n$. To prove the result, one additional technical assumption on the sequence k_n is required, which can be regarded as very light.

Assumption 3.5
There exists some $p \in \mathbb{N}$ such that $n/k_n^p = o(1)$.

Proposition 3.6
Suppose that Assumptions 3.1, 3.2 and 3.5 hold. Then, under H_0^Λ,

$$(\mathbb{G}_n, \mathbb{G}_{n,\xi^{(1)}}, \ldots, \mathbb{G}_{n,\xi^{(B)}}) \rightsquigarrow (\mathbb{G}_\Lambda, \mathbb{G}_\Lambda^{(1)}, \ldots, \mathbb{G}_\Lambda^{(B)})$$

in $(\mathcal{B}_\infty([0,1] \times \mathbb{E}), d)^{B+1}$, *where* $\mathbb{G}_\Lambda^{(1)}, \ldots, \mathbb{G}_\Lambda^{(B)}$ *are independent copies of* $\mathbb{G}_\Lambda$.

For $b = 1, \ldots, B$, define $\mathcal{S}_{n,\xi^{(b)}}$ and $\mathcal{T}_{n,\xi^{(b)}}$ by

$$\mathcal{S}_{n,\xi^{(b)}} = \hat{\lambda}_n^{-1} \int_0^1 \{\mathbb{G}_{n,\xi^{(b)}}(s,1,1)\}^2 ds, \quad \mathcal{T}_{n,\xi^{(b)}} = \int_{[0,1]^2} \{\mathbb{G}_{n,\xi^{(b)}}(s, 2-2t, 2t)\}^2 d(s,t).$$

We obtain the following tests for H_0^λ and H_0^Λ, respectively.

TDC-Test 2. Reject H_0^λ for $\mathcal{S}_n \geq \hat{q}_{\mathcal{S}_n, 1-\alpha}$, where $\hat{q}_{\mathcal{S}_n,1-\alpha}$ denotes the $(1-\alpha)$-sample quantile of $\mathcal{S}_{n,\xi^{(1)}}, \ldots, \mathcal{S}_{n,\xi^{(B)}}$.

TC-Test. Reject H_0^Λ for $\mathcal{T}_n \geq \hat{q}_{\mathcal{T}_n,1-\alpha}$, where $\hat{q}_{\mathcal{T}_n,1-\alpha}$ denotes the $(1-\alpha)$-sample quantile of $\mathcal{T}_{n,\xi^{(1)}}, \ldots, \mathcal{T}_{n,\xi^{(B)}}$.

The final result of this subsection shows that all proposed tests in this paper asymptotically hold their level.

Corollary 3.7
Suppose that Assumptions 3.1 and 3.2 hold and that H_0^Λ is valid. Then TDC-Test 1 is an asymptotic level α test for H_0^λ. If, additionally, Assumption 3.5 holds, then TDC-Test 2 and TC-Test are asymptotic level α tests for H_0^λ and H_0^Λ, respectively, in the sense that, for any $\alpha \in (0,1)$,

$$\lim_{B\to\infty}\lim_{n\to\infty} \mathbb{P}(\mathcal{S}_n \geq \hat{q}_{\mathcal{S}_n,1-\alpha}) = \alpha, \qquad \lim_{B\to\infty}\lim_{n\to\infty} \mathbb{P}(\mathcal{T}_n \geq \hat{q}_{\mathcal{T}_n,1-\alpha}) = \alpha.$$

3.3.3 Asymptotics under fixed alternatives

In the present subsection we are going to show consistency of the proposed test statistics under fixed alternatives. We observe a triangular array of row-wise independent random vectors $(X_{i,n}, Y_{i,n})$, $i = 1, \ldots, n$, such that $X_{i,n} \sim F$ and $Y_{i,n} \sim G$ for all i and n and such that the copula $C_{i,n}$ of $(X_{i,n}, Y_{i,n})$ may vary over time. Slightly abusing notation, we omit the index n wherever it does not cause any ambiguity. For the sake of a clear exposition, we first consider the following two simple alternatives for H_0^λ and H_0^Λ. Later on, we provide a discussion on how to detect multiple break-points and how the test statistics behave in the presence of smooth changes.

H_1^λ : there exists $\bar{s} \in (0,1), \lambda^{(1)} \neq \lambda^{(2)}$ such that
$$\lambda_i = \lambda^{(1)} \text{ for } i = 1, \ldots, \lfloor n\bar{s} \rfloor \text{ and } \lambda_i = \lambda^{(2)} \text{ for } i = \lfloor n\bar{s} \rfloor + 1, \ldots, n.$$
H_1^Λ : there exists $\bar{s} \in (0,1), \Lambda^{(1)} \not\equiv \Lambda^{(2)}$ such that
$$\Lambda_i = \Lambda^{(1)} \text{ for } i = 1, \ldots, \lfloor n\bar{s} \rfloor \text{ and } \Lambda_i = \Lambda^{(2)} \text{ for } i = \lfloor n\bar{s} \rfloor + 1, \ldots, n.$$

Proposition 3.8
Suppose that Assumptions 3.1 and 3.2 hold.

(i) If H_1^λ and H_1^Λ are true, then

$$\sup_{s\in[0,1]} \left| \frac{1}{\sqrt{k_n}} \mathbb{G}_n(s,1,1) - A_\lambda(s) \right| = o_P(1)$$

where $A_\lambda(s) = s(1-\bar{s})(\lambda^{(1)} - \lambda^{(2)})$ for $s \leq \bar{s}$ and $A_\lambda(s) = \bar{s}(1-s)(\lambda^{(1)} - \lambda^{(2)})$ for $s > \bar{s}$. Moreover, $\mathcal{S}_n$ converges to infinity in probability.

(ii) If H_1^Λ is true, then

$$\sup_{s\in[0,1],(x,y)\in T_m} \left| \frac{1}{\sqrt{k_n}} \mathbb{G}_n(s,x,y) - A_\Lambda(s,x,y) \right| = o_P(1)$$

for any $m \in \mathbb{N}$, where $A_\Lambda(s,x,y) = s(1-\bar{s})\{\Lambda^{(1)}(x,y) - \Lambda^{(2)}(x,y)\}$ for $s \leq \bar{s}$ and $A_\Lambda(s,x,y) = \bar{s}(1-s)\{\Lambda^{(1)}(x,y) - \Lambda^{(2)}(x,y)\}$ for $s > \bar{s}$. Moreover, $\mathcal{T}_n$ converges to infinity in probability.

As already mentioned after Corollary 3.4, it is not necessary to assume global constancy of the tail copulas in the respective subsamples in part (i) of Proposition 3.8, constancy in a neighborhood of $(1,1)$ is sufficient. Moreover, Proposition 3.8 implies consistency of the proposed tests.

Corollary 3.9
Suppose that Assumptions 3.1 and 3.2 are satisfied. Then TDC-Test 1 is consistent for H_1^λ. If, additionally, Assumption 3.5 holds, then TDC-Test 2 and TC-Test are consistent for H_1^λ and H_1^Λ, respectively, in the sense that, for any $B \in \mathbb{N}$ and $\alpha \in (0,1)$,

$$\lim_{n\to\infty} \mathbb{P}(\mathcal{S}_n \geq \hat{q}_{\mathcal{S}_n,1-\alpha}) = 1, \qquad \lim_{n\to\infty} \mathbb{P}(\mathcal{T}_n \geq \hat{q}_{\mathcal{T}_n,1-\alpha}) = 1.$$

Under H_1^λ and H_1^Λ, consistent estimators for the break-point $\bar{s}$ are given by $\hat{s}^\lambda := \operatorname{argmax}_{s\in[0,1]} |\mathbb{G}_n(s,1,1)|$ and $\hat{s}^\Lambda := \operatorname{argmax}_{s\in[0,1]} \sup_{t\in[0,1]} |\mathbb{G}_n(s,2-2t,2t)|$, respectively.

Proposition 3.10
Suppose that Assumptions 3.1 and 3.2 hold.

(i) If H_1^λ and H_1^Λ are true, $\hat{s}^\lambda \to_p \bar{s}$.

(ii) If H_1^Λ is true, $\hat{s}^\Lambda \to_p \bar{s}$.

Note that, if one of the alternatives H_1^λ or H_1^Λ holds, then the other one cannot hold with a different value for $\bar{s}$. Hence, the break-point $\bar{s}$ in Proposition 3.10 (i) is well-defined.

Up to now, we have assumed the existence of at most one single break-point. As is shown in the end of this subsection, an analog consistency result for the test can be obtained in the case of an arbitrary finite number of break-points between which the tail copula is constant, respectively. For example, a corresponding alternative for H_0^λ would then read as: there exists a finite number of points $0 = s_0 < s_1 < \ldots < s_\ell < \ldots < s_L = 1$ such that, for any $\ell \in \{1,\ldots,L\}$, the TDC of the sample $(X_{\lfloor ns_{\ell-1}\rfloor+1}, Y_{\lfloor ns_{\ell-1}\rfloor+1}), \ldots, (X_{\lfloor ns_\ell\rfloor}, Y_{\lfloor ns_\ell\rfloor})$ is given by $\lambda^{(\ell)}$, with $\lambda^{(\ell)} \neq \lambda^{(\ell+1)}$.

Estimating the break-points $s_1, s_2, \ldots, s_{L-1}$ is slightly more complicated than it is in the case of just one break-point. In principle, it is also possible to work with the argmax-estimator $\hat{s}^\lambda$ here, but, by construction, this estimator only estimates a single break-point. The number and the location of the other break-points can be estimated by a binary segmentation algorithm going back to Vostrikova (1981). This procedure is for instance applied in Galeano and Wied (2014) to the problem of detecting changing correlations. The basic principle is as follows: at first, the test is applied to the whole sample. If the null hypothesis gets rejected, the argmax-estimator $\hat{s}^\lambda$ can be shown to be a consistent estimator for the *dominating* break-point (see Galeano and Wied, 2014). In the next step, the sample is divided into two parts with the split point given by $\lfloor n\hat{s}^\lambda \rfloor$. The test is applied to both parts separately to decide whether one gets additional break-points in the corresponding subsamples. In that case, the respective subsample is further divided at the corresponding estimated break-point. This procedure is repeated until no further break-points are detected.

The setting with a fixed number of break-points as described above is a special case of a general class of alternatives in which Λ_i (and thus also λ_i) is described by a nonconstant function g. More precisely, let $\mathcal{G}$ denote the class of all functions $g : [0,1] \times \mathbb{E} \to \mathbb{R}$ such that $g(s,\cdot,\cdot)$ is a tail copula for any $s \in [0,1]$ and such that, for any $m \in \mathbb{N}$,

$$\lim_{n\to\infty} \sup_{(s,x,y)\in S_m} \left| \frac{1}{n} \sum_{i=1}^{\lfloor ns \rfloor} g\left(\frac{i}{n}, x, y\right) - \int_0^s g(z,x,y)\, dz \right| = 0.$$

The class $\mathcal{G}$ allows to consider the following general class of alternatives, see also Wied

et al. (2012):

$$H_{1,\mathcal{G}}^{\lambda}: \text{ there exists } g \in \mathcal{G} \text{ such that } \Lambda_i = g(i/n,\cdot,\cdot) \text{ and such that } \int_0^s g(z,1,1)\,dz \neq s\int_0^1 g(z,1,1)\,dz \text{ for some } s \in [0,1],$$

$$H_{1,\mathcal{G}}^{\Lambda}: \text{ there exists } g \in \mathcal{G} \text{ such that } \Lambda_i = g(i/n,\cdot,\cdot) \text{ and such that } \int_0^s g(z,x,y)\,dz \neq s\int_0^1 g(z,x,y)\,dz \text{ for some } (s,x,y) \in [0,1]\times\mathbb{E}.$$

The former setting with a fixed number of break-points corresponds to a function g that is piecewise constant in s, but in the general case, continuous functions are explicitly allowed. The latter, for instance, may occur in models with time varying copula parameters (see, e.g., Hafner and Manner, 2012 or Patton, 2006).

In general, CUSUM-type procedures as those considered in Section 3.3.2 are not constructed for detecting smooth changes in the first place. Here, it would perhaps be more advisable to consider a setup based on locally stationary processes. Nevertheless, the test statistics converge to infinity in probability under smooth alternatives.

Proposition 3.11
Suppose that Assumptions 3.1 and 3.2 hold.

(i) If $H_{1,\mathcal{G}}^{\lambda}$ is true, then

$$\sup_{s\in[0,1]}\left|\frac{1}{\sqrt{k_n}}\mathbb{G}_n(s,1,1) - A_{\lambda}^{g}(s)\right| = o_P(1),$$

where $A_{\lambda}^{g}(s) = \int_0^s g(z,1,1)dz - s\int_0^1 g(z,1,1)dz$. Moreover, $\mathcal{S}_n$ converges to infinity in probability.

(ii) If $H_{1,\mathcal{G}}^{\Lambda}$ is true, then

$$\sup_{s\in[0,1],(x,y)\in T_m}\left|\frac{1}{\sqrt{k_n}}\mathbb{G}_n(s,x,y) - A_{\Lambda}^{g}(s,x,y)\right| = o_P(1),$$

for any $m \in \mathbb{N}$, where $A_{\Lambda}^{g}(s,x,y) = \int_0^s g(z,x,y)dz - s\int_0^1 g(z,x,y)dz$. Moreover, $\mathcal{T}_n$ converges to infinity in probability.

As a simple consequence, we obtain consistency of TDC-Test 1 under the setting of Proposition 3.11(i).

3.3.4 Testing for a break at a specific time point

In certain applications, one might have a reasonable guess for a potential break-point in the tail dependence of a time series. Important econometric examples can be seen in Black Monday on 19th of October 1987, the introduction of the Euro on 1st of January 1999 or the bankruptcy of Lehman Brothers Inc. on 15th of September 2008. In that case, it might be beneficial to test for constancy against a break at that specific time point rather than testing against the existence of *some* unspecified break-point. The results in the previous subsections easily allow to obtain simple tests in this setting.

Under the situation of Section 3.3.1, let $\bar{s} \in (0,1)$ be some fixed time point of interest. Suppose we know that the tail dependence is constant in the two subsamples before

$\lfloor n\bar{s} \rfloor$ and after $\lfloor n\bar{s} \rfloor + 1$, which, in practice, can be verified by the tests in the preceding subsections. Then, to test for H_0^λ against

$$H_1^\lambda(\bar{s}): \text{ there exists } \lambda^{(1)} \neq \lambda^{(2)} \text{ such that } \lambda_i = \lambda^{(1)} \text{ for } i = 1, \ldots, \lfloor n\bar{s} \rfloor \text{ and } \lambda_i = \lambda^{(2)} \text{ for } i = \lfloor n\bar{s} \rfloor + 1, \ldots, n,$$

we propose to use the test statistic

$$\mathcal{S}_n(\bar{s}) := \left(\bar{s}\hat{\lambda}_n\right)^{-1} \mathbb{G}_n(\bar{s}, 1, 1)^2. \tag{3.11}$$

It easily follows from Proposition 3.3 that, under the null hypothesis, $\mathcal{S}_n(\bar{s})$ weakly converges to a chi-squared distribution with one degree of freedom. Under the alternative, it follows from Proposition 3.8 that $\mathcal{S}_n(\bar{s})$ converges to infinity, in probability. Hence, rejecting H_0^λ if $\mathcal{S}_n(\bar{s})$ exceeds a corresponding quantile of the chi-squared distribution, yields a consistent test for H_0^λ against $H_1^\lambda(\bar{s})$, which asymptotically holds its significance level. Similar results can be obtained for the bootstrap analog and for the test for constancy of the entire tail copula, the details are omitted for the sake of brevity.

3.3.5 Choice of the parameter k

As usual in extreme-value theory, the choice of k_n plays a crucial role for statistical applications. The asymptotic properties of the tests proposed in this paper hold as long as the assumptions on the sequence k_n from Assumption 3.2 (and of course other assumptions) hold. This, of course, allows for a large number of possible choices of k_n. However, the results of the testing procedures may depend crucially on the specific choice of k_n.

The common approach in extreme-value theory to cope with this problem is to consider the outcome of statistical procedures, for instance of an estimator, for several different values of k. The set of all these outcomes should give a clearer picture of the underlying data-generating process. This, for instance, is the basic motivation for the Hill plot used in univariate extreme-value theory for estimating the extreme-value index, see, e.g., Embrechts et al. (1997). Additionally, in certain univariate settings some refined data-adaptive choices to estimate an *optimal* k have been developed, see for instance Drees and Kaufmann (1998) or Danielsson et al. (2001).

In the specific context of estimating tail dependence, Frahm et al. (2005) use plots of the function $k \mapsto \mathrm{TDC}(k)$ to define a *plateau-finding* algorithm that provides a single data-adaptive choice of k. In most of the application in this paper, we closely follow their approach for which reason we briefly summarize this algorithm in the following.

The aim of the algorithm is to search for a value k^* such that the TDC, as a function of k, is *as constant as possible* in a suitable neighborhood of k^*. This is achieved by accomplishing the following steps: first, the function $k \mapsto \mathrm{TDC}(k)$ is smoothed by a box kernel depending on a bandwidth b; we denote the smoothed plot by $k \mapsto \tilde{\lambda}_b(k), k = 1, \ldots, n - 2b$. In our simulation study, we use $b = \lfloor 0.005n \rfloor$. In a second step, we consider a rolling window of vectors or plateaus (having length $\ell = \lfloor \sqrt{n - 2b} \rfloor$) with their entries consisting of successive values of the smoothed TDC-plot, formally defined as $P(k) = (\tilde{\lambda}_b(k), \tilde{\lambda}_b(k+1), \ldots, \tilde{\lambda}_b(k+\ell-1)) \in \mathbb{R}^\ell$, where $k = 1, \ldots, n - 2b - \ell + 1$. We calculate the sum of the absolute deviations between all entries and the first entry in each vector, i.e., $\mathrm{MAD}(k) = \sum_{j=1}^{\ell} |(P(k))_1 - (P(k))_j|$. The algorithm searches for the first vector such that $\mathrm{MAD}(k)$ is smaller than two times the sample standard deviation of all values of the smoothed TDC-plot $\tilde{\lambda}_b(1), \ldots, \tilde{\lambda}_b(n - 2b)$. Finally, k^* is defined as the index which corresponds to the middle entry (the floor function if the length is even) of this vector. For further details, we refer to Frahm et al. (2005).

3.3.6 Higher dimensions

Although we have focused on the case of two dimensions so far, it is basically straightforward (although notationally more involved) to deal with d-dimensional random vectors for a fixed number d. Consider a sequence of marginally i.i.d. random vectors $(X_{i1}, \dots, X_{id})_{i\in\{1,\dots,n\}}$ with continuous marginal c.d.f.s $F_1, \dots, F_d$ and d-dimensional copulas C_i. We suppose that the corresponding lower tail copulas

$$\Lambda_i(x_1, \dots, x_d) := \lim_{t\to\infty} tC_i(x_1/t, \dots, x_d/t).$$

exist for all $x = (x_1, \dots, x_d) \in \mathbb{E}_d = [0,\infty]^d \setminus \{(\infty, \dots, \infty)\}$. Note that Λ_i is in one-to-one correspondence to the familiar d-dimensional stable tail dependence function of $(X_{i1}, \dots, X_{id})$, see, e.g., Einmahl et al. (2012) for its definition. Define pseudo-observations $(\hat{U}_{i1}, \dots, \hat{U}_{id})$ from the copula C_i by $\hat{U}_{ij} = \frac{n}{n+1} F_{nj}(X_{ij})$, $j = 1, \dots, d$, where F_{nj} denote the marginal empirical c.d.f.s. The d-dimensional sequential empirical tail copula process is defined, for any $(s, x_1, \dots, x_d) \in [0,1] \times \mathbb{E}_d$, by

$$\mathbb{G}_n(s, x_1, \dots, x_d) = \sqrt{k} \left\{ \hat{\Lambda}_n^\circ(s, x_1, \dots, x_d) - s\hat{\Lambda}_n^\circ(1, x_1, \dots, x_d) \right\},$$

where $\hat{\Lambda}_n^\circ(s, x_1, \dots, x_d) = \frac{1}{k} \sum_{i=1}^{\lfloor ns \rfloor} \mathbb{1}(\hat{U}_{i1} \le kx_1/n, \dots, \hat{U}_{id} \le kx_d/n)$. A test statistic only focusing on the d-dimensional TDC can be defined analog to the 2-dimensional case,

$$\mathcal{S}_n := \left\{ \hat{\Lambda}_n^\circ(1, 1, \dots, 1) \right\}^{-1} \int_0^1 \left\{ \mathbb{G}_n(s, 1, \dots, 1) \right\}^2 ds,$$

while test statistics focusing on the entire tail copula look slightly more complicated. For instance, one might use

$$\mathcal{T}_n := \int_{[0,1]\times\Delta} \left\{ \mathbb{G}_n(s, \boldsymbol{t}) \right\}^2 d(s, \boldsymbol{t}),$$

where $\Delta := \{\boldsymbol{t} \in (t_1, \dots, t_d) \in \mathbb{E} \mid \text{at least 2 of the } t_j \text{ are } \neq \infty, \sum_{j=1, t_j\neq\infty}^d t_j = 1\}$. Note that the restriction of a tail copula to Δ uniquely determines the whole tail copula by homogeneity. Bootstrap statistics can be defined analogously. For the asymptotic results, one has to modify the metric defined in the beginning of Section 3.3.2 such that

$$T_m := \bigcup_{j=0}^{d-1} \bigcup_{\ell=1}^{\binom{d}{j}} U_{m,j,\ell},$$

where, for each $m \in \mathbb{N}$ and $j = 0, \dots, d-1$, the $U_{m,j,\ell}$ are the $\binom{d}{j}$ different d-fold cartesian products that contain j times $\{\infty\}$ and $d-j$ times $[0, m]$.

3.3.7 Testing for a break under non-stationarity of the marginals

Throughout the previous subsections, we made the assumption that the marginal laws of (X_i, Y_i) are constant over time. A less stringent assumption would be to allow for breaks in the marginal laws. In the present subsection, we outline how the proposed methods can be adapted to that setting.

For the sake of brevity, we restrict ourselves to the case of one known break in each marginal. Let (X_i, Y_i) be an independent sequence of random variables with copula C_i and continuous marginal c.d.f.s $F^{(i)}$ and $G^{(i)}$, respectively. Suppose that there exist

$t_F, t_G \in (0,1)$ such that $F^{(1)} = \cdots = F^{(\lfloor nt_F \rfloor)} \neq F^{(\lfloor nt_F \rfloor + 1)} = \cdots = F^{(n)}$ and $G^{(1)} = \cdots = G^{(\lfloor nt_G \rfloor)} \neq G^{(\lfloor nt_G \rfloor + 1)} = \cdots = G^{(n)}$. Define pseudo-observations $(\hat{U}_i, \hat{V}_i)$ of C_i through

$$\hat{U}_i = \begin{cases} F_{1:\lfloor nt_F \rfloor}(X_i), & i \leq \lfloor nt_F \rfloor, \\ F_{\lfloor nt_F \rfloor + 1:n}(X_i), & i > \lfloor nt_F \rfloor, \end{cases} \quad \hat{V}_i = \begin{cases} G_{1:\lfloor nt_G \rfloor}(Y_i), & i \leq \lfloor nt_G \rfloor, \\ G_{\lfloor nt_G \rfloor + 1:n}(Y_i), & i > \lfloor nt_G \rfloor, \end{cases} \tag{3.12}$$

where $F_{(k+1):\ell}(x) := (\ell - k + 1)^{-1} \sum_{j=k+1}^{\ell} \mathbb{1}(X_j \leq x)$, and similarly for the second coordinate. Define $\mathbb{G}_n$ exactly as in (3.7). For the derivation of asymptotic properties, we need an additional smoothness assumption on Λ.

Assumption 3.12
The first order partial derivative $\dot{\Lambda}_x = \frac{\partial}{\partial x}\Lambda$ exists and is continuous on $\{(x,y) \in \mathbb{E} : 0 < x < \infty\}$. The first order partial derivative $\dot{\Lambda}_y = \frac{\partial}{\partial y}\Lambda$ exists and is continuous on $\{(x,y) \in \mathbb{E} : 0 < y < \infty\}$.

Proposition 3.13
Suppose that Assumptions 3.1, 3.2 and 3.12 are satisfied. Then, under H_0^{Λ}, we have $\mathbb{G}_n \rightsquigarrow \mathbb{G}_{\Lambda,t_F,t_G}$ in $(\mathcal{B}_\infty([0,1] \times \mathbb{E}), d)$, where

$$\mathbb{G}_{\Lambda,t_F,t_G}(s,x,y) = \mathbb{G}_\Lambda(s,x,y) - \dot{\Lambda}_x(x,y)\frac{s \wedge t_F - st_F}{t_F(1-t_F)}\mathbb{G}_\Lambda(t_F,x,\infty) - \dot{\Lambda}_y(x,y)\frac{s \wedge t_G - st_G}{t_G(1-t_G)}\mathbb{G}_\Lambda(t_G,\infty,y).$$

The limiting distribution is different from the one under constant margins in Proposition 3.3. As a consequence, for approximating critical values of an appropriate test statistic, one needs to modify the methods described in the previous subsections. In the following, we restrict ourselves to the case of testing for a constant coefficient of tail dependence. Let $\hat{\Lambda}_{x,n}(1,1)$ and $\hat{\Lambda}_{y,n}(1,1)$ denote estimators for the partial derivatives of Λ at $(1,1)$ which are consistent under the null hypothesis, for instance

$$\hat{\Lambda}_{x,n}(1,1) := \frac{k^{1/2}}{2}\left\{\hat{\Lambda}_n(1 + k^{-1/2}, 1) - \hat{\Lambda}_n(1 - k^{-1/2}, 1)\right\},$$

and similar for the partial derivative with respect to y (Bücher and Dette, 2013). Furthermore, let $\mathcal{S}_n$ be defined as in (3.8) with pseudo-observations as in (3.12). Observing that $s \mapsto \lambda^{-1/2}\mathbb{G}_\Lambda(s,1,1)$ is a standard Brownian bridge, Proposition 3.13 suggests the following test procedure.

TDC$^{\text{MB}}$-Test. Reject H_0^{λ} if the test statistic $\mathcal{S}_n$ is larger than the $(1-\alpha)$-quantile of the distribution of the random variable $\int_0^1 \{\hat{B}_{t_F,t_G}(s)\}^2\, ds$, where

$$\hat{B}_{t_F,t_G}(s) := B(s) - \hat{\Lambda}_{x,n}(1,1)\frac{s \wedge t_F - st_F}{t_F(1-t_F)}B(t_F) - \hat{\Lambda}_{y,n}(1,1)\frac{s \wedge t_G - st_G}{t_G(1-t_G)}B(t_G),$$

with marginal break points t_F and t_G, and a standard Brownian bridge B.

Analogs of the tests in Section 3.3.4 for the detection of breaks at a given time point $\bar{s}$ are straightforward. In practice, the marginal break points t_F and t_G are rarely known. However, they can usually be estimated at rate n^{-1} which suggests that the previous results remain valid provided t_F and t_G are replaced by suitable estimators $\hat{t}_F$ and $\hat{t}_G$ (see, e.g., Dümbgen, 1991) both within the definition of the pseudo-observations in (3.12) and the approximation of the limit distribution stated in Proposition 3.13. For instance, in

a model with a structural break in the (unconditional) mean for the first marginal, one might use

$$\hat{t}_F = \frac{1}{n} \operatorname*{argmax}_{j=1,\dots,n} \left| \frac{1}{\sqrt{n}} \left(\sum_{i=1}^{j} X_i - \frac{j}{n} \sum_{i=1}^{n} X_i \right) \right|, \tag{3.13}$$

(see, e.g., Bai, 1997; Aue and Horváth, 2013). The simulation results in Section 3.4 show that, indeed, the approximation of the nominal size is quite good.

3.4 Evidence in finite samples

This section investigates the finite sample properties of the proposed testing procedures by means of a simulation study. We observe that the tests are slightly conservative and that they have reasonable power properties. As a main conclusion, we obtain that the tests based on i.i.d. observations and on time series residuals show the same asymptotic behavior.

3.4.1 Setup

As outlined in Jäschke (2014) (see also McNeil et al., 2005, Section 7.5), many commonly applied symmetric tail copulas exhibit a quite similar behavior. When comparing, for instance, the Gumbel model (Gumbel, 1960), the Galambos model (Galambos, 1975) or the Hüsler-Reiss model (Hüsler and Reiss, 1989), the plots of $t \mapsto \Lambda(1-t,t)$, which uniquely determine the tail copula by homogeneity, are nearly indistinguishable. We therefore stick to two cases of one common symmetric and one common asymmetric tail copula model as follows.

(Λ1) The **negative logistic** or Galambos model (Galambos, 1975), defined by

$$\Lambda(1-t,t) = \left\{ (1-t)^{-\theta} + t^{-\theta} \right\}^{-1/\theta}, \quad t \in [0,1],$$

where we chose the parameter $\theta \in [1,\infty)$ such that $\lambda = \Lambda(1,1) = 2^{-1/\theta}$ varies in the set $\{0.25, 0.50, 0.75\}$.

(Λ2) The **asymmetric negative logistic** model (Joe, 1990), defined by

$$\Lambda(1-t,t) = \left\{ (\psi_1(1-t))^{-\theta} + (\psi_2 t)^{-\theta} \right\}^{-1/\theta}, \quad t \in [0,1],$$

with two fixed parameters $\psi_1 = 2/3$, $\psi_2 = 1$ and parameter $\theta \in [1,\infty)$ such that $\lambda = \Lambda(1,1) = 2\left((\psi_1/2)^{-\theta} + (\psi_2/2)^{-\theta}\right)^{-1/\theta}$ varies in the set $\{0.2, 0.4, 0.6\}$.

Note that (Λ1) is a special case of (Λ2) with $\psi_1 = \psi_2 = 1$. Tail copulas being directional derivatives of copulas in the origin, there are of course many copulas that result in the same tail copula. In our simulation study, we basically stick to simulating from one of following two copula families.

(C1) The **Clayton copula**, defined by

$$C(u,v) = \left(u^{-\theta} + v^{-\theta} - 1 \right)^{-1/\theta}, \quad u,v \in [0,1],$$

possesses the negative logistic tail copula as specified in (Λ1). The Clayton copula is widely used for modeling negative tail dependent data.

(C2) The **survival copula of the extreme-value copula**, defined by

$$C(u,v) = \exp\left\{\log(uv)A\left(\frac{\log(v)}{\log(uv)}\right)\right\} \quad u,v \in [0,1], \tag{3.14}$$

where $A(t) = 1 - \Lambda(1-t,t)$ with Λ as in (Λ2), see Segers (2012b), possesses the asymmetric negative logistic tail copula specified in (Λ2).

In order to show that our methods have better power properties than tests for constancy of the whole copula, provided the change only takes place in the tail, we consider a third model.

(C3) Instead of giving a closed form expression for the copula, we state the simulation algorithm for generating a pair (U,V) from that copula.

(a) First, generate $(\tilde{U},\tilde{V}) \sim C$, with C being one of the aforementioned copulas (C1) or (C2).

(b) Then, if $(\tilde{U},\tilde{V}) \in [a,1]^2$, set $(X,Y) = (\tilde{U},\tilde{V})$. If $(\tilde{U},\tilde{V}) \in [0,1]^2 \setminus [a,1]^2$, toss a coin with success probability p. In case of success, define $(X,Y) = (a\bar{U}, a\bar{V})$ with $(\bar{U},\bar{V}) \sim C$, independent of $(\tilde{U},\tilde{V})$, otherwise set $(X,Y) = (\tilde{U},\tilde{V})$.

Note that, for $p = 0$, (X,Y) is distributed according to the initial copula C. Some tedious calculations show that

$$\begin{aligned} H(x,y) &= \mathbb{P}(X \le x, Y \le y) \\ &= \begin{cases} \mu p C(x_{\min}, y_{\min}) + (1-p)C(x,y), & (x,y) \in [0,1]^2 \setminus [a,1]^2, \\ \mu p + C(x,y) - p\{C(x,a) + C(a,y) - C(a,a)\}, & (x,y) \in [a,1]^2, \end{cases} \end{aligned}$$

where $x_{\min} := \min(x/a, 1)$, $y_{\min} := \min(y/a, 1)$ and $\mu := C(a,1) + C(1,a) - C(a,a)$ denotes the C-measure of $[0,1]^2 \setminus [a,1]^2$.

(c) Finally, define (U,V) by $U = H(X,1)$ and $V = H(1,Y)$.

(Estimated) densities of the resulting copulas are depicted in Fig. 3.1 for the Clayton copula with $\theta = 0.5$ (or equivalently $\lambda = 0.25$), for $a = 0.1$ and for $p \in \{0, 0.3\}$. One can clearly see that the two densities are very close to each other on $[a,1]^2$, while they differ significantly in the tail.

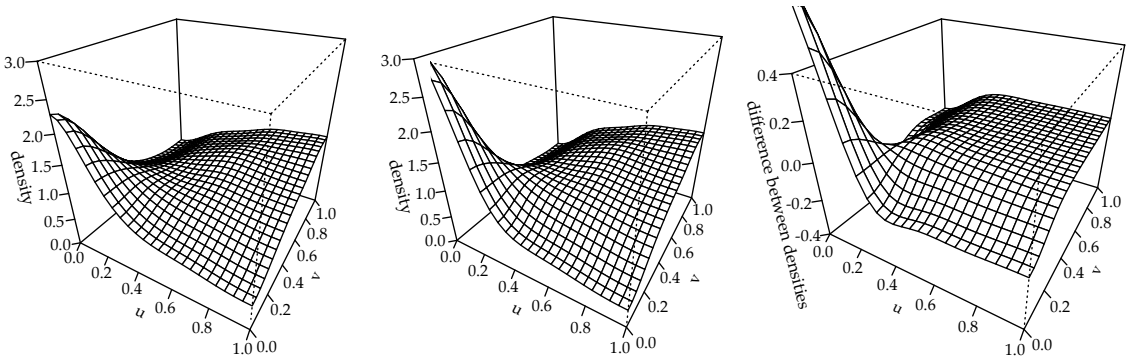

Fig. 3.1. Left: (estimated) copula density from the Clayton copula with $\lambda = 0.25$. Middle: (estimated) copula density from the transformed Clayton copula described in (C3). Right: difference between the two densities.

Our simulation results will show that the distribution of the test statistic based on estimated *marginally almost i.i.d.* residuals is the same as the one of the test statistic based on the unobservable, marginally i.i.d. innovations. Regarding the marginal time series behavior, we consider three different cases. We begin with a consideration of i.i.d. marginals. Subsequently, the simulation results in this case will serve as a benchmark for the application of the tests to *marginally almost i.i.d.* residuals of AR and GARCH time series models. Note that, under the null hypothesis, the latter two models satisfy the assumptions that Rémillard (2010) imposed in the context of related residual-based tests for constancy of the entire copula.

(T1) **Serial independence.** Here, we generate independent random vectors (U_i, V_i), $i = 1, \dots, n$, of one of the aforementioned copulas (C1), (C2) or (C3). Note that, without loss of generality, the marginal distribution can be chosen as standard uniform in this case, since all estimators in this paper are rank-based and hence invariant with respect to monotone transformations.

(T2) **AR(1) residuals.** This setting considers the (under H_0 stationary) solution (Q_i, R_i) of the first order autoregressive process

$$\begin{cases} Q_i = \beta_1 Q_{i-1} + X_i, \\ R_i = \beta_2 R_{i-1} + Y_i, \end{cases} \quad i \in \mathbb{Z}, \tag{3.15}$$

where (X_i, Y_i), $i \in \mathbb{Z}$, are serially independent bivariate random vectors (innovations) whose copula is either from model (C1) or (C2). Here, the (stationary) marginals X_i, $i \in \mathbb{Z}$, are standard normally distributed and Y_i, $i \in \mathbb{Z}$, are t_3-distributed, respectively. The coefficients (β_1, β_2) of the lagged variables vary in the set $\{1/3, 1/2, 2/3\}$. We simulate a time series of length n of this model as follows:

(a) choose some reasonably large negative number M, e.g., $M = -100$;

(b) generate a serially independent sequence $(U_i, V_i) \sim C_i$, $i = M, \dots, n$ of one of the aforementioned copulas C and apply the inverse of the marginal c.d.f.s F and G to the copula sample, vis. $(X_i, Y_i) = (F^{-1}(U_i), G^{-1}(V_i))$;

(c) calculate recursively the values (Q_i, R_i) according to (3.15) for all $i = M + 1, \dots, n$, starting with $(Q_M, R_M) = (X_M, Y_M)$; the last n observations form the final sample.

Since we do not observe the innovations (X_i, Y_i), $i = 1, \dots, n$, we estimate β_1 and β_2 by the Yule-Walker estimators and obtain an *marginally almost i.i.d.* sample (see Section 3.3.1) by considering the time series $(\hat{X}_i, \hat{Y}_i)$ of corresponding estimated residuals defined as

$$\hat{X}_i = Q_i - \hat{\beta}_1 Q_{i-1}, \quad \hat{Y}_i = R_i - \hat{\beta}_2 R_{i-1}, \quad i = 1, \dots, n.$$

(T3) **GARCH(1,1) residuals.** The final setting analyses a two-dimensional time series model which is based on the frequently applied univariate GARCH(1,1) model. More precisely, for $i \in \mathbb{Z}$, we consider the (under H_0 stationary) solution (Q_i, R_i) of

$$\begin{cases} Q_i = \sigma_{i,1} X_i, & \sigma_{i,1}^2 = \omega_1 + \alpha_1 Q_{i-1}^2 + \beta_1 \sigma_{i-1,1}^2, \\ R_i = \sigma_{i,2} Y_i, & \sigma_{i,2}^2 = \omega_2 + \alpha_2 R_{i-1}^2 + \beta_2 \sigma_{i-1,2}^2, \end{cases} \tag{3.16}$$

where (X_i, Y_i), $i \in \mathbb{Z}$, are serially independent bivariate random vectors (innovations) whose copula is again either from model (C1) or (C2). This time, the (stationary) marginals X_i, $i \in \mathbb{Z}$, are standard normally distributed and Y_i, $i \in \mathbb{Z}$, are *normalized* t_3-distributed (i.e., $\sqrt{3}Y_i$, $i \in \mathbb{Z}$, are t_3-distributed), respectively. Following the empirical application of modeling volatility of S&P 500 and DAX daily log-returns in Jondeau et al. (2007) we set the coefficients $\omega_1 = 0.012$, $\omega_2 = 0.037$, $\alpha_1 = 0.072$, $\alpha_2 = 0.115$, $\beta_1 = 0.919$ and $\beta_2 = 0.868$. The long run average variances in this model are given by $\sigma_{M,j} = \sqrt{\omega_j/(1-\alpha_j-\beta_j)}$ which also serve as initial values for simulating a sample from (3.16). The simulation algorithm reads as follows:

(a) generate an independent sample (X_i, Y_i), $i = M, \ldots, n$, as described in steps (a) and (b) of the previous AR(1) setting;

(b) recursively calculate the values (Q_i, R_i) according to (3.16) for all $i = M+1, \ldots, n$, starting with $(Q_M, R_M) = (\sigma_{M,1}X_M, \sigma_{M,2}Y_M)$; again, the last n observations form the final sample.

A *marginally almost i.i.d.* sample $(\hat{X}_i, \hat{Y}_i)$, $i = 1, \ldots, n$, to which we apply the tests is obtained by estimating the standardized residuals

$$\hat{X}_i := \sigma_{i,1}^{-1}(\hat{\omega}_1, \hat{\alpha}_1, \hat{\beta}_1)Q_i, \quad \hat{Y}_i := \sigma_{i,2}^{-1}(\hat{\omega}_2, \hat{\alpha}_2, \hat{\beta}_2)R_i, \quad i = 1, \ldots, n,$$

where the estimates $\hat{\omega}_j, \hat{\alpha}_j$ and $\hat{\beta}_j$, $j = 1, 2$, are calculated by applying standard constraint nonlinear optimization routines.

3.4.2 Results and discussion

The target values of our finite sample study are the simulated rejection probabilities (s.r.p.s) of the Cramér-von Mises tests described in Sections 3.3.2 and 3.3.7 under the null hypothesis and under various alternatives. We calculate the s.r.p.s for three levels of significance $\alpha \in \{1\%, 5\%, 10\%\}$, for two different sample sizes $n = 1000$ and $n = 3000$ and for all of the previously described models. Due to close similarity of some of the results, we report them only partially. The results are based on $N = 5000$ repetitions, unless stated otherwise.

In Table 3.1, we present the results for TDC-Test 1 under 7×3 different null hypotheses. The s.r.p.s for the different levels are stated in columns 3–5 ($n = 1000$) and 8–10 ($n = 3000$), respectively. The parameter k is determined by the plateau algorithm described in Section 3.3.5. The properties of this algorithm are summarized in columns 6 and 7 ($n = 1000$) and 11 and 12 ($n = 3000$), where we state the mean and the sample standard deviation of the estimate k^*. We observe an accurate approximation of the nominal level in all cases, with a tendency of a slight underestimation of the significance level in most of the cases. As already mentioned in Section 3.3, the additional initial estimation step of applying univariate filtering to the time series does not significantly influence the finite sample properties. The slight conservative behavior of the test can be explained by the constancy of the copula in most of our settings: defining $\hat{C}_n^\circ(s,u,v) = \frac{1}{n}\sum_{i=1}^{\lfloor ns \rfloor} \mathbb{1}(\hat{U}_i \le u, \hat{V}_i \le v)$ the test statistic $\mathcal{S}_n$ from Equation (3.8) can be rewritten as

$$\mathcal{S}_n = \left\{\hat{C}_n^\circ(1,k/n,k/n)\right\}^{-1} \int_0^1 \left[\sqrt{n}\left\{\hat{C}_n^\circ(s,k/n,k/n) - s\hat{C}_n^\circ(1,k/n,k/n)\right\}\right]^2 ds.$$

If k was chosen such that $u = k/n > 0$ is constant in n and if, additionally to the tail copula, the copula remained constant over time, it would follow from Corollary 3.3 (a)

in Bücher and Volgushev (2013) that $\mathcal{S}_n$ weakly converges to $\{1 - C(u,u)\} \int_0^1 B^2(s)\, ds$, where B denotes a standard Brownian bridge. Since the critical values of TDC-Test 1 are the quantiles of $\int_0^1 B^2(s)\, ds$, we can easily see that the test rejects too rarely, provided that $C(u,u) > 0$. Note that this argument remains valid if the copula is constant over time only in a neighborhood of (u,u).

A more enlightening view on this issue can be gained from the results in the third block of Table 3.1. Here, we first simulate the first half of the dataset from model (C1) whereas the second half is simulated from model (C2). The parameters are chosen in such a way that both models exhibit the same tail dependence coefficient. Hence, we are still simulating under the null hypothesis but this time the hybrid (copula) model is not constant (over time) at any point on the diagonal of the interior of the unit square. Within the serially independent setting we observe that this is the only case where the s.r.p.s (slightly) exceed some levels of significance.

In Table 3.2, we present simulation results for TDC-Test 1 under 8×3 different alternatives. We consider only the case of one break-point, which is either located at $\bar{s} = 0.25$ or at $\bar{s} = 0.5$, and of three different upward jumps. Note that, for symmetry reasons, the results are essentially the same for corresponding downward jumps at $1 - \bar{s}$. The second column of the table indicates the coefficient of tail dependence before and after the break-point. As one might have expected, higher jumps in the TDC are detected more frequently. Also, breaks at $\bar{s} = 0.5$ are more likely to be detected than breaks at $\bar{s} = 0.25$. Similar as for the null hypotheses presented in Table 3.1, the discrepancy between the corresponding results for the serially independent case and for the time series residuals appears to be negligible. Overall, one can conclude that TDC-Test 1 shows reasonable power properties.

Table 3.1. Simulated rejection probabilities of TDC-Test 1 under various null hypotheses H_0^{Λ}. In the AR(1) scenario the marginals X_i, $i = 1, \ldots, n$, are standard normally distributed and Y_i, $i = 1, \ldots, n$, are t_3-distributed, respectively. The parameters are set to $\beta_1 = 1/3$ and $\beta_2 = 2/3$. In the GARCH(1,1) setting, $\sqrt{3}Y_i$, $i = 1, \ldots, n$, are t_3-distributed.

Tail copula	$\Lambda(1,1)$	$n = 1000$					$n = 3000$				
		$\alpha = 1\%$	$\alpha = 5\%$	$\alpha = 10\%$	avg(k^*)	std(k^*)	$\alpha = 1\%$	$\alpha = 5\%$	$\alpha = 10\%$	avg(k^*)	std(k^*)
Serial independence											
	0.25	0.008	0.046	0.092	52	23	0.008	0.044	0.093	97	49
$(\Lambda 1)$	0.50	0.007	0.044	0.092	71	29	0.009	0.047	0.091	134	59
	0.75	0.007	0.039	0.085	127	46	0.008	0.038	0.088	237	97
	0.20	0.009	0.047	0.095	44	20	0.009	0.045	0.100	80	40
$(\Lambda 2)$	0.40	0.010	0.042	0.091	61	26	0.009	0.047	0.093	113	52
	0.60	0.007	0.046	0.090	84	34	0.008	0.045	0.098	153	67
	0.20	0.010	0.053	0.106	47	21	0.010	0.056	0.098	86	44
$(\Lambda 1)$, $(\Lambda 2)$	0.40	0.008	0.044	0.091	62	26	0.010	0.048	0.092	114	52
	0.60	0.009	0.047	0.092	87	33	0.010	0.048	0.093	159	69
AR(1) residuals											
	0.25	0.008	0.046	0.098	52	23	0.011	0.047	0.099	97	49
$(\Lambda 1)$	0.50	0.009	0.049	0.091	72	29	0.011	0.049	0.096	134	60
	0.75	0.007	0.036	0.081	126	46	0.008	0.041	0.090	235	95
	0.20	0.007	0.042	0.093	44	20	0.009	0.049	0.099	81	40
$(\Lambda 2)$	0.40	0.007	0.046	0.092	61	25	0.009	0.045	0.098	112	42
	0.60	0.009	0.043	0.091	83	34	0.010	0.045	0.094	154	67
GARCH(1,1) residuals											
	0.25	0.008	0.047	0.092	52	23	0.008	0.047	0.096	96	48
$(\Lambda 1)$	0.50	0.007	0.045	0.090	72	29	0.007	0.048	0.093	134	59
	0.75	0.006	0.038	0.083	127	45	0.007	0.041	0.087	235	94
	0.20	0.007	0.043	0.095	44	20	0.008	0.046	0.092	81	42
$(\Lambda 2)$	0.40	0.009	0.045	0.090	61	25	0.010	0.043	0.095	113	52
	0.60	0.007	0.044	0.088	85	33	0.008	0.047	0.089	154	68

Table 3.2. Simulated rejection probabilities of TDC-Test 1 under various alternatives H_1^{λ}. The marginal time series models are the same as in Table 3.1 except that $\beta_1 = 1/2 = \beta_2$.

Tail copula	$\Lambda(1,1)$	$n = 1000$					$n = 3000$				
		$\alpha = 1\%$	$\alpha = 5\%$	$\alpha = 10\%$	avg(k^*)	std(k^*)	$\alpha = 1\%$	$\alpha = 5\%$	$\alpha = 10\%$	avg(k^*)	std(k^*)
Serial independence, $\bar{s} = 0.5$											
	0.25 to 0.50	0.051	0.165	0.261	61	26	0.136	0.309	0.426	113	53
(Λ1)	0.25 to 0.75	0.321	0.563	0.694	76	30	0.679	0.845	0.904	140	64
	0.50 to 0.75	0.073	0.211	0.321	93	35	0.185	0.389	0.507	171	71
	0.20 to 0.40	0.054	0.175	0.279	52	22	0.128	0.306	0.431	94	45
(Λ2)	0.20 to 0.60	0.247	0.485	0.613	60	25	0.547	0.752	0.830	111	52
	0.40 to 0.60	0.044	0.139	0.231	71	29	0.105	0.258	0.369	130	59
Serial independence, $\bar{s} = 0.25$											
	0.25 to 0.50	0.019	0.091	0.174	66	27	0.054	0.173	0.277	122	52
(Λ1)	0.25 to 0.75	0.125	0.340	0.478	95	36	0.394	0.650	0.763	174	74
	0.50 to 0.75	0.036	0.129	0.217	107	40	0.077	0.225	0.339	197	82
	0.20 to 0.40	0.022	0.092	0.172	56	24	0.050	0.161	0.265	104	49
(Λ2)	0.20 to 0.60	0.090	0.262	0.395	71	29	0.252	0.498	0.640	129	60
	0.40 to 0.60	0.017	0.079	0.154	77	31	0.046	0.148	0.238	144	63
AR(1) residuals, $\bar{s} = 0.5$											
	0.25 to 0.50	0.050	0.164	0.256	61	26	0.125	0.300	0.420	114	53
(Λ1)	0.25 to 0.75	0.329	0.567	0.690	76	30	0.686	0.849	0.904	138	62
	0.50 to 0.75	0.073	0.205	0.311	92	35	0.190	0.390	0.506	169	72
	0.20 to 0.40	0.052	0.170	0.262	52	22	0.133	0.295	0.413	96	48
(Λ2)	0.20 to 0.60	0.256	0.489	0.614	61	25	0.565	0.766	0.838	111	53
	0.40 to 0.60	0.044	0.148	0.242	71	29	0.109	0.268	0.386	131	59
GARCH(1,1) residuals, $\bar{s} = 0.5$											
	0.25 to 0.50	0.051	0.159	0.256	61	25	0.138	0.316	0.439	113	52
(Λ1)	0.25 to 0.75	0.335	0.575	0.685	76	30	0.682	0.849	0.906	141	63
	0.50 to 0.75	0.076	0.213	0.320	91	35	0.192	0.387	0.511	169	70
	0.20 to 0.40	0.053	0.174	0.278	52	23	0.137	0.317	0.429	95	45
(Λ2)	0.20 to 0.60	0.262	0.487	0.619	60	25	0.550	0.747	0.830	111	53
	0.40 to 0.60	0.046	0.147	0.237	71	29	0.106	0.262	0.375	132	61

Table 3.3. Simulated rejection probabilities of TDC-Test 2 and the TC-Test under the null hypothesis and one alternative using the Clayton copula within the serial independence setting.

Scenario	$\Lambda(1,1)$	$n = 1000$					$n = 3000$				
		$\alpha = 1\%$	$\alpha = 5\%$	$\alpha = 10\%$	avg(k^*)	std(k^*)	$\alpha = 1\%$	$\alpha = 5\%$	$\alpha = 10\%$	avg(k^*)	std(k^*)
TDC-Test 2											
	0.25	0.007	0.046	0.088	52	23	0.007	0.049	0.096	97	51
H_0^Λ	0.50	0.010	0.052	0.116	73	28	0.011	0.052	0.099	135	62
	0.75	0.009	0.052	0.110	129	47	0.012	0.044	0.092	239	96
	0.25 to 0.50	0.053	0.179	0.277	61	26	0.159	0.320	0.455	113	52
$H_1^\lambda, \bar{s} = 0.5$	0.25 to 0.75	0.353	0.579	0.695	77	31	0.688	0.855	0.901	138	61
	0.50 to 0.75	0.091	0.256	0.359	93	34	0.225	0.425	0.541	171	72
TC-Test											
	0.25	0.017	0.045	0.100	51	23	0.006	0.051	0.091	95	48
H_0^Λ	0.50	0.012	0.044	0.099	70	29	0.008	0.039	0.089	135	58
	0.75	0.010	0.046	0.103	127	46	0.013	0.060	0.105	239	95
	0.25 to 0.50	0.049	0.152	0.246	61	25	0.150	0.312	0.416	116	52
$H_1^\lambda, \bar{s} = 0.5$	0.25 to 0.75	0.276	0.530	0.639	76	30	0.619	0.813	0.882	141	64
	0.50 to 0.75	0.063	0.169	0.267	91	35	0.125	0.302	0.416	169	72

Table 3.4. Simulated rejection probabilities of TDC-Test 1 and the TC-Test in the serial independence setting: The parameters are chosen such that the TDC remains constant over time while the tail copula does not.

Scenario	$\Lambda(1,1)$	$n = 1000$					$n = 3000$				
		$\alpha = 1\%$	$\alpha = 5\%$	$\alpha = 10\%$	avg(k^*)	std(k^*)	$\alpha = 1\%$	$\alpha = 5\%$	$\alpha = 10\%$	avg(k^*)	std(k^*)
TDC-Test 1											
	0.20	0.009	0.048	0.102	45	21	0.010	0.053	0.103	95	46
$H_0^\lambda \cap H_1^\Lambda$	0.40	0.009	0.049	0.103	63	26	0.009	0.048	0.101	120	53
	0.60	0.010	0.053	0.107	89	35	0.012	0.050	0.101	168	72
TC-Test											
	0.20	0.032	0.183	0.355	45	20	0.236	0.566	0.744	92	44
$H_0^\lambda \cap H_1^\Lambda$	0.40	0.047	0.219	0.447	60	25	0.279	0.666	0.835	122	54
	0.60	0.024	0.160	0.381	91	34	0.140	0.509	0.747	169	72

Table 3.3 briefly presents simulation results for TDC-Test 2 and the TC-Test. For the sake of brevity, we only report the s.r.p.s for the Clayton tail copula model and the serially independent case, since the results for the other cases do not convey any additional insights. The s.r.p.s are based on $N = 1000$ simulation runs, while the sample size is again either $n = 1000$ or $n = 3000$ with $B = 500$ bootstrap replications ($B = 300$ for the TC-Test) and multipliers $\xi_i^{(b)}$ that are uniformly distributed on the set $\{-1, 1\}$. In comparison to its competitor TDC-Test 1, we observe that with TDC-Test 2, there seems to be slight evidence that the rejection probabilities are higher both under the null hypothesis as well as under the alternative. Regarding the null hypothesis, a comparable observation can be made for the TC-Test, but the power under the alternative is even lower than that of TDC-Test 1.

The next results of this subsection, presented in Table 3.4, concern a setting where the tail dependence coefficient stays constant over time whereas the tail copula may change at points $(x, y) \neq (1, 1)$ (cf. third block of Table 3.1). From theory, one would expect that the TC-Test should be able to detect those breaks, whereas the TDC-Tests should hold the nominal size. We only consider breaks at $\bar{s} = 0.5$ and model $(\Lambda 2)$ (i.e., we simulate from (C2)) which will allow to construct tail copulas that are equal in $(1, 1)$, but sufficiently different in other points. More precisely, for a given $\lambda \in \{0.2, 0.4, 0.6\}$, we choose $\psi_1 = \lambda$, $\psi_2 = 1$ and $\theta = 100$ for $s \leq \bar{s}$ and we set $\psi_1 = 1$, $\psi_2 = \lambda$ and $\theta = 100$ for $s > \bar{s}$. For $\lambda = 0.4$, the corresponding graphs of $t \mapsto \Lambda(2 - 2t, 2t)$ are shown in Fig. 3.2. Note that, for fixed ψ_1, ψ_2, we have

$$\Lambda_\infty(1 - t, t) := \lim_{\theta \to \infty} \Lambda(1 - t, t) = \{\psi_1(1 - t)\} \wedge (\psi_2 t).$$

The corresponding *limit* copula defined in (3.14) is the well-known Marshall–Olkin copula, whose TDC is given by $\min(\psi_1, \psi_2)$, see Segers (2012b). With our choice of $\theta = 100$ in $(\Lambda 2)$, the difference between the TDC and $\min(\psi_1, \psi_2) = \lambda$ is less than the machine accuracy 10^{-16}.

The results in Table 3.4 confirm the expectations: the TC-Test (again based on $N = 1000$ simulation runs and $B = 300$ bootstrap replications) has considerable power while TDC-Test 1 basically keeps the nominal size. As a conclusion, the developed testing procedures allow for empirically distinguishing between constant tail dependence coefficient and constant tail copula.

Next, we investigate a scenario (for sample size $n = 1000$) where the simulated copula is constant at the center of the distribution throughout the sample period but exhibiting a significant structural break in the tail. For that purpose, we consider one break at $\bar{s} = 0.5$, and we simulate from the Clayton copula with $\lambda = 0.25$ before the break, and from the copula described in (C3), with $a = 0.1$, $p \in \{0, 0.25, 0.5, 0.75, 1\}$ and the Clayton copula with $\lambda = 0.25$, after the break. The results for TDC-Test 1 can be found in the right part of Table 3.5. As expected, the significant break in the tail is well detected by our methods.

Since our methods focus on the tail dependence, they should have, at least in this particular setting, more power than related tests for constancy of the whole copula. This is confirmed by the results in the left part of Table 3.5, which show the s.r.p.s for an L^2-type version of the tests for constancy of the copula proposed in Rémillard (2010); Bücher and Ruppert (2013). More precisely, recalling that $\hat{C}_n^\circ(s, u, v) = \frac{1}{n} \sum_{i=1}^{\lfloor ns \rfloor} \mathbb{1}(\hat{U}_i \leq u, \hat{V}_i \leq v)$, the results are based on the test statistic

$$\mathcal{R}_n := n \int_{[0,1]^3} \left\{ \hat{C}_n^\circ(s, u, v) - s\hat{C}_n^\circ(1, u, v) \right\}^2 d(s, u, v),$$

along with the bootstrap approximation $\mathcal{R}_{n,\xi^{(b)}} := \int_{[0,1]^3} \mathbb{G}_{n,\xi^{(b)}}(s, u, v)^2 \, d(s, u, v)$ with $\mathbb{G}_{n,\xi^{(b)}}$ as defined in (3.10) based on the choice $k = n$. In practice, we approximate the

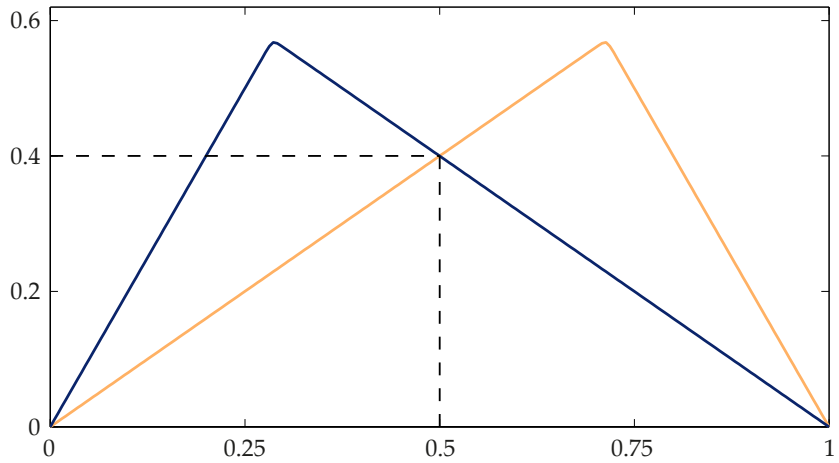

Fig. 3.2. Negative asymmetric logistic model ($\Lambda 2$) for $\psi_1 = 0.4$, $\psi_2 = 1$, $\theta = 100$ (blue) and $\psi_1 = 1$, $\psi_2 = 0.4$, $\theta = 100$ (yellow) evaluated on the straight line $(2 - 2t, 2t)$, $t \in [0, 1]$. Both models exhibit the same tail dependence coefficient $\lambda = 0.4$.

integral through a sum over a finite grid. We use $N = 500$ repetitions and $B = 300$ bootstrap replications with multipliers that are uniformly distributed on the set $\{-1, 1\}$. It is clearly visible that, as expected, the power of the copula constancy test is lower than that of TDC-Test 1.

Finally, we investigate the detection of breaks in the tail dependence coefficient under the potential presence of breaks in the marginal laws. We restrict ourselves to a comparison of the TDC^{MB}-Test to TDC-Test 1 in a serially independent case. Table 3.6 shows the s.r.p.s for the TDC^{MB}-Test, based on samples from copula (C1) with or without a break in the TDC at $\bar{s} = 0.5$ and with marginal laws being either uniform on $[0, 1]$ for the entire sample or being uniform on $[0, 1]$ before $t_F = 0.25$ and $t_G = 0.5$ and uniform on $[5, 6]$ after t_F and t_G, respectively. The marginal breaks are estimated by (3.13). Critical values are obtained by simulating 500 times from the respective limiting distribution, where the Brownian bridge is simulated based on a grid of length $1/500$. When comparing the simulations results in the case of a constant mean to the ones from TDC-Test 1 (see the first block of Table 3.1 and Table 3.2, respectively), the TDC^{MB}-Test has better power properties. On the other hand, it seems to be quite liberal compared to the slightly conservative TDC-Test 1. Moreover, the computational costs are substantially increased compared to TDC-Test 1: first, marginal breaks have to be estimated, and second, as the limiting distribution is not pivotal, additional estimation of the partial derivatives of Λ and simulations of a Brownian bridge are necessary. Finally, note that applying TDC-Test 1 to observations underlying a mean change in the marginal laws seems to be useless as under both H_0^{Λ} and H_1^{λ} all s.r.p.s are very close to 1.

Table 3.5. Simulated rejection probabilities of a test for constancy of the entire copula and TDC-Test 1 in the serial independence setting ($n = 1000$) in which there is a structural break in the tail but not in the center of the distribution.

Scenario	p	Copula-Test			TDC-Test 1				
		$\alpha = 1\%$	$\alpha = 5\%$	$\alpha = 10\%$	$\alpha = 1\%$	$\alpha = 5\%$	$\alpha = 10\%$	avg(k^*)	std(k^*)
H_0^Λ	0.00	0.010	0.046	0.086	0.008	0.040	0.091	52	23
$H_1^\lambda, \bar{s} = 0.5$	0.25	0.014	0.060	0.120	0.041	0.128	0.199	67	32
	0.50	0.022	0.070	0.124	0.187	0.340	0.436	84	43
	0.75	0.040	0.126	0.236	0.346	0.481	0.554	102	57
	1.00	0.070	0.230	0.330	0.430	0.542	0.609	121	73

Table 3.6. Simulated rejection probabilities for the TDC$^{\text{MB}}$-Test in a serially independent setting with and without a mean change in the margins.

Scenario	$\Lambda(1,1)$	$n = 1000$					$n = 3000$				
		$\alpha = 1\%$	$\alpha = 5\%$	$\alpha = 10\%$	avg(k^*)	std(k^*)	$\alpha = 1\%$	$\alpha = 5\%$	$\alpha = 10\%$	avg(k^*)	std(k^*)
TDC$^{\text{MB}}$-Test, constant mean											
H_0^Λ	0.25	0.014	0.061	0.111	52	24	0.013	0.063	0.117	98	49
	0.50	0.017	0.070	0.120	71	29	0.021	0.073	0.122	133	58
	0.75	0.022	0.072	0.122	120	44	0.025	0.075	0.130	231	95
$H_1^\lambda, \bar{s} = 0.5$	0.25 to 0.50	0.122	0.262	0.370	61	26	0.300	0.500	0.609	113	53
	0.25 to 0.75	0.640	0.807	0.871	73	30	0.912	0.963	0.979	138	62
	0.50 to 0.75	0.229	0.420	0.532	98	34	0.502	0.693	0.779	168	72
TDC$^{\text{MB}}$-Test, mean change											
H_0^Λ	0.25	0.014	0.061	0.116	53	23	0.017	0.065	0.120	99	50
	0.50	0.015	0.062	0.122	71	28	0.019	0.066	0.121	132	58
	0.75	0.013	0.053	0.103	120	43	0.013	0.054	0.104	231	94
$H_1^\lambda, \bar{s} = 0.5$	0.25 to 0.50	0.129	0.288	0.408	61	26	0.310	0.512	0.619	112	53
	0.25 to 0.75	0.688	0.847	0.898	73	31	0.920	0.968	0.979	136	61
	0.50 to 0.75	0.252	0.449	0.560	90	35	0.511	0.703	0.788	167	70

3.5 Empirical applications

3.5.1 Energy sector

In this subsection, we reinvestigate the bivariate dataset from Jäschke (2014) consisting of $n = 1001$ daily closing quotes of the WTI Cushing Crude Oil Spot and the Bloomberg European Dated Brent from October 2, 2006, to October 1, 2010, collected from Bloomberg's Financial Information Services. The analysis of the extremal dependence between the log-returns of the two time series in Jäschke (2014) is based on the implicit assumption that the tail dependence structure, more precisely their lower tail copula, remains constant over time. We are going to verify this assumption by applying the tests developed in Section 3.3.

As pointed out in Jäschke (2014), the assumption of a serially independent sample is unrealistic. To account for autocorrelation and volatility clustering, it is shown that an ARMA(0,0)-EGARCH(2,3)-model including an explanatory variable (U.S. crude oil inventory) and the skewed generalized error distribution adequately describes the data generating process for the log-returns of the WTI time series. Regarding the daily Brent spot log-returns, an ARMA(1,1)-EGARCH(2,3)-model including U.S. crude oil inventory as an explanatory variable and the skewed generalized error distribution provides an adequate fit. In particular, there is no clear evidence against the assumption of marginal stationarity in both time series.

We calculate standardized residuals on the basis of the preceding time series models. A first view on the lower tail dependence between these residuals can be gained from the diagnostic plot in Fig. 3.3. For various values of k such that k/n lies in the set $\{0.05, 0.06, \ldots, 0.15\}$, we depict the points in time where the pseudo-observations in both coordinates fall simultaneously below the value k/n. Note that these are exactly the joint extreme events inside the indicators in the definition of the empirical tail dependence coefficient. As the points are quite equally spaced in time, the picture suggests that the tail dependence remains rather constant.

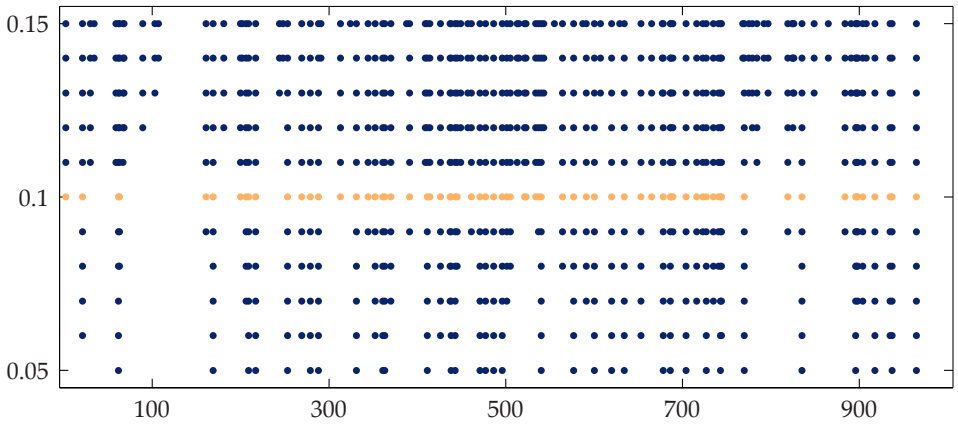

Fig. 3.3. (WTI and Brent time series) Points in time where pseudo-observations in both coordinates fall simultaneously below the value k/n, for $k/n \in \{0.05, 0.06, \ldots, 0.15\}$. The yellow row corresponds to the plateau ratio $k^*/n = 104/1001 \approx 10\%$.

More formally, we proceed by checking the hypothesis H_0^λ of constancy of the tail dependence coefficients by an application of TDC-Test 1. First, in order to obtain a reasonable choice for the parameter k, we use the plateau algorithm from Section 3.3.5 with bandwidth $b = \lfloor 0.005n \rfloor = 5$. This yields a value of $k^* = 104$ (which is also depicted

in yellow in Fig. 3.3) and a plateau of length $\ell = 31$. Following Frahm et al. (2005), the average of the 31 empirical lower tail dependence coefficients on this plateau, given by $\hat{\lambda} = 0.732$, provides a good estimate for λ. Figure 3.4 shows the corresponding standardized sequential empirical tail copula process $ns \mapsto \hat{\lambda}^{-1/2}\mathbb{G}_n(s,1,1)$ for $k^* = 104$. The graph seems to be indistinguishable from a simulated path of a one-dimensional standard Brownian bridge which indicates that the null hypothesis cannot be rejected. In Fig. 3.5 we depict both the value of the Cramér-von Mises type test statistic $\mathcal{S}_n$ defined in (3.8) (yellow) as well as the corresponding p-values (blue) as a function of k. The dashed vertical line shows the outcomes for the plateau optimal $k^* = 104$, in which case we obtain $\mathcal{S}_n = 0.285$ with a resulting p-value of 0.15. Consequently, the null hypothesis H_0^λ cannot be rejected at a 5% level of significance. Moreover, Fig. 3.5 shows that this conclusion is robust with respect to different choices of k. Results for TDC-Test 2 are very similar and are not depicted for the sake of brevity.

Finally, the assumption of a constant lower tail copula is verified by testing for the hypothesis H_0^Λ. We apply the TC-Test from Section 3.3.2 with $B = 2000$ bootstrap replications using the plateau optimal $k^* = 104$. We obtain $\mathcal{T}_n = 0.069$ with a resulting p-value of 0.29. Again, the null hypothesis cannot be rejected at a 5% level of significance. Similar as for the tests for H_0^λ, this conclusion is robust with respect to different choices of k.

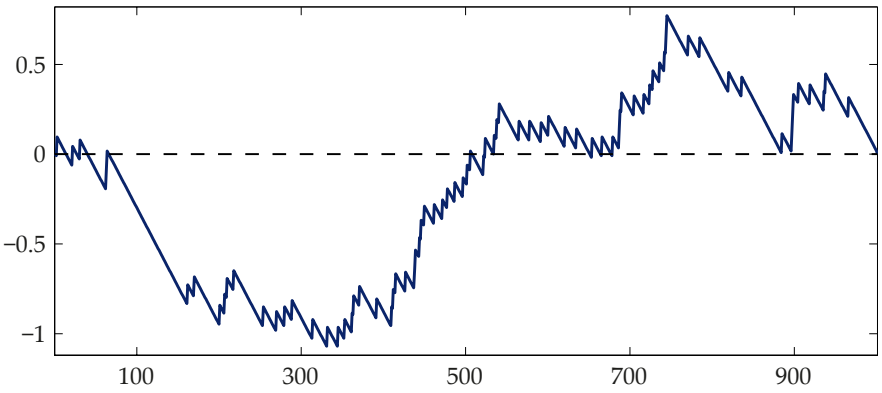

Fig. 3.4. (WTI and Brent time series) Standardized sequential empirical tail copula process $\hat{\lambda}^{-1/2}\mathbb{G}_n(s,1,1)$ for $k^* = 104$ with respect to ns, $s \in [0,1]$.

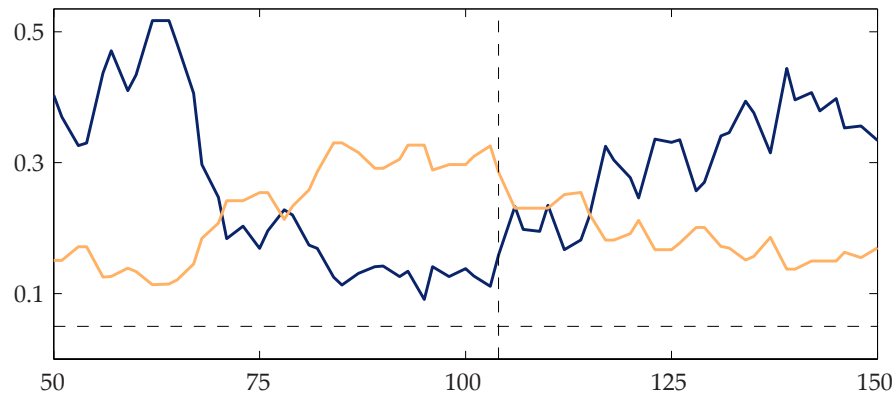

Fig. 3.5. (WTI and Brent time series) Test statistics $\mathcal{S}_n$ (yellow) and corresponding p-values (blue) for different k. The horizontal line indicates the 5% level of significance, the vertical one the plateau $k^* = 104$.

3.5.2 Financial markets

As an empirical application from the finance sector, we consider the Dow Jones Industrial Average and the Nasdaq Composite time series around Black Monday on 19th of October 1987. This dataset covers $n = 1768$ log-returns from daily closing quotes between January 4, 1984, and December 31, 1990, collected from Datastream. Related studies in Wied et al. (2014) and Dehling et al. (2013) try to examine whether Black Monday constitutes a break in the dependence structure between the two time series. The outcomes of their studies do not provide a clear picture, as the answer depends on the applied test statistic. While the test for a constant Pearson correlation rejects the null hypothesis of constant correlation, the more robust (rank-based) tests for constant Spearman's rho and Kendall's tau yield no evidence for breaks. In these papers, the contrasting result is explained by the fact that the (unfiltered) time series contain several heavy outliers around Black Monday which seriously affect the Pearson-, but not the rank-based tests for Spearman's rho and Kendall's tau.

For our analysis, we begin by an investigation of the univariate time series. Applying the model selection and verification criteria from Jäschke (2014), we find that an ARMA(0,0)-GARCH(1,1)-model with t-distribution for the Dow Jones log-returns and an ARMA(1,0)-GARCH(1,1)-model with skewed t-distribution for the Nasdaq equivalent provide the best fits among a number of common stationary time series models. Details on the parameter estimation are given in Table 3.7. Note that more suitable models might be found by considering piecewise stationary models and by subsequently applying the tests from Section 3.3.7 where necessary. For our illustrative purposes, we restrict ourselves to the former models and to the tests from Sections 3.3.2 and 3.3.4 in the following.

Along the lines of Dehling et al. (2013) we first seek to answer the question whether Black Monday constitutes a break in the tail dependence between the two time series. A positive answer would indicate that the market conditions have substantially changed after this date. For the ease of a clear exposition, we restrict ourselves to an investigation of the lower tail dependence coefficient. A first visual description of the joint tail behavior similar to the one in Fig. 3.3 can be found in Fig. 3.6 which, however, does not provide a clear picture: even though there seems to be a tendency of stronger tail dependence for later dates in the time series, it is unclear whether this is due to a break on Black Monday (second dashed vertical line).

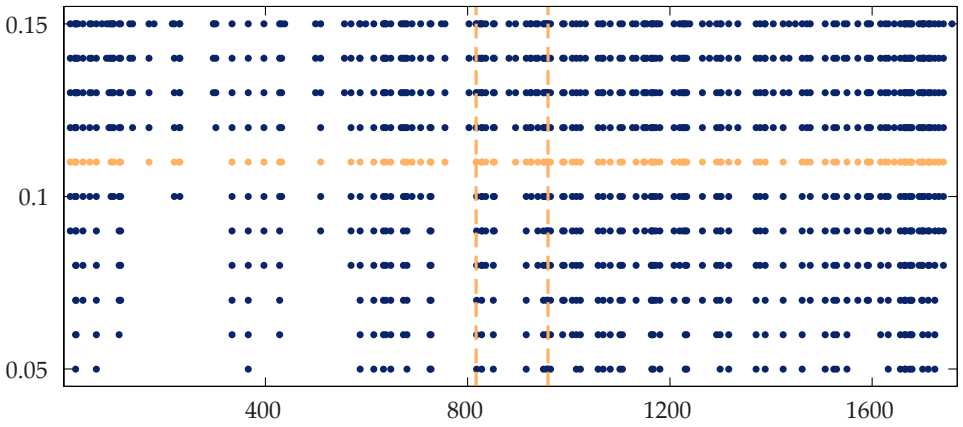

Fig. 3.6. (Dow Jones and Nasdaq time series) Points in time where pseudo-observations in both coordinates fall simultaneously below the value k/n, for $k/n \in \{0.05, 0.06, \ldots, 0.15\}$. The yellow row corresponds to the plateau ratio $k^*/n \approx 11\%$. The first yellow vertical line reflects the argmax-estimator $\lfloor n\hat{s}^{\lambda} \rfloor = 817$, the second equivalent indicates Black Monday $\lfloor n\bar{s}_{BM} \rfloor = 959$.

Table 3.7. Maximum likelihood estimates together with their corresponding standard errors for the Dow Jones ARMA(0,0)-GARCH(1,1)-model with t-distribution and the Nasdaq ARMA(1,0)-GARCH(1,1)-model including the skewed t-distribution. All estimates but the additive constant ω are significant at the 1% level.

Parameter	Dow Jones log-returns		Nasdaq log-returns	
	Estimate	std. error	Estimate	std. error
Mean equation				
μ	0.0006	0.0002	0.0005	0.0002
θ_1	–	–	0.2714	0.0234
Variance equation				
ω	0.0000	0.0000	0.0000	0.0000
α_1	0.0349	0.0084	0.1407	0.0179
β_1	0.9373	0.0080	0.7914	0.0182
Distribution				
ξ	–	–	0.8531	0.0294
ν	4.2016	0.4390	5.3001	0.4135

In the following, we examine this formally by applying the tests from Section 3.3, in particular the test from Section 3.3.4 for a specific break-point. First, a careful inspection of the plot $k \mapsto \mathrm{TDC}(k)$ and the statistics defining the plateau algorithm (which are not depicted for the sake of brevity) suggests that $k^* = 191$ is a reasonable choice for the parameter k, with a corresponding length of the plateau of $\ell = 41$. The average of the empirical lower tail dependence coefficients over the corresponding values $k \in \{171, \dots, 211\}$ is given by $\hat{\lambda} = 0.620$.

Now, we apply the test from Section 3.3.4 for a specific break-point at $\lfloor n\bar{s}_{\mathrm{BM}} \rfloor = 959$, the date of Black Monday. The results are depicted in Fig. 3.7, where we plot the p-values of the test against the parameter k. For $k^* = 191$, the resulting p-value of 0.082 does not allow for a clear rejection of the null hypothesis. In contrast to this, slightly lower values of k yield a rejection at the 5% level of significance, whence, as a summary, there seems to be some light, but disputable evidence against H_0. However, the rejection of the null hypothesis might be due to different reasons than a break precisely on Black Monday. To conclude upon the latter, one would have to accept the hypothesis of constancy of the lower tail dependence coefficient in the subsamples before and after Black Monday. Therefore, we perform the corresponding TDC-Test 1 in the subsamples, whose results are depicted in Figs. 3.8 and 3.9 in a similar manner as before; in particular, they are based on new (plateau-based) choices of k for the reduced samples. We can accept constancy after Black Monday, but have to reject it for the subsample before Black Monday. A summary of the results can also be found in the first two columns of Table 3.8.

In principal, one could now proceed by a refined analysis of the subsample before Black Monday in order to identify potential additional break-points. Motivated by the diagnostic plot in Fig. 3.6, we prefer an application of TDC-Test 1 to the whole sample since this might reveal that a model with at most one break-point is also appropriate. In other words, we dismiss the initial guess of a break precisely on Black Monday and rather split the sample at an estimated break-point, hoping that the latter yields a simpler model with at most one break-point.

We do not depict the results of the corresponding test, since it clearly rejects the null hypothesis H_0^λ at the 1% level of significance for almost all choices of k. A short summary can be found in the last column of Table 3.8. More enlightening conclusions can be drawn from the plot of the function $ns \mapsto |\hat{\lambda}^{-1/2}\mathbb{G}_n(s,1,1)|$ in Fig. 3.10, for $k^* = 191$. The dashed

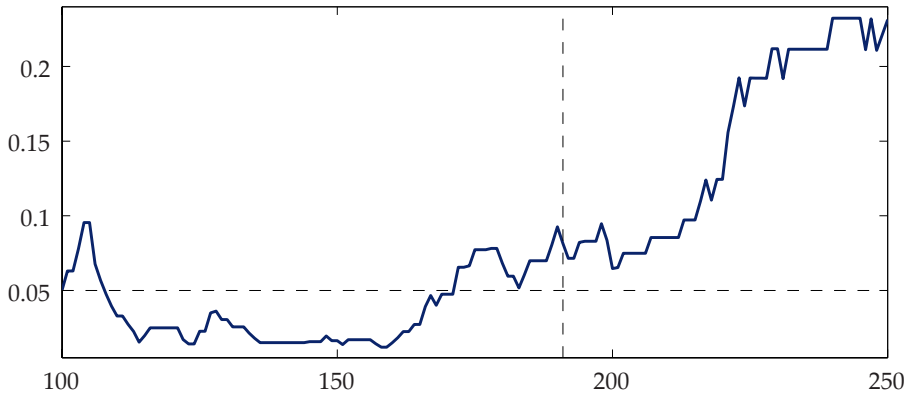

Fig. 3.7. (Dow Jones and Nasdaq time series) Chi-squared test for a specific break at $\lfloor n\bar{s}_{\mathrm{BM}} \rfloor = 959$: p-values for different k. The horizontal line indicates the 5% level of significance, the vertical one the plateau $k^* = 191$.

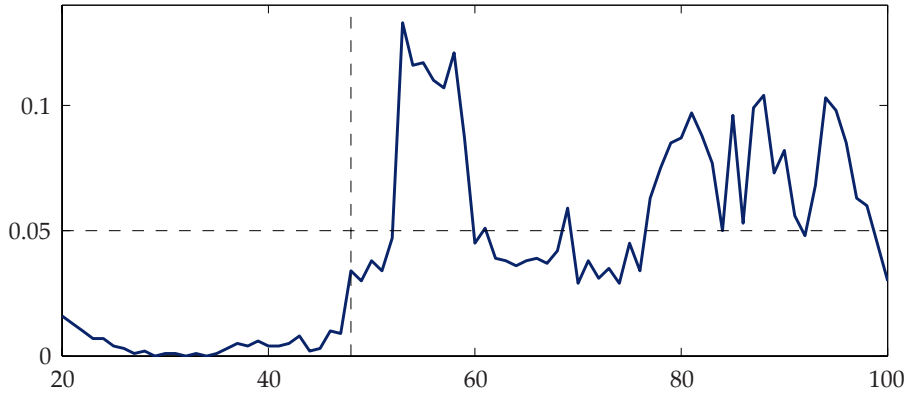

Fig. 3.8. (Dow Jones and Nasdaq time series) TDC-Test 1 for the subsample before $\lfloor n\bar{s}_{\mathrm{BM}} \rfloor = 959$: p-values for different k. The horizontal line indicates the 5% level of significance, the vertical one the plateau $k^* = 48$.

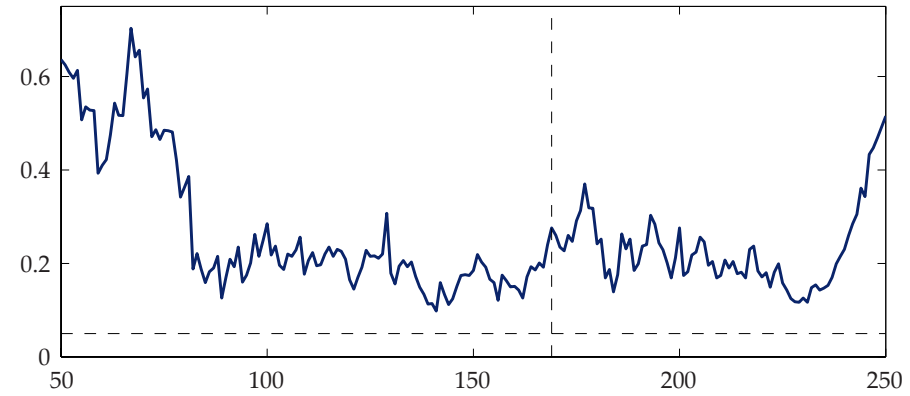

Fig. 3.9. (Dow Jones and Nasdaq time series) TDC-Test 1 for the subsample after $\lfloor n\bar{s}_{\mathrm{BM}} \rfloor = 959$ (including Black Monday): p-values for different k. The horizontal line indicates the 5% level of significance, the vertical one the plateau $k^* = 169$.

Table 3.8. Summary of results for TDC-Test 1 applied to the subsample before Black Monday, to the subsample after Black Monday and to the full sample.

Parameter	before Black Monday	after Black Monday	full sample size
n	958	810	1768
k^*	48	169	191
ℓ	30	28	41
$\hat{\lambda}$	0.449	0.678	0.620
$\mathcal{S}_n$	0.546	0.211	1.064
p-value	0.028	0.244	0.003

vertical lines denote Black Monday $\lfloor n\bar{s}_{BM} \rfloor = 959$ (second line) and the value $\lfloor n\hat{s}^{\lambda} \rfloor = 817$ where the graph attains its maximum. The latter corresponds to the 27th of March 1987 and appears to be the argmax for most choices of k in a neighborhood of $k^* = 191$. We split the sample at this estimated break-point and conduct a refined analysis in the respective subsamples. The procedure is similar to what we have done before, whence we restrict ourselves to a brief summary of the results: in both subsamples, we cannot reject the null hypothesis for all reasonable choices of k, including the values obtained from the plateau algorithm, with p-values lying between 0.2 and 0.5. Similar to the values in Table 3.8 we find $\hat{\lambda} = 0.430$ for the first subsample ($k^* = 43$) and $\hat{\lambda} = 0.656$ for the second one ($k^* = 57$), respectively.

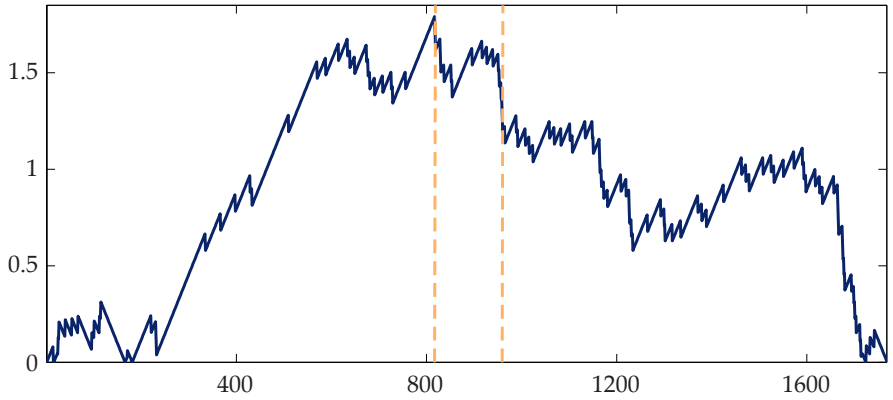

Fig. 3.10. (Dow Jones and Nasdaq time series) Absolute standardized sequential empirical tail copula process $|\hat{\lambda}^{-1/2}\mathbb{G}_n(s,1,1)|$ for $k^* = 191$ with respect to ns, $s \in [0,1]$. The first yellow vertical line indicates the argmax estimator $\lfloor n\hat{s}^{\lambda} \rfloor = 817$, the second one shows Black Monday $\lfloor n\bar{s}_{\mathrm{BM}} \rfloor = 959$.

We conclude this application with a short summary of the main findings:

(i) The test for a break on Black Monday does not yield entirely unambiguous results; in particular, we have to reject the null hypothesis of constant tail dependence in the subsample before Black Monday resulting in an overall model with more than one break-point.

(ii) Testing against the existence of *some* unspecified break-point in the full sample clearly rejects the null, with an estimated break-point at $\lfloor n\hat{s}^{\lambda} \rfloor = 817$. Since we cannot reject the null hypothesis in the corresponding subsamples, an overall model with only one break-point can be accepted.

3.6 Conclusion and Outlook

We developed new tests for detecting structural breaks in the tail dependence of multivariate time series, derived their theoretical properties, investigated their finite-sample performance and applied them to energy and financial market data.

Our work hints at interesting directions for further research. First of all, we did not give a formal proof for the conjecture derived from the simulation study, that the test statistics based on estimated residuals show the same asymptotic behavior as the ones based on i.i.d. samples. To the best of our knowledge, this problem is also unsolved for the estimation techniques described in Section 3.2: under what conditions does (or does not) the additional estimation step of forming *marginally almost i.i.d.* residuals influence the asymptotic behavior of the nonparametric estimators for the tail dependence? Second, extensions to the case of serially dependent datasets (e.g., to mixing sequences) would allow to check for constant tail dependence of the raw data which might also be of interest for practitioners. In particular with a view on the necessary (block) bootstrap procedure this could be a quite challenging task.

Finally, a deeper investigation of the results in Section 3.3.7 would be a worthwhile topic of future research: under what conditions can one replace the (unknown) marginal break points in Proposition 3.13 by their empirical counterparts? How can one treat the case of an unknown number of breaks in the marginals, and how can one adapt the bootstrap methodology to these settings?

3.7 Proof of the results in the main text

For all proofs, by asymptotic equicontinuity, we may redefine $\hat{U}_i = F_n(X_i)$ and $\hat{V}_i = G_n(Y_i)$. Now, for any $s \in [0,1]$ and $(x,y) \in \mathbb{E}$, let

$$\tilde{\Lambda}_n^\circ(s,x,y) = \frac{1}{k} \sum_{i=1}^{\lfloor ns \rfloor} \mathbb{1}(U_i \leq kx/n, V_i \leq ky/n). \tag{3.17}$$

Under H_0^Λ, this is a sequential (oracle) estimator for $\Lambda^\circ(s,x,y) = s\Lambda(x,y)$. The asymptotic behavior of $\tilde{\Lambda}_n^\circ$ can be derived under the following general condition, which allows for rather general changes of the tail copula Λ_i (see also Section 3.3.3).

Assumption 3.14
There exists some function $g : [0,1] \times \mathbb{E} \to \mathbb{R}$ such that $\Lambda_i(\cdot,\cdot) = g(i/n,\cdot,\cdot)$ and such that, for any $m \in \mathbb{N}$,

$$\sup_{(s,x,y)\in S_m} \left| \frac{1}{n} \sum_{i=1}^{\lfloor ns \rfloor} g(i/n,x,y) - G(s,x,y) \right| = o(1), \quad n \to \infty, \tag{3.18}$$

where $G(s,x,y) = \int_0^s g(z,x,y)\,dz$.

Note that, under H_0^Λ, Assumption 3.14 is trivially met with $g(z,x,y) = \Lambda(x,y)$, $G(s,x,y) = \Lambda^\circ(s,x,y) = s\Lambda(x,y)$ and with the expression on the left-hand side of (3.18) being of order $O(1/n)$. Now, consider the following sequential empirical process $\mathbb{B}_n$ defined as

$$\mathbb{B}_n(s,x,y) = \sqrt{k}\left\{\tilde{\Lambda}_n^\circ(s,x,y) - G(s,x,y)\right\},$$

and its corresponding centered version

$$\mathbb{B}'_n(s,x,y) = \frac{1}{\sqrt{k}} \sum_{i=1}^{\lfloor ns \rfloor} \mathbb{1}(U_i \leq kx/n, V_i \leq ky/n) - C_i(kx/n, ky/n).$$

The proof of the following central lemma is given in Section 3.7.1.

Lemma 3.15
Suppose that Assumptions 3.1, 3.2 (a) and 3.14 hold. Then

$$\mathbb{B}'_n \rightsquigarrow \mathbb{B}'_g \quad \text{in } (\mathcal{B}_\infty([0,1] \times \mathbb{E}), d),$$

where $\mathbb{B}'_g$ denotes a tight centered Gaussian process with covariance given by

$$\mathrm{Cov}\{\mathbb{B}'_g(s_1,x_1,y_1), \mathbb{B}'_g(s_2,x_2,y_2)\} = G(s_1 \wedge s_2, x_1 \wedge x_2, y_1 \wedge y_2).$$

If, additionally, Assumption 3.2 (b) is met and if the convergence in (3.18) in Assumption 3.1 is of order $o(k_n^{-1/2})$, then $d(\mathbb{B}'_n, \mathbb{B}_n) = o(1)$.

Note that, under H_0^Λ, the distribution of $\mathbb{B}'_g$ is equal to the distribution of $\mathbb{B}_\Lambda$ as defined in Proposition 3.3.

Proof of Proposition 3.3. Since the rank of X_i among $X_1, \ldots, X_n$ is the same as the rank of U_i among $U_1, \ldots, U_n$ (similar for the second coordinate) we may assume without loss of generality that (X_i, Y_i) is distributed according to C_i, i.e., $F(x) = G(x) = x$ for all $x \in [0,1]$. Some thoughts reveal that

$$|\hat{\Lambda}^\circ_n(s,x,y) - \bar{\Lambda}^\circ_n(s,x,y)| \leq 2/k,$$

uniformly in $(s,x,y) \in S_m$, where

$$\bar{\Lambda}^\circ_n(s,x,y) := \frac{1}{k} \sum_{i=1}^{\lfloor ns \rfloor} \mathbb{1}\left\{ X_i \leq F_n^-(kx/n), Y_i \leq G_n^-(ky/n) \right\}$$

and where F_n^- and G_n^- denote the generalized inverse functions of F_n and G_n, respectively. Note that $\bar{\Lambda}^\circ_n$ can be expressed in terms of $\tilde{\Lambda}^\circ_n$ as

$$\bar{\Lambda}^\circ_n(s,x,y) = \tilde{\Lambda}^\circ_n\left\{ s, \frac{n}{k} F_n^-\left(\frac{kx}{n}\right), \frac{n}{k} G_n^-\left(\frac{ky}{n}\right) \right\}.$$

Now, we have $n/kF_n(kx/n) = \tilde{\Lambda}^\circ_n(1,x,\infty)$ and $n/kG_n(kx/n) = \tilde{\Lambda}^\circ_n(1,\infty,y)$, whence, by Hadamard-differentiability of the inverse mapping as stated in Bücher and Dette (2013),

$$\sup_{x \in [0,M]} \left| \frac{n}{k} F_n^-\left(\frac{kx}{n}\right) - x \right| = o_P(1), \quad \sup_{y \in [0,M]} \left| \frac{n}{k} G_n^-\left(\frac{ky}{n}\right) - y \right| = o_P(1) \tag{3.19}$$

for any $M > 0$ (this result can also be obtained by deducing weak convergence of $x \mapsto \mathbb{B}_n(1,x,\infty)$ as an element of the càdlàg space $D([0,M])$ with the Skorohod topology (from Lemma 3.15), invoking a Skorohod construction and applying Vervaat's Lemma, see Vervaat (1972) or Lemma A.0.2 in de Haan and Ferreira (2006)). Therefore, by asymptotic

equicontinuity of $\mathbb{B}_n$ from Lemma 3.15, uniformly on S_m,

$$\begin{aligned}\mathbb{G}_n(s,x,y) &= \sqrt{k}\left\{\bar{\Lambda}_n^{\circ}(s,x,y) - s\bar{\Lambda}_n^{\circ}(1,x,y)\right\} + O(k^{-1/2}) \\ &= \mathbb{B}_n\left\{s, \frac{n}{k}F_n^-\left(\frac{kx}{n}\right), \frac{n}{k}G_n^-\left(\frac{ky}{n}\right)\right\} \\ &\qquad - s\mathbb{B}_n\left\{1, \frac{n}{k}F_n^-\left(\frac{kx}{n}\right), \frac{n}{k}G_n^-\left(\frac{ky}{n}\right)\right\} + O(k^{-1/2}) \\ &= \mathbb{B}_n(s,x,y) - s\mathbb{B}_n(1,x,y) + o_P(1), \end{aligned} \tag{3.20}$$

which converges weakly to $\mathbb{G}_\Lambda(s,x,y) = \mathbb{B}_\Lambda(s,x,y) - s\mathbb{B}_\Lambda(1,x,y)$ on $(S_m, \|\cdot\|_{S_m})$, for any $m \in \mathbb{N}$. The proposition is proven. □

Remark 3.16
A crucial argument in the preceding proof is the decomposition (3.20) of $\mathbb{G}_n$ into a sum involving $\mathbb{B}_n$ from Lemma 3.15. A similar decomposition is possible with $\mathbb{B}_n$ replaced by $\mathbb{B}'_n$ from Lemma 3.15, and weak convergence of the latter holds without imposing Assumption 3.2 (b). Therefore, a relaxation of the assumptions for Proposition 3.3 seems to be possible. Indeed, a sufficient condition that makes occurring bias terms in an alternative version of (3.20) negligible and allows to dispense with Assumption 3.2 (b) is given by

$$\sup_{(s,x,y)\in S_m} \frac{\sqrt{k}}{n}\left|\sum_{i=1}^{\lfloor ns\rfloor}\frac{n}{k}C_i(kx/n,ky/n) - s\sum_{i=1}^{n}\frac{n}{k}C_i(kx/n,ky/n)\right| = o(1),$$

as $n \to \infty$. In case $C_i \equiv C$ is constant over time, this condition reduces to $\sqrt{k}/n = o(1)$, which is satisfied anyway since $k = o(n)$.

Proof of Corollary 3.4. It follows from Proposition 3.3 that

$$s \mapsto \left\{\hat{\Lambda}_n^{\circ}(1,1,1)\right\}^{-1/2}\mathbb{G}_n(s,1,1)$$

converges to a standard Brownian bridge. Therefore, both assertions are simple consequences of the continuous mapping theorem. □

Proof of Proposition 3.6. Let us first fix a $b \in \{1,\dots,B\}$ and show that $\mathbb{G}_{n,\xi^{(b)}}$ weakly converges to $\mathbb{G}_{\Lambda^{(b)}}$. For the sake of a clear notation, we omit the index b for the proof of this result. In light of the continuous mapping theorem, it is sufficient to prove that $\mathbb{B}_{n,\xi}$ weakly converges to $\mathbb{B}_\Lambda$. As in the proof of Proposition 3.3, we may assume that the marginal distributions are standard uniform. Let us suppose that we have proven $\tilde{\mathbb{B}}_{n,\xi} \rightsquigarrow \mathbb{B}_\Lambda$, where

$$\tilde{\mathbb{B}}_{n,\xi}(s,x,y) := \frac{1}{\sqrt{k}}\sum_{i=1}^{\lfloor ns\rfloor}\xi_i\left\{\mathbb{1}\left(U_i \le kx/n, V_i \le ky/n\right) - \tilde{C}_n(kx/n,ky/n)\right\}$$

and where $\tilde{C}_n(u,v) := n^{-1}\sum_{i=1}^n \mathbb{1}(U_i \le u, V_i \le v)$. Then, by a similar reasoning as in the proof of Proposition 3.3,

$$\mathbb{B}_{n,\xi}(s,x,y) = \tilde{\mathbb{B}}_{n,\xi}\left\{s, \frac{n}{k}F_n^-\left(\frac{kx}{n}\right), \frac{n}{k}G_n^-\left(\frac{ky}{n}\right)\right\} + O\left(k^{-1/2}\max_{i=1}^{n}|\xi_i|\right). \tag{3.21}$$

By (3.19) and asymptotic equicontinuity of $\tilde{\mathbb{B}}_{n,\xi}$, the first expression on the right-hand side weakly converges to $\mathbb{B}_\Lambda$ in $\ell^\infty(S_m)$, for any fixed S_m. In light of the fact that ξ_1 has

finite moments of any order we have $\mathbb{P}(|\xi_1| > x) = O(x^{-q})$ for any $q \in \mathbb{N}$. Therefore, the estimation

$$\mathbb{P}(k^{-1/2} \max_{i=1}^{n} |\xi_i| > \varepsilon) \leq n\mathbb{P}(|\xi_1| > \varepsilon\sqrt{k}/2) = nO(k^{-q/2})$$

shows that the O-term in (3.21) converges to 0 in probability, by choosing q sufficiently large. This proves that $\mathbb{G}_{n,\xi^{(b)}}$ weakly converges to $\mathbb{G}_{\Lambda^{(b)}}$.

It remains to be shown that $\tilde{\mathbb{B}}_{n,\xi} \rightsquigarrow \mathbb{B}_\Lambda$ in $\ell^\infty(S_m)$, for any fixed S_m. We have

$$\tilde{\mathbb{B}}_{n,\xi}(s,x,y) = A_{n1}(s,x,y) + A_{n2}(s,x,y) + A_{n3}(s,x,y),$$

where

$$\begin{aligned}
A_{n1} &:= \frac{1}{\sqrt{k}} \sum_{i=1}^{\lfloor ns \rfloor} \xi_i \left\{ \mathbb{1}(U_i \leq kx/n, V_i \leq ky/n) - C_i(kx/n, ky/n) \right\}, \\
A_{n2} &:= \frac{1}{\sqrt{k}} \sum_{i=1}^{\lfloor ns \rfloor} \xi_i \left\{ C_i(kx/n, ky/n) - \Lambda(kx/n, ky/n) \right\}, \\
A_{n3} &:= \frac{1}{\sqrt{k}} \sum_{i=1}^{\lfloor ns \rfloor} \xi_i \left\{ \Lambda(kx/n, ky/n) - \tilde{C}_n(kx/n, ky/n) \right\}.
\end{aligned}$$

The fact that $\tilde{C}_n(kx/n, ky/n) - \Lambda(kx/n, ky/n) = \sqrt{k}/n \times \mathbb{B}_n(s,x,y) = O_P(\sqrt{k}/n)$ from Lemma 3.15 together with Donsker's invarance principle implies that the last term A_{n3} is of order $O_P(1/\sqrt{n}) = o_P(1)$, uniformly on each S_m. Furthermore, $C_i(kx/n, ky/n) - \Lambda(kx/n, ky/n) = k/n \times O(S(n/k))$ by Assumption 3.1, uniformly in i and uniformly on T_m, whence

$$\sup_{(s,x,y) \in S_m} |A_{n2}(s,x,y)| \leq \frac{1}{n} \sum_{i=1}^{n} |\xi_i| \times \sqrt{k} O(S(n/k)).$$

The right-hand side is $o_P(1)$ by Assumption 3.2 (b). Hence, it remains to consider the leading term A_{n1}. Its conditional weak convergence follows from Theorem 11.19 in Kosorok (2008) and the proof of Lemma 3.15 below. Further note that conditional weak convergence as considered by the last named author implies unconditional weak convergence.

Now, let us give the proof of the proposition. On each S_m, the sequence $(\mathbb{G}_n, \mathbb{G}_{n,\xi^{(1)}}, \ldots, \mathbb{G}_{n,\xi^{(B)}})$ is jointly asymptotically tight by Lemma 1.4.3 in Van der Vaart and Wellner (1996). Hence, it remains to consider weak convergence of the finite-dimensional distributions. It suffices to consider the finite-dimensional distributions of the sequence $(\mathbb{B}_n, \mathbb{B}_{n,\xi^{(1)}}, \ldots, \mathbb{B}_{n,\xi^{(B)}})$. By a similar argumentation as above in the case of a fixed $b \in \{1, \ldots, B\}$, we may replace each coordinate $\mathbb{B}_{n,\xi^{(b)}}$ by

$$\frac{1}{\sqrt{k}} \sum_{i=1}^{\lfloor ns \rfloor} \xi_i^{(b)} \left\{ \mathbb{1}(U_i \leq kx/n, V_i \leq ky/n) - C_i(kx/n, ky/n) \right\}.$$

Then, the coordinates are uncorrelated and row-wise independent, whence the finite-dimensional distributions weakly converge to those of $(\mathbb{B}_\Lambda, \mathbb{B}_\Lambda^{(1)}, \ldots, \mathbb{B}_\Lambda^{(B)})$ by the central limit theorem for row-wise independent triangular arrays. □

Proof of Corollary 3.7. For TDC-Test 1, this is a direct consequence of Corollary 3.4 (i). The proofs of TDC-Test 2 and TC-Test being essentially the same, we restrict ourselves to the proof of TDC-Test 2. For monotonicity reasons it suffices to consider $\alpha \in \mathbb{R} \setminus \mathbb{Q}$.

Let K denote the c.d.f. of $\mathcal{S}$ and define

$$K_{n,B}(x) = B^{-1} \sum_{b=1}^{B} \mathbb{1}(\mathcal{S}_{n,\xi^{(b)}} \leq x), \qquad K_B(x) = B^{-1} \sum_{b=1}^{B} \mathbb{1}(\mathcal{S}^{(b)} \leq x),$$

where $\mathcal{S}^{(1)}, \ldots, \mathcal{S}^{(B)}$ denote independent copies of $\mathcal{S}$. Consequently, we can write $\mathbb{P}(\mathcal{S}_n \geq \hat{q}_{\mathcal{S}_n, 1-\alpha}) = \mathbb{P}\{K_{n,B}(\mathcal{S}_n) \geq 1-\alpha\}$. Let us first show that, for any $B \in \mathbb{N}$ fixed, we have

$$\lim_{n\to\infty} \mathbb{P}\{K_{n,B}(\mathcal{S}_n) \geq 1-\alpha\} = \mathbb{P}\{K_B(S) \geq 1-\alpha\}. \tag{3.22}$$

For that purpose, let $\varepsilon > 0$ be given. Define a map $\Psi : \mathbb{R}^{B+1} \to \mathbb{R}$ by $\Psi(t_0, \ldots, t_B) = B^{-1} \sum_{b=1}^{B} \mathbb{1}(t_b \leq t_0)$ and note that Ψ is continuous at any point $(t_0, \ldots, t_B)$ with pairwise different coordinates (i.e., $t_i \neq t_j$ for $i \neq j$). Then, observing that $(\mathcal{S}_n, \mathcal{S}_{n,\xi^{(1)}}, \ldots, \mathcal{S}_{n,\xi^{(B)}}) \rightsquigarrow (\mathcal{S}, \mathcal{S}^{(1)}, \ldots, \mathcal{S}^{(B)})$ with the limit having pairwise different coordinates, almost surely, the continuous mapping theorem implies that $K_{n,B}(\mathcal{S}_n) \rightsquigarrow K_B(\mathcal{S})$, for $n \to \infty$. The Portmanteau-Theorem implies that there exists some $n_0 = n_0(\varepsilon, B)$ such that

$$|\mathbb{P}\{K_{n,B}(\mathcal{S}_n) \geq 1-\alpha\} - \mathbb{P}\{K_B(\mathcal{S}) \geq 1-\alpha\}| < \varepsilon$$

(note that $\mathbb{P}(K_B(\mathcal{S}) = 1-\alpha) = 0$ since $\alpha \in \mathbb{R} \setminus \mathbb{Q}$), which proves (3.22).

It remains to be shown that

$$\lim_{B\to\infty} \mathbb{P}\{K_B(\mathcal{S}) \geq 1-\alpha\} = \alpha. \tag{3.23}$$

By the Glivenko-Cantelli Theorem, we may choose $B_0 = B_0(\varepsilon) \in \mathbb{N}$ such that

$$\mathbb{P}\left\{\sup_{x\in\mathbb{R}} |K_B(x) - K(x)| > \varepsilon\right\} \leq \varepsilon.$$

for all $B \geq B_0$. For all such B,

$$\mathbb{P}\{K_B(\mathcal{S}) \geq 1-\alpha\} \leq \mathbb{P}\{K(\mathcal{S}) \geq 1-\alpha-\varepsilon) + \varepsilon = \alpha + 2\varepsilon,$$

and similarly,

$$\mathbb{P}\{K_B(\mathcal{S}) \geq 1-\alpha\} \geq \mathbb{P}\{K(\mathcal{S}) \geq 1-\alpha+\varepsilon) = \alpha - \varepsilon,$$

which implies that

$$|\mathbb{P}\{K_B(\mathcal{S}) \geq 1-\alpha\} - \alpha| \leq 2\varepsilon.$$

This proves (3.23) and hence the Corollary. □

Proof of Proposition 3.8. The result is a special case of Proposition 3.11 which is proven below. □

Proof of Corollary 3.9. For TDC-Test 1, this is a direct consequence of Proposition 3.8 (i). The proofs for TDC-Test 2 and TC-Test being essentially the same, we only consider the TC-Test.

Let us first show that $\mathcal{T}_{n,\xi}$ is stochastically bounded. This follows if we prove that $\sup_{(s,x,y)\in S_m} |\mathbb{B}_{n,\xi}(s,x,y)| = O_P(1)$, for $n \to \infty$. By a similar reasoning as in (3.21) and the subsequent paragraph, it suffices to show the same for $\tilde{\mathbb{B}}_{n,\xi}(s,x,y)$. Since

$$\sup_{(s,x,y)\in S_m} |\tilde{\mathbb{B}}_{n,\xi}(s,x,y)| = \max\left\{ \sup_{s\le\bar{s},(x,y)\in T_m} |\tilde{\mathbb{B}}_{n,\xi}(s,x,y)|, \sup_{s\ge\bar{s},(x,y)\in T_m} |\tilde{\mathbb{B}}_{n,\xi}(s,x,y)| \right\}, \quad (3.24)$$

we can verify the claim for each of the suprema in the maximum separately. Let us first treat the notationally simpler first supremum. We can decompose $\tilde{\mathbb{B}}_{n,\xi}(s,x,y) = \sum_{\ell=1}^{4} A_{n\ell}(s,x,y)$, where

$$A_{n1} := \frac{1}{\sqrt{k}} \sum_{i=1}^{\lfloor ns\rfloor} \xi_i \left\{ \mathbb{1}(U_i \le kx/n, V_i \le ky/n) - C_i(kx/n, ky/n) \right\},$$

$$A_{n2} := \frac{1}{\sqrt{k}} \sum_{i=1}^{\lfloor ns\rfloor} \xi_i \left\{ C_i(kx/n, ky/n) - \Lambda^{(1)}(kx/n, ky/n) \right\},$$

$$A_{n3} := \frac{1}{\sqrt{k}} \sum_{i=1}^{\lfloor ns\rfloor} \xi_i (1-\bar{s}) \left\{ \Lambda^{(1)}(kx/n, ky/n) - \Lambda^{(2)}(kx/n, ky/n) \right\},$$

$$A_{n4} := \frac{1}{\sqrt{k}} \sum_{i=1}^{\lfloor ns\rfloor} \xi_i \left\{ \bar{s}\Lambda^{(1)}(kx/n, ky/n) + (1-\bar{s})\Lambda^{(2)}(kx/n, ky/n) - \tilde{C}_n(kx/n, ky/n) \right\}.$$

Since $s \le \bar{s}$, the first term A_{n1} converges weakly by the same arguments as in the proof of Proposition 3.6. Also as in that proof, $A_{n2} = o_P(1)$. Negligibility of A_{n3} follows from Donsker's invariance principle and the fact that $\Lambda(kx/n, ky/n) \le (x \wedge y) \times k/n$ for any tail copula Λ. Hence, it remains to consider A_{n4}. Again exploiting Donsker's invariance principle, it is certainly sufficient to show $\Delta_n := \tilde{C}_n(kx/n, ky/n) - \bar{s}\Lambda^{(1)}(kx/n, ky/n) - (1-\bar{s})\Lambda^{(2)} = O_P(\sqrt{k}/n)$. This, however, follows from the fact that we can write

$$\frac{n}{\sqrt{k}}\Delta_n = \sqrt{k}\Bigg\{ \frac{1}{k} \sum_{i=1}^{\lfloor n\bar{s}\rfloor} \mathbb{1}(U_i \le kx/n, V_i \le ky/n) - \bar{s}\Lambda^{(1)}(x,y) + \frac{1}{k} \sum_{\lfloor n\bar{s}\rfloor+1}^{n} \mathbb{1}(U_i \le kx/n, V_i \le ky/n) - (1-\bar{s})\Lambda^{(2)}(x,y) \Bigg\},$$

which is $O_P(1)$ by two suitable applications of Lemma 3.15.

Regarding the second supremum on the left-hand side of (3.24), write

$$\tilde{\mathbb{B}}_{n,\xi}(s,x,y) = \tilde{\mathbb{B}}_{n,\xi}(\bar{s},x,y) + k^{-1/2} \sum_{i=\lfloor n\bar{s}\rfloor+1}^{\lfloor ns\rfloor} \xi_i \left\{ \mathbb{1}(U_i \le kx/n, V_i \le ky/n) - \tilde{C}_n(kx/n, ky/n) \right\}. \quad (3.25)$$

The first term on the left-hand side has already been handled above, and the second one can be treated by a similar decomposition.

Now, fix $B \in \mathbb{N}$ and let $\varepsilon > 0$ be given. Then, since $\mathcal{T}_{n,\xi^{(b)}} = O_P(1)$ for each $b = 1, \dots, B$, we may choose $K = K(\varepsilon, B) > 0$ such that

$$\sup_{n\in\mathbb{N}} \mathbb{P}\left(\max_{b=1}^{B} |\mathcal{T}_{n,\xi^{(b)}}| > K \right) \le \varepsilon.$$

Therefore, $\hat{q}_{\mathcal{T}_n,1-\alpha} > K$ with probability of at least ε, and since $\mathcal{T}_n \to \infty$ in probability, we get that

$$\liminf_{n\to\infty} \mathbb{P}(\mathcal{T}_n \geq \hat{q}_{\mathcal{T}_n,1-\alpha}) \geq \liminf_{n\to\infty} \{\mathbb{P}(\mathcal{T}_n \geq K) - \mathbb{P}(\hat{q}_{\mathcal{T}_n,1-\alpha} > K)\} \geq 1 - \varepsilon.$$

As $\varepsilon > 0$ was arbitrary, the assertion is proven. □

Proof of Proposition 3.11. As in the proof of Proposition 3.3 we may assume without loss of generality that the marginals are standard uniform. We only prove (i), the proof of (ii) is completely analogous. By the continuous mapping theorem, it suffices to show that

$$\sup_{s\in[0,1]} \left| \frac{1}{k} \sum_{i=1}^{\lfloor ns \rfloor} \mathbb{1}\left(\hat{U}_i \leq k/n, \hat{V}_i \leq k/n\right) - \int_0^s g(z,1,1)dz \right| = o_P(1).$$

As in the proof of Proposition 3.3, we may replace the indicators in the previous expression by $\mathbb{1}\{U_i \leq F_n^-(k/n), V_i \leq G_n^-(k/n)\}$. Now, we decompose

$$\frac{1}{k} \sum_{i=1}^{\lfloor ns \rfloor} \mathbb{1}\left\{U_i \leq F_n^-(k/n), V_i \leq G_n^-(k/n)\right\} - \int_0^s g(z,1,1)dz = \sum_{\ell=1}^{4} A_\ell(s)$$

where

$$\begin{aligned}
A_1(s) &:= k^{-1/2}\mathbb{B}_n'\left\{(n/k)F_n^-(k/n), (n/k)G_n^-(k/n)\right\},\\
A_2(s) &:= \frac{1}{k}\sum_{i=1}^{\lfloor ns \rfloor} C_i\left\{F_n^-(k/n), G_n^-(k/n)\right\} - C_i(k/n, k/n),\\
A_3(s) &:= \frac{1}{n}\sum_{i=1}^{\lfloor ns \rfloor} (n/k)C_i(k/n,k/n) - g(i/n,1,1),\\
A_4(s) &:= \frac{1}{n}\sum_{i=1}^{\lfloor ns \rfloor} g(i/n,1,1) - \int_0^s g(z,1,1)dz.
\end{aligned}$$

$A_1(s)$ converges to 0, uniformly in $s \in [0,1]$, by Lemma 3.15. The second term is uniformly $o_P(1)$ by Lipschitz continuity of C_i and (3.19). By Assumption 3.2, the third term is of order $O(S(n/k)) = o(1)$. $A_4(s)$ goes to 0, uniformly in s, by the assumption in H_1^λ. □

Proof of Proposition 3.13. For $i = 1, \ldots, \lfloor nt_F \rfloor$, the rank of X_i among $X_1, \ldots, X_{\lfloor nt_F \rfloor}$ is the same as the rank of U_i among $U_1, \ldots, U_{\lfloor nt_F \rfloor}$, and similar for the second subsample and for the second coordinate. Hence, we may assume without loss of generality that (X_i, Y_i) is distributed according to C_i, for all $i = 1, \ldots, n$. Moreover, by asymptotic equicontinuity, we may redefine $F_{(k+1):\ell}(x) := (\ell - k)^{-1} \sum_{j=k+1}^{\ell} \mathbb{1}(X_j \leq x)$, and similar for the second coordinate.

In the following, we suppose that $t_F \leq t_G$, the other case is treated similarly. We restrict ourselves to show weak convergence on $\ell^\infty([0,1] \times [\varepsilon, m]^2)$ for $0 < \varepsilon < m < \infty$; the boundary cases can be treated similarly, following arguments in Bücher and Dette (2013) for x or y smaller than ε. Let n be large enough such that $t_F, t_G \in (1/n, 1 - 1/n)$.

Define

$$\begin{aligned}\bar{\Lambda}_n^\circ(s,x,y;t_F,t_G) = \frac{1}{k}\sum_{i=1}^{\lfloor n(s\wedge t_F)\rfloor} \mathbb{1}\Big\{X_i \le F^-_{1:\lfloor nt_F\rfloor}(kx/n), Y_i \le G^-_{1:\lfloor nt_G\rfloor}(ky/n)\Big\}\\ + \frac{1}{k}\sum_{i=\lfloor n(s\wedge t_F)\rfloor+1}^{\lfloor n(s\wedge t_G)\rfloor} \mathbb{1}\Big\{X_i \le F^-_{\lfloor nt_F\rfloor+1:n}(kx/n), Y_i \le G^-_{1:\lfloor nt_G\rfloor}(ky/n)\Big\}\\ + \frac{1}{k}\sum_{i=\lfloor n(s\wedge t_G)\rfloor+1}^{\lfloor ns\rfloor} \mathbb{1}\Big\{X_i \le F^-_{\lfloor nt_F\rfloor+1:n}(kx/n), Y_i \le G^-_{\lfloor nt_G\rfloor+1:n}(ky/n)\Big\}\end{aligned}$$

and note that

$$|\hat{\Lambda}_n^\circ(s,x,y) - \bar{\Lambda}_n^\circ(s,x,y;t_F,t_G)| = O(1/k),$$

uniformly in $(s,x,y) \in [0,1]\times[\varepsilon,m]^2$. Therefore, it suffices to prove weak convergence of

$$\sqrt{k}\left\{\bar{\Lambda}_n^\circ(s,x,y;t_F,t_G) - s\bar{\Lambda}_n^\circ(1,x,y;t_F,t_G)\right\}.$$

For $(t_1,t_2)\in[0,1]^2$ with $t_2 > t_1 + 1/n$ define

$$\alpha_n(t_1,t_2,x) = \frac{n}{k}F^-_{\lfloor nt_1\rfloor+1:\lfloor nt_2\rfloor}\left(\frac{kx}{n}\right), \qquad \beta_n(t_1,t_2,y) = \frac{n}{k}G^-_{\lfloor nt_1\rfloor+1:\lfloor nt_2\rfloor}\left(\frac{ky}{n}\right).$$

Recall the definition of $\tilde{\Lambda}_n^\circ$ in (3.17) and note that

$$\begin{aligned}&\bar{\Lambda}_n^\circ(s,x,y;t_F,t_G) = \tilde{\Lambda}_n^\circ\{s\wedge t_F, \alpha_n(0,t_F,x), \beta_n(0,t_G,y)\}\\ &+\tilde{\Lambda}_n^\circ\{s\wedge t_G, \alpha_n(t_F,1,x), \beta_n(0,t_G,y)\} - \tilde{\Lambda}_n^\circ\{s\wedge t_F, \alpha_n(t_F,1,x), \beta_n(0,t_G,y)\}\\ &+\tilde{\Lambda}_n^\circ\{s, \alpha_n(t_F,1,x), \beta_n(t_G,1,y)\} - \tilde{\Lambda}_n^\circ\{s\wedge t_G, \alpha_n(t_F,1,x), \beta_n(t_G,1,y)\}.\end{aligned}$$

In particular, we can write $\sqrt{k}\left\{\bar{\Lambda}_n^\circ(s,x,y;t_F,t_G) - s\bar{\Lambda}_n^\circ(1,x,y;t_F,t_G)\right\}$ as

$$\begin{aligned}&\mathbb{B}_n\{s\wedge t_F, \alpha_n(0,t_F,x), \beta_n(0,t_G,y)\}\\ &\quad+\mathbb{B}_n\{s\wedge t_G, \alpha_n(t_F,1,x), \beta_n(0,t_G,y)\} - \mathbb{B}_n\{s\wedge t_F, \alpha_n(t_F,1,x), \beta_n(0,t_G,y)\}\\ &\quad+\mathbb{B}_n\{s, \alpha_n(t_F,1,x), \beta_n(t_G,1,y)\} - \mathbb{B}_n\{s\wedge t_G, \alpha_n(t_F,1,x), \beta_n(t_G,1,y)\}\\ &-s\Big[\mathbb{B}_n\{1\wedge t_F, \alpha_n(0,t_F,x), \beta_n(0,t_G,y)\}\\ &\quad+\mathbb{B}_n\{1\wedge t_G, \alpha_n(t_F,1,x), \beta_n(0,t_G,y)\} - \mathbb{B}_n\{1\wedge t_F, \alpha_n(t_F,1,x), \beta_n(0,t_G,y)\}\\ &\quad+\mathbb{B}_n\{1, \alpha_n(t_F,1,x), \beta_n(t_G,1,y)\} - \mathbb{B}_n\{1\wedge t_G, \alpha_n(t_F,1,x), \beta_n(t_G,1,y)\}\Big]\\ &+R_n\end{aligned} \tag{3.26}$$

where the remainder R_n is given by

$$\begin{aligned}\sqrt{k}\Big\{&(s\wedge t_F - st_F)\Big[\Lambda\{\alpha_n(0,t_F,x), \beta_n(0,t_G,y)\} - \Lambda\{\alpha_n(t_F,1,x), \beta_n(0,t_G,y)\}\Big]\\ &+(s\wedge t_G - st_G)\Big[\Lambda\{\alpha_n(t_F,1,x), \beta_n(0,t_G,y)\} - \Lambda\{\alpha_n(t_F,1,x), \beta_n(t_G,1,y)\}\Big]\Big\}.\end{aligned}$$

The functional delta method applied to the inverse mapping (see the proof of Lemma A.1 in Bücher and Dette, 2013) shows that

$$\sup_{x\in[0,M]}\left|\sqrt{k}\{\alpha_n(0,t_F,x)-x\}+t_F^{-1}\mathbb{B}_n(t_F,x,\infty)\right|=o_P(1),$$
$$\sup_{x\in[0,M]}\left|\sqrt{k}\{\alpha_n(t_F,1,x)-x\}+(1-t_F)^{-1}\{\mathbb{B}_n(1,x,\infty)-\mathbb{B}_n(t_F,x,\infty)\}\right|=o_P(1),$$
$$\sup_{y\in[0,M]}\left|\sqrt{k}\{\beta_n(0,t_G,y)-y\}+t_G^{-1}\mathbb{B}_n(t_G,\infty,y)\right|=o_P(1),$$
$$\sup_{y\in[0,M]}\left|\sqrt{k}\{\beta_n(t_G,1,y)-y\}+(1-t_G)^{-1}\{\mathbb{B}_n(1,\infty,y)-\mathbb{B}_n(t_G,\infty,y)\}\right|=o_P(1),$$

for any $M\in\mathbb{N}$. In particular,

$$\sup_{x\in[0,M]}|\alpha_n(0,t_F,x)-x|=o_P(1),\qquad \sup_{x\in[0,M]}|\alpha_n(t_F,1,x)-x|=o_P(1)$$
$$\sup_{y\in[0,M]}|\beta_n(0,t_G,y)-y|=o_P(1),\qquad \sup_{y\in[0,M]}|\beta_n(t_G,1,y)-y|=o_P(1),$$

which implies, by asymptotic equicontinuity of $\mathbb{B}_n$, that the first six lines of the decomposition (3.26) are equal to $\mathbb{B}_n(s,x,y)-s\mathbb{B}_n(1,x,y)$, up to a term of uniform order $o_P(1)$. Regarding R_n, a Taylor expansion of Λ based on Assumption 3.12 shows that

$$\begin{aligned}\sqrt{k}\Big[\Lambda\{\alpha_n(0,t_F,x),\beta_n(0,t_G,y)\}-\Lambda\{\alpha_n(t_F,1,x),\beta_n(0,t_G,y)\}\Big]&\\ =-\frac{\dot\Lambda_x(x,y)}{t_F(1-t_F)}\Big[(1-t_F)\mathbb{B}_n(t_F,x,\infty)-t_F\{\mathbb{B}_n(1,x,\infty)-\mathbb{B}_n(t_F,x,\infty)\}\Big]+o_P(1)&\\ =-\frac{\dot\Lambda_x(x,y)}{t_F(1-t_F)}\{\mathbb{B}_n(t_F,x,\infty)-t_F\mathbb{B}_n(1,x,\infty)\}+o_P(1).&\end{aligned}$$

A similar calculation yields

$$\begin{aligned}\sqrt{k}\Big[\Lambda\{\alpha_n(t_F,1,x),\beta_n(0,t_G,y)\}-\Lambda\{\alpha_n(t_F,1,x),\beta_n(t_G,1,y)\}\Big]&\\ =-\frac{\dot\Lambda_y(x,y)}{t_G(1-t_G)}\{\mathbb{B}_n(t_G,\infty,y)-t_G\mathbb{B}_n(1,\infty,y)\}+o_P(1).&\end{aligned}$$

Assembling terms yields the assertion. □

3.7.1 Proofs of additional results

Proof of Lemma 3.15. First, consider the assertion regarding $\mathbb{B}_n'$. It suffices to fix one set S_m and to show weak convergence in $\ell^\infty(S_m)$. The latter can be accomplished by a suitable application of Theorem 11.16 in Kosorok (2008), see also Bücher and Dette (2013) for a similar proof for the i.i.d. and nonsequential case. Write $\mathbb{B}_n'(s,x,y)=\mathbb{B}_n'(s,x,y,\omega)$ as

$$\mathbb{B}_n'(s,x,y,\omega)=\sum_{i=1}^n f_{n,i}(s,x,y,\omega)-\mathbb{E}[f_{n,i}(s,x,y,\cdot)],$$

where $f_{n,i}(s,x,y,\omega)=k^{-1/2}\mathbb{1}(U_i(\omega)\le kx/n,V_i(\omega)\le ky/n)\mathbb{1}(i\le\lfloor ns\rfloor)$. Moreover define envelopes $F_{n,i}$ for $f_{n,i}$ as

$$F_{n,i}(\omega)=k^{-1/2}\mathbb{1}(U_i(\omega)\le km/n\ \text{ or }\ V_i(\omega)\le km/n)\mathbb{1}(i\le\lfloor ns\rfloor).$$

By Theorem 11.16 in Kosorok (2008), the assertion in Lemma 3.15 regarding $\mathbb{B}_n'$ is proven if we show that

(i) *The $f_{n,i}$ are manageable with envelopes $F_{n,i}$.*

(ii) *The limit $H((s_1,x_1,y_1),(s_1,x_1,y_1)) = \lim_{n\to\infty} \mathbb{E}[\mathbb{B}'_n(s_1,x_1,y_1)\mathbb{B}'_n(s_2,x_2,y_2)]$ exists for every $(s_1,x_1,y_1),(s_2,x_2,y_2) \in S_m$.*

(iii) $\limsup_{n\to\infty} \sum_{i=1}^n \mathbb{E}F_{n,i}^2 < \infty$.

(iv) $\lim_{n\to\infty} \sum_{i=1}^n \mathbb{E}F_{n,i}^2 \mathbb{1}\{F_{n,i} > \varepsilon\} = 0$ *for all* $\varepsilon > 0$.

(v) *The limit $\lim_{n\to\infty} \rho_n((s_1,x_1,y_1),(s_2,x_2,y_2)) = \rho((s_1,x_1,y_1),(s_2,x_2,y_2))$ exists for all $(s_1,x_1,y_1),(s_2,x_2,y_2) \in S_m$, where*

$$\rho_n((s_1,x_1,y_1),(s_2,x_2,y_2)) = \left(\sum_{i=1}^n \mathbb{E}\left|f_{n,i}(s_1,x_1,y_1,\cdot) - f_{n,i}(s_2,x_2,y_2,\cdot)\right|^2\right)^{1/2}.$$

Furthermore, for all sequences $(s_{1n},x_{1n},y_{1n})_{n\in\mathbb{N}}, (s_{2n},x_{2n},y_{2n})_{n\in\mathbb{N}} \in S_m$, the convergence $\rho_n((s_{1n},x_{1n},y_{1n}),(s_{2n},x_{2n},y_{2n})) \to 0$ holds, under the condition that $\rho((s_{1n},x_{1n},y_{1n}),(s_{2n},x_{2n},y_{2n})) \to 0$.

(vi) *$\{f_{n,1}(s,x,y,\omega),\ldots,f_{n,n}(s,x,y,\omega) : (s,x,y) \in S_m\}$ is almost measurable Suslin.*

For the proof of (i) note that we can write $f_{n,i}$, when indexed by the extended domain $[0,1]\times([0,m]\cup\{\infty\})^2$ instead of S_m, as a product of three nondecreasing functions in s, x and y, respectively. Manageability with respect to the envelopes $F_{n,i}$ then follows from the discussion on Page 221 in Kosorok (2008) and two applications of Theorem 11.17 (iv) in that reference. Then, also the restriction to S_m is manageable with envelopes $F_{n,i}$.

In the following, we omit the argument ω. For the proof of (ii), we have the decomposition $\mathbb{E}[\mathbb{B}'_n(s_1,x_1,y_1)\mathbb{B}'_n(s_2,x_2,y_2)] = A_{n1} + A_{n2}$, where

$$A_{n1} := \frac{1}{k_n} \sum_{i=1}^{\lfloor n(s_1\wedge s_2)\rfloor} C_i\left(k(x_1\wedge x_2)/n, k(y_1\wedge y_2)/n\right),$$
$$A_{n2} := \frac{1}{k_n} \sum_{i=1}^{\lfloor n(s_1\wedge s_2)\rfloor} C_i(kx_1/n, ky_1/n) C_i(kx_2/n, ky_2/n).$$

Exploiting that $C_i(u,v) \le u\wedge v$, the second summand A_{n2} is uniformly bounded by $km/n = o(1)$. For the first summand, we write

$$A_{n1} = \frac{1}{n} \sum_{i=1}^{\lfloor n(s_1\wedge s_2)\rfloor} \Lambda_i(x_1\wedge x_2, y_1\wedge y_2) + \frac{1}{n} \sum_{i=1}^{n(s_1\wedge s_2)} \frac{n}{k} C_i(k(x_1\wedge x_2)/n, k(y_1\wedge y_2)/n) - \Lambda_i(x_1\wedge x_2, y_1\wedge y_2).$$

The second sum is of order $O(S(n/k)) = o(1)$ by Assumption 3.1, and the first sum converges to $G(s_1\wedge s_2, x_1\wedge x_2, y_1\wedge y_2) < \infty$.

For the proof of (iii) note that $\mathbb{E}F_{n,i}^2 = 2m/n - C_i(km/n, km/n)/k$. Therefore,

$$\sum_{i=1}^n \mathbb{E}\left[F_{n,i}^2\right] = 2m - \frac{1}{n}\sum_{i=1}^n \frac{n}{k} C_i(km/n, km/n).$$

As in the proof of (ii), the second sum converges to $\int_0^1 g(z,m,m)\,dz$.

For the proof of (iv), note that $\mathbb{E}[F_{n,i}^2 \mathbb{1}(F_{n,i} > \varepsilon)] \leq \mathbb{P}(F_{n,i} > \varepsilon)$, and the right-hand side is equal to 0 for sufficiently large n.

For the proof of (v), note that

$$\rho_n((s_1, x_1, y_1), (s_2, x_2, y_2))^2 = \frac{1}{n} \sum_{i=1}^{\lfloor ns_1 \rfloor} \frac{k}{n} C_i(kx_1/n, ky_1/n) - \frac{2}{n} \sum_{i=1}^{\lfloor n(s_1 \wedge s_2) \rfloor} \frac{k}{n} C_i(k(x_1 \wedge x_2)/n, k(y_1 \wedge y_2)/n) + \frac{1}{n} \sum_{i=1}^{\lfloor ns_2 \rfloor} \frac{k}{n} C_i(kx_2/n, ky_2/n).$$

Similar calculations as before show that this expression converges uniformly (on S_m) to

$$\rho((s_1, x_1, y_1), (s_2, x_2, y_2))^2 = G(s_1, x_1, y_1) - 2G(s_1, \wedge s_2, x_1 \wedge x_2, y_1 \wedge y_2) + G(s_2, x_2, y_2).$$

Finally, the assertion in (vi) follows from separability of $\mathbb{B}_n'$ and Lemma 11.15 in Kosorok (2008).

Now, consider the assertion regarding $\mathbb{B}_n$. We have

$$\begin{aligned} |\mathbb{B}_n'(s, x, y) - \mathbb{B}_n(s, x, y)| &= \sqrt{k_n} \left| \frac{1}{k_n} \sum_{i=1}^{\lfloor ns \rfloor} C_i(k_n x/n, k_n y/n) - G(s, x, y) \right| \\ &\leq \sqrt{k_n} \frac{\lfloor ns \rfloor}{n} \max_{i=1}^{n} \left| \frac{n}{k_n} C_i(k_n x/n, k_n y/n) - g(i/n, x, y) \right| \\ &\quad + \sqrt{k_n} \left| \frac{1}{n} \sum_{i=1}^{\lfloor ns \rfloor} g(i/n, x, y) - G(s, x, y) \right|. \end{aligned}$$

Since we assume that the convergence in Assumption 3.1 is of order $o(k_n^{-1/2})$, we immediately obtain negligibility of the second term on the right-hand side. By (3.9), the first term on the right-hand side is of order $O(\sqrt{k_n} S(n/k_n))$, uniformly on each S_m. Hence, by Assumption 3.2 (b), this term converges to 0 as well. □

Appendix A

Commented code

The next part consists of selected Matlab source code and algorithms used for obtaining the results presented in the preceding articles. It is organized as follows: Section A.1 presents the implementation of the goodness-of-fit test for both copulas and tail copulas applied in Chapter 2. Section A.2 provides a useful algorithm to simulate from arbitrary copulas, particularly convenient for singular copulas. Further, the simulation algorithm of copula model (C3) from Section 3.4.1 is presented. Finally, Section A.3 lists two test procedures from Chapter 3: the application of TDC-Test 1 to a bivariate dataset and the TC-Test used in the finite sample studies. Note that some symbols have been adjusted to improve readability.

A.1 Goodness-of-fit tests

Code A.1. One-level parametric bootstrap-based goodness-of-fit test for the t-copula including calculation of the cross-validation Copula Information Criterion.

```
% goodness-of-fit test for the t-copula with calculation of the CIC

% load data
WTI = xlsread('...');
Brent = xlsread('...');

% initialization
n = length(WTI);
tau_data = corr(WTI,Brent,'type','Kendall');

% rank-based analysis
rcl = zeros(n,1);
[hv,ar] = sort(WTI);
for i = 1:n
   rcl(ar(i)) = i;
end
rcl = rcl/(n+1);

rhh = zeros(n,1);
[hv,ar] = sort(Brent);
for i = 1:n
   rhh(ar(i)) = i;
end
rhh = rhh/(n+1);

% maximum pseudo likelihood estimator and cross-validation CIC
theta = linspace(0,0.999,100)';
```

```
nu = linspace(3,7,100)';
mple = zeros(100,100);

for i = 1:100
   for j = 1:100
      mple(i,j) = sum(log(copulapdf('t',[rcl rhh],theta(i),nu(j))));
   end
end
[maximum posrow] = max(mple);
[maximum poscol] = max(maximum);
h = 10^(-5);

p = 1/(2*h)*(log(copulapdf('t',[rcl rhh], theta(posrow(poscol))+h,
  nu(poscol))) - log(copulapdf('t',[rcl rhh], theta(posrow(poscol))-h,
  nu(poscol))));
jhat = 1/n*sum(1/(h^2)*(log(copulapdf('t',[rcl rhh], theta(posrow(poscol))+h,
  nu(poscol))) - log(copulapdf('t',[rcl rhh], theta(posrow(poscol))-h,
  nu(poscol))) - ...
      2*log(copulapdf('t',[rcl rhh], theta(posrow(poscol)), nu(poscol)))));
jinvhat = -1/(jhat);
phat = 1/n*sum(p.^2*jinvhat);

z1 = zeros(n,1);
z2 = zeros(n,1);
for i = 1:n
   z1(i) = 1/n*sum(1/(4*h^2)*((log(copulapdf('t',[rcl+h rhh],
     theta(posrow(poscol))+h, nu(poscol))) - log(copulapdf('t',[rcl+h rhh],
     theta(posrow(poscol))-h, nu(poscol)))) - ...
         (log(copulapdf('t',[rcl-h rhh], theta(posrow(poscol))+h, nu(poscol)))
           - log(copulapdf('t',[rcl-h rhh], theta(posrow(poscol))-h,
           nu(poscol))))) .* ...
         ((rcl ≤ rcl(i)) - rcl(i)));
   z2(i) = 1/n*sum(1/(4*h^2)*((log(copulapdf('t',[rcl rhh+h],
     theta(posrow(poscol))+h, nu(poscol))) - log(copulapdf('t',[rcl rhh+h],
     theta(posrow(poscol))-h, nu(poscol)))) - ...
         (log(copulapdf('t',[rcl rhh-h], theta(posrow(poscol))+h, nu(poscol)))
           - log(copulapdf('t',[rcl rhh-h], theta(posrow(poscol))-h,
           nu(poscol))))) .* ...
         ((rhh ≤ rhh(i)) - rhh(i)));
end
z = (z1+z2);
qhat = 1/n*sum(jinvhat*p.*z);

zeta1 = 1/(2*h)*(log(copulapdf('t',[rcl+h rhh], theta(posrow(poscol)),
  nu(poscol))) - log(copulapdf('t',[rcl-h rhh], theta(posrow(poscol)),
  nu(poscol))));
zeta2 = 1/(2*h)*(log(copulapdf('t',[rcl rhh+h], theta(posrow(poscol)),
  nu(poscol))) - log(copulapdf('t',[rcl rhh-h], theta(posrow(poscol)),
  nu(poscol))));
rhat = 1/n*sum(sum([zeta1 zeta2].*(1 - [rcl rhh])));

CIC = 2*maximum - 2*(phat + qhat + rhat);

% obtaining the degrees of freedom via maximum likelihood
corr_data = copulaparam('t',tau_data);
nu_vec = linspace(4,6,100);

maxlike = zeros(length(nu_vec),1);
for i = 1:length(nu_vec)
   maxlike(i) = sum(log(copulapdf('t',[rcl rhh],corr_data,nu_vec(i))));
end
```

```
[value, pos] = max(maxlike);
nu_data = nu_vec(pos);

% begin bootstrap-based goodness-of-fit test
for i = 1:n
   G(i) = sum((rcl ≤ rcl(i)).*(rhh ≤ rhh(i)));
end
G = G/n;

C = copulacdf('t',[rcl rhh],corr_data,nu_data);
errt1 = sum((C-G').^2);
resultt = 0;

for t = 1:N
   % generation of an independent random sample of the t-copula
   data = copularnd('t',corr_data,nu_data,n);

   t1 = data(:,1);
   [hv,ar] = sort(t1);
   rt1 = zeros(n,1);
   for i = 1:n
      rt1(ar(i)) = i;
   end
   rt1 = rt1/(n+1);

   t2 = data(:,2);
   [hv,ar] = sort(t2);
   rt2 = zeros(n,1);
   for i = 1:n
      rt2(ar(i)) = i;
   end
   rt2 = rt2/(n+1);

   tau = corr(data(:,1),data(:,2),'type','Kendall');
   cor = copulaparam('t',tau,nu_data);
   maxlike = zeros(length(nu_vec),1);

   for i = 1:length(nu_vec)
      maxlike(i) = sum(log(copulapdf('t',[rcl rhh],cor,nu_vec(i))));
   end
   [value, pos] = max(maxlike);
   nu = nu_vec(pos);

   for i = 1:n
      T(i) = sum((rt1 ≤ rt1(i)).*(rt2 ≤ rt2(i)));
   end
   T = T/n;

   C = copulacdf('t',[rt1 rt2],cor,nu);
   errt2 = sum((C-T').^2);
   vergleich = errt2 > errt1;
   resultt = resultt + vergleich;
end
% result goodness-of-fit test
tfit = resultt/N
```

Code A.2. Partial derivatives multiplier goodness-of-fit test for tail copulas using the example of the Hüsler-Reiss model.

```
% partial derivatives multiplier bootstrap goodness-of-fit test for tail
  copulas

% load data
WTI = xlsread('...');
Brent = xlsread('...');

% initialization
n = length(WTI);
N = 10000;
k = 200;
delta = 0.001;
steps = round(pi/(2*delta) + 1);
s = linspace(0.0001,pi/2,steps);
t = (tan(s)./(1+tan(s)))';
tau_data = corr(WTI,Brent,'type','Kendall');

% definition of the Pickands dependence function (nonsymbolic)
A = @(t,theta) (1-t).*normcdf(theta + 1/(2*theta)*log((1-t)./t)) +
  t.*normcdf(theta + 1/(2*theta)*log(t./(1-t))); % Hüsler-Reiss model

% lower tail copula evaluated on the unit circle
APrime = @(t,theta) (1 - A(t,theta))./(sqrt(2*t.^2 - 2*t + 1));

% rank-based analysis
rcl = zeros(n,1);
[hv,ar] = sort(WTI);
for i = 1:n
   rcl(ar(i)) = i;
end
rcl = rcl/(n+1);

rhh = zeros(n,1);
[hv,ar] = sort(Brent);
for i = 1:n
   rhh(ar(i)) = i;
end
rhh = rhh/(n+1);

% parametrisation of the unit circle
x = cos(s)';
y = sin(s)';

% transformation to unit simplex
xnorm = x./(x+y);
ynorm = y./(x+y);

% calculation of the empirical lower tail copula (evaluated on the unit circle)
U = zeros(steps,1);
for i = 1:steps
   U(i) = sum((rcl <= k*x(i)/(n+1)).*(rhh <= k*y(i)/(n+1)));
end
U = U/k;

% applying the minimum distance estimator
z = linspace(0,1,1000)';
dist = zeros(length(z),1);
for i = 1:length(z)
   dist(i) = delta*sum((U - LPrime(t,z(i))).^2);
```

```
end
[minimum pos] = min(dist);
theta = z(pos);

% calculation of the reference statistic
ref_stat = k*minimum;

% partial derivatives lower tail copula
h = 1/sqrt(k);

partial_x = zeros(steps,1);
for i = 1:steps
   if x(i) ≥ h
      partial_x(i) = (sum((rcl ≤ k*(x(i)+h)/(n+1)).*(rhh ≤ k*y(i)/(n+1))) -
        sum((rcl ≤ k*(x(i)-h)/(n+1)).*(rhh ≤ k*y(i)/(n+1))))/(2*h);
   else
      partial_x(i) = (sum((rcl ≤ k*(x(i)+2*h)/(n+1)).*(rhh ≤ k*y(i)/(n+1))) -
        sum((rcl ≤ 0).*(rhh ≤ k*y(i)/(n+1))))/(2*h);
   end
end
partial_x = max(min(partial_x./k,1),0);

partial_y = zeros(steps,1);
for i = 1:steps
   if y(i) ≥ h
      partial_y(i) = (sum((rcl ≤ k*x(i)/(n+1)).*(rhh ≤ k*(y(i)+h)/(n+1))) -
        sum((rcl ≤ k*x(i)/(n+1)).*(rhh ≤ k*(y(i)-h)/(n+1)))./(2*h);
   else
      partial_y(i) = (sum((rcl ≤ k*x(i)/(n+1)).*(rhh ≤ k*(y(i)+2*h)/(n+1))) -
        sum((rcl ≤ k*x(i)/(n+1)).*(rhh ≤ 0)))./(2*h);
   end
end
partial_y = max(min(partial_y./k,1),0);

% partial derivative of the assumed lower tail copula with respect to theta
  solved by symbolic equations
syms a p q

integralBody = exp(-q^2/2);
symNormA = (1/sqrt(2*sym(pi)))*int(integralBody, -Inf, p +
  1/(2*p)*log((1-a)/a));
symNormB = (1/sqrt(2*sym(pi)))*int(integralBody, -Inf, p +
  1/(2*p)*log(a/(1-a)));
A = (1-a)*symNormA + a*symNormB; % Hüsler-Reiss model

partial_theta = (-1)*diff(A,p);
partial_theta = subs(partial_theta, {a, p}, {t, repmat(theta,steps,1)});

num_partial_theta = partial_theta./sqrt(2*t.^2 - 2*t + 1);
A_theta = delta*sum(num_partial_theta.^2);
A_theta_inv = 1/A_theta;

% begin multiplier bootstrap
statistik = zeros(N,1);
result = 0;

for j = 1:N
   % generation of multiplier sample ξ_{i,1},...,ξ_{i,T}
   multiplier = zeros(n,1);
   for i = 1:n
      if unidrnd(2) == 1;
```

```
            multiplier(i) = 0;
        else
            multiplier(i) = 2;
        end
    end
    mu = mean(multiplier);
    sigma = sqrt(var(multiplier));
    multiplier = multiplier/mu;

    % calculation of the process beta_T^pdm
    beta = zeros(steps,1);
    for i = 1:steps
        beta(i) = sum((multiplier-1).*(rcl <= k*x(i)/(n+1)).*(rhh <=
          k*y(i)/(n+1)));
    end
    beta = (mu/sigma)*(1/sqrt(k))*beta;

    % beta infinity values
    betainf_x = zeros(steps,1);
    for i = 1:steps
        betainf_x(i) = sum((multiplier -1).*(rcl <= k*n^2/(n+1)).*(rhh <=
          k*y(i)/(n+1)));
    end
    betainf_x = (mu/sigma)*(1/sqrt(k))*betainf_x;

    betainf_y = zeros(steps,1);
    for i = 1:steps
        betainf_y(i) = sum((multiplier -1).*(rcl <= k*x(i)/(n+1)).*(rhh <=
          k*n^2/(n+1)));
    end
    betainf_y = (mu/sigma)*(1/sqrt(k))*betainf_y;

    % calculation of the process alpha_{i,T}^pdm
    alpha = beta - partial_x.*betainf_y - partial_y.*betainf_x;

    % evaluation of the loop statistic
    stat = delta*sum((alpha -
      num_partial_theta*delta*sum(A_theta_inv*num_partial_theta.*alpha)).^2);

    % comparing results
    vergleich = stat > ref_stat;
    result = result + vergleich;
    multiplier = [];
    beta = [];
    betainf_x = [];
    betainf_y = [];
    alpha = [];
end
% result goodness-of-fit test
result = result/N
```

A.2 Simulation of copulas

Code A.3. Simulation of arbitrary copulas with a grid approach using the example of the upper Fréchet-Hoeffding bound.

```
function [simU simV] = SimulationCop(n,m,p)

% simulation of arbitrary copula families

% calling the subfunction GridCalc to obtain probabilities in each cell of
% an equidistant (n × m)-partition of the square [0,1]^2
[u,v,C] = GridCalc(n,m);

% preparing the simulation vector with p independent copies
simU = zeros(p,1);
simV = zeros(p,1);

for k = 1:p
   % generate uniform distribution to choose relevant cell
   c = rand(1);

   % searching for the corresponding cell
   i = 1;
   while C(2,i) < c
      i = i + 1;
   end
   simU(k) = u(C(4,i));
   simV(k) = v(C(3,i));
end

end

function [u,v,C] = GridCalc(n,m)

% defining the copula function, here the upper Fréchet-Hoeffding bound
f = @(u,v) min(u,v);

% initial settings
P = zeros(m-1,n-1);
C = zeros(4,(m-1)*(n-1));
u = linspace(0,1,n);
v = linspace(0,1,m);

% probability calculation
for i = 2:m
   for j = 2:n
      if (i == 2) && (j == 2)
         P(i-1,j-1) = f(u(j),v(i)) - f(u(j-1),v(i)) - f(u(j),v(i-1));
      else
         P(i-1,j-1) = f(u(j),v(i)) - f(u(j-1),v(i)) - f(u(j),v(i-1)) +
           f(u(j-1),v(i-1));
      end
   end
end

% reshaping, cumulating, storing positions
sum = 0;

for i = 1:m-1
   for j = 1:n-1
      C(1,(i-1)*(n-1)+j) = P(i,j);
```

```
        sum = sum + P(i,j);
        C(2,(i-1)*(n-1)+j) = sum;
        C(3,(i-1)*(n-1)+j) = i+1;
        C(4,(i-1)*(n-1)+j) = j+1;
    end
end

end
```

Code A.4. Simulation of the copula (C3) from Section 3.4.1 with underlying Clayton family.

```
function [simU simV] = SimAlgorithm(n,a,p,tailindex)

% simulation of copula family (C3) from Section 3.4.1

% using the inverse Clayton tail dependence coefficient relation to obtain
% parameter of the corresponding copula
theta = -log(2)/log(tailindex);

% generate the pair (X,Y)
U = copularnd('Clayton',theta,n/2);
subsetU = find(U(:,1) <= a | U(:,2) <= a);
binom = binornd(1,p,length(subsetU),1);
multBinom = subsetU.*binom;
multBinom = multBinom(multBinom ~= 0);
tailU = a*copularnd('Clayton',theta,length(multBinom));

for j = 1:length(multBinom)
    U(multBinom(j),:) = tailU(j,:);
end

% calculate the distribution H and return marginals
Caa = copulacdf('Clayton', [a a], theta);
mu = 2*a - Caa;

for j = 1:length(U(:,1))
    % obtaining first marginal H(X,1)
    if U(j,1) <= a
        U(j,1) = mu*p*U(j,1)/a + (1-p)*U(j,1);
    else
        Cxa = copulacdf('Clayton', [U(j,1) a], theta);
        U(j,1) = mu*p + (1-p)*(Cxa + a - Caa) + U(j,1) - Cxa - a + Caa;
    end

    % obtaining second marginal H(1,Y)
    if U(j,2) <= a
        U(j,2) = mu*p*U(j,2)/a + (1-p)*U(j,2);
    else
        Cay = copulacdf('Clayton', [a U(j,2)], theta);
        U(j,2) = mu*p + (1-p)*(a + Cay - Caa) + U(j,2) - a - Cay + Caa;
    end
end

simU = U(:,1);
simV = U(:,2);
end
```

A.3 Tests for constant tail dependence

Code A.5. Application of TDC-Test 1 to the bivariate energy dataset for different k.

```
% empirical application of TDC-Test 1

% loading data
WTI = xlsread('...');
Brent = xlsread('...');

% initialization
n = length(WTI);
steps = n;
ns = floor(linspace(0,1,steps).*n);
sopt = floor(linspace(100,250,150));
teststat = linspace(0,0,length(sopt));
pvalue = linspace(0,0,length(sopt));

% calculating pseudo-observations
rcl = zeros(n,1);
[hv,ar] = sort(WTI);
for l = 1:n
   rcl(ar(l)) = l;
end
rcl = rcl/(n+1);

rhh = zeros(n,1);
[hv,ar] = sort(Brent);
for l = 1:n
   rhh(ar(l)) = l;
end
rhh = rhh/(n+1);

% test statistic and p-value
for r = 1:length(sopt)
   EmpLtdc = linspace(0,0,length(ns));
   for j = 1:length(ns)
      EmpLtdc(j) = 1/sopt(r)*sum((rcl(1:ns(j)) <= ...
        sopt(r)/(n+1)).*(rhh(1:ns(j)) <= sopt(r)/(n+1)));
   end
   stat = sqrt(sopt(r)).*(EmpLtdc - EmpLtdc(length(ns))*ns/n);
   stat = stat.*(EmpLtdc(length(ns)).^(-1/2));

   teststat(r) = mean(stat.^2);
   pvalue(r) = pvaluebrownianbridge(teststat(r),0,1000,1000,2);
end

% additional functions to be copied in a separate m-file

function [pbb] = pvaluebrownianbridge(x,s,numsim,steps,norm)

% finds the p-value of two functionals of the Brownian Bridge
% s ratio, numsim number of simulations, steps discretization for the
% interval [0,1], norm applies either the supremumsnorm
% or euclidean norm

maxbb = zeros(steps,1);
for i = 1:numsim
   [bb] = brownianbridge(steps);
   if norm == 1
      maxbb(i,1) = max(abs(bb((floor(s*steps)+1):steps,1)));
```

```
   else
      maxbb(i,1) = mean(bb((floor(s*steps)+1):steps,1).^2);
   end
end
pbb = mean(maxbb(:,1) ≥ x);
end

function [bb] = brownianbridge(steps)

% simulates a Brownian Bridge between 0 and 1

bm = 1/sqrt(steps)*cumsum(randn(steps,1));
bb = bm - (1:steps)'./steps.*bm(steps,1);
end
```

Code A.6. Simulated rejection probabilities of the TC-Test under the null hypothesis using the Clayton copula within the serial independence setting.

```
% simulated rejection probabilities of the TC-Test

% setup simulation parameter and bootstrap replications
N = 1000;
B = 300;
n = 1000;

steps = 200;
stepst = 20;
ns = floor(linspace(0,1,steps).*n);
tparam = linspace(1/(stepst+1),1-1/(steps+1),stepst);
x = 1 - tparam;
y = tparam;

tailindex = 0.75;
theta = -log(2)/log(tailindex);

sopt = floor(linspace(1,n,n));
quantilefix = [0.9 0.95 0.99];
PlateauLowLtdcNull = linspace(0,0,N);
ResultNull = linspace(0,0,N);
normstat = linspace(0,0,N);
bootquantile = zeros(N,length(quantilefix));

% begin simulation run
for i = 1:N
   % simulate from Clayton copula
   U = copularnd('Clayton',theta,n);
   WTI = U(:,1);
   Brent = U(:,2);

   rcl = zeros(n,1);
   [hv,ar] = sort(WTI);
   for l = 1:n
      rcl(ar(l)) = l;
   end
   rcl = rcl/(n+1);

   rhh = zeros(n,1);
   [hv,ar] = sort(Brent);
   for l = 1:n
      rhh(ar(l)) = l;
   end
```

```
    rhh = rhh/(n+1);

    LowLtdc = linspace(0,0,length(sopt));
    % calculation of lower tail dependence coefficient
    for r = 1:length(sopt)
       LowLtdc(r) = 1/sopt(r)*sum((rcl ≤ sopt(r)/(n+1)).*(rhh ≤
         sopt(r)/(n+1)));
    end

    % box kernel to smooth
    b = floor(0.005*n);
    EmpLtcBar = linspace(0,0,length(n-2*b));
    for j = 1:(n - 2*b);
       EmpLtcBar(j) = mean(LowLtdc(j:2*b+j));
    end
    sigma = 2*std(EmpLtcBar);
    l = floor(sqrt(n-2*b));

    % calculate the difference within each block
    sumLtdc = linspace(0,0,length(n-2*b-l+1));
    for k = 1:(n-2*b-l+1)
       sumLtdc(k) = sum(abs(EmpLtcBar(k)-EmpLtcBar(k:k+l-1)));
       if sumLtdc(k) < sigma
          PlateauLowLtdcNull(i) = mean(EmpLtcBar(k:k+l-1));
          ResultNull(i) = k + floor(1/2*l);
          break
       end
    end
    k = k + floor(1/2*l);

    % empirical lower tail copula
    EmpLtc = zeros(length(tparam),length(ns));
    for m = 1:length(tparam)
       for j = 1:length(ns)
          % rows tparam, columns ns
          EmpLtc(m,j) = 1/k*sum((rcl(1:ns(j)) ≤ k*2*x(m)/(n+1)).*(rhh(1:ns(j))
            ≤ k*2*y(m)/(n+1)));
       end
    end
    stat = sqrt(k).*(EmpLtc - EmpLtc(:,length(ns))*ns/n);
    normstat(i) = mean(mean(stat.^2,1));

    % begin multiplier bootstrap
    bootstat = linspace(0,0,B);
    for b = 1:B
       % generation of multiplier sample ξ_1^(b),...,ξ_n^(b)
       multiplier = zeros(n,1);
       for p = 1:n
          if unidrnd(2) == 1;
              multiplier(p) = -1;
          else
              multiplier(p) = 1;
          end
       end

       % empirical lower tail copula bootstrap
       EmpLtcBoot = zeros(length(tparam),length(ns));
       for m = 1:length(tparam)
          for j = 1:length(ns)
             % rows tparam, columns ns
```

```
            EmpLtcBoot(m,j) = 1/k*sum(multiplier(1:ns(j)).*((rcl(1:ns(j)) ≤
              k*2*x(m)/(n+1)).*(rhh(1:ns(j)) ≤ k*2*y(m)/(n+1)) -
              k/n*EmpLtc(m,length(ns))));
        end
    end
    statboot = sqrt(k).*(EmpLtcBoot - EmpLtcBoot(:,length(ns))*ns/n);
    bootstat(b) = mean(mean(statboot.^2,1));
  end
  bootquantile(i,:) = quantile(bootstat,quantilefix);
end

% calculate finite sample results
sum(normstat' > bootquantile(:,1))/N
sum(normstat' > bootquantile(:,2))/N
sum(normstat' > bootquantile(:,3))/N
mean(ResultNull)
std(ResultNull)
```

List of Figures

1 Daily quotes in USD/barrel of the WTI Cushing Crude Oil Spot and the Bloomberg European Dated Brent from October 2, 2006 to October 1, 2010 2

2 Scatter plot of the WTI Cushing Crude Oil Spot and the Bloomberg European Dated Brent log-returns from October 2, 2006 to October 1, 2010 (left) and enlarged third quadrant (right) 2

1.1 Log-returns of the one-month-ahead futures on crude oil (top) and natural gas (bottom) between July 2, 2007 and July 2, 2010 9

1.2 Standardized residuals of the individual time series models for the daily log-returns of the crude oil (top) and natural gas (bottom) futures 10

1.3 Scatter plot of the ranks of the standardized residuals u_t and v_t 12

1.4 Empirical lower tail copula $\hat{\Lambda}_L$ of the log-returns of the crude oil and natural gas futures 15

1.5 Empirical upper tail copula $\hat{\Lambda}_U$ of the log-returns of the crude oil and natural gas futures 15

1.6 Parametrization of the circle around the origin through the point $(1,1)$ in the first quadrant with values of the empirical lower tail copula $\hat{\Lambda}_L$ as well as the lower tail copulas of the Pareto copula, $\hat{\theta}_T = 0.545$, and the t-copula, $\hat{\theta}_T = 0.330$, $\nu = 2.7$ 17

1.7 Parametrization of the circle around the origin through the point $(1,1)$ in the first quadrant with values of the empirical upper tail copula $\hat{\Lambda}_U$ as well as the upper tail copulas of the Gumbel copula, $\hat{\theta}_T = 1.272$, and the t-copula, $\hat{\theta}_T = 0.330$, $\nu = 2.7$ 17

2.1 Log-returns of the WTI Cushing Crude Oil Spot (top) and the Bloomberg European Dated Brent (bottom) from October 2, 2006 to October 1, 2010 . 24

2.2 Standardized residuals of both WTI Cushing Crude Oil Spot (top) and Bloomberg European Dated Brent (bottom) log-return time series 26

2.3 QQ-plots of standardized residuals for the WTI Cushing Crude Oil Spot (top) and the Bloomberg European Dated Brent (bottom) 27

2.4 Scatter plot of the rank-based representation of the standardized residuals 30

2.5 Simulation of Frank copula (top left), copula (4.1.14) (center left), Plackett copula (bottom left), Gaussian copula (top right), copula (4.1.12) (center right) and t-copula (bottom right) 35

2.6 Plot of the empirical lower tail copula $\hat{\Lambda}_L$, Gumbel model, mixed model and the overall range for both the Pickands framework (top) and the tail copula approach (bottom) 38

2.7 In sample one day-ahead simulated portfolio ($\omega_1 = \omega_2 = 0.5$) Value-at-Risk for a given level of confidence $\alpha = 95\%$ for the Gumbel model and the realized (observed) returns 40

3.1 Left: (estimated) copula density from the Clayton copula with $\lambda = 0.25$. Middle: (estimated) copula density from the transformed Clayton copula described in (C3). Right: difference between the two densities 60
3.2 Negative asymmetric logistic model $(\Lambda 2)$ for $\psi_1 = 0.4$, $\psi_2 = 1$, $\theta = 100$ and $\psi_1 = 1$, $\psi_2 = 0.4$, $\theta = 100$ evaluated on the straight line $(2-2t, 2t)$, $t \in [0,1]$ 68
3.3 (WTI and Brent time series) Points in time where pseudo-observations in both coordinates fall simultaneously below the value k/n, for $k/n \in \{0.05, 0.06, \ldots, 0.15\}$ 70
3.4 (WTI and Brent time series) Standardized sequential empirical tail copula process $\hat{\lambda}^{-1/2}\mathbb{G}_n(s,1,1)$ for $k^* = 104$ with respect to ns, $s \in [0,1]$ 71
3.5 (WTI and Brent time series) Test statistics $\mathcal{S}_n$ and corresponding p-values for different k 71
3.6 (Dow Jones and Nasdaq time series) Points in time where pseudo-observations in both coordinates fall simultaneously below the value k/n, for $k/n \in \{0.05, 0.06, \ldots, 0.15\}$ 72
3.7 (Dow Jones and Nasdaq time series) Chi-squared test for a specific break at $\lfloor n\bar{s}_{\mathrm{BM}} \rfloor = 959$: p-values for different k 74
3.8 (Dow Jones and Nasdaq time series) TDC-Test 1 for the subsample before $\lfloor n\bar{s}_{\mathrm{BM}} \rfloor = 959$: p-values for different k 74
3.9 (Dow Jones and Nasdaq time series) TDC-Test 1 for the subsample after $\lfloor n\bar{s}_{\mathrm{BM}} \rfloor = 959$ (including Black Monday): p-values for different k 74
3.10 (Dow Jones and Nasdaq time series) Absolute standardized sequential empirical tail copula process $|\hat{\lambda}^{-1/2}\mathbb{G}_n(s,1,1)|$ for $k^* = 191$ with respect to ns, $s \in [0,1]$ 75

List of Tables

1.1 Maximum likelihood estimates together with their corresponding standard errors for the crude oil APARCH(1,1)-model with skewed normal distribution and the natural gas GARCH(1,1)-model including the skewed Student's t-distribution 11
1.2 Test results for the goodness-of-fit test of different copula models in ascending order (p-value) 13
1.3 Tail dependence coefficients of the copulas considered for the goodness-of-fit test presented in Table 1.2 16

2.1 Mean values and maximum likelihood estimates together with their corresponding standard errors for the WTI ARMA(0,0)-EGARCH(2,3)-model and the Brent ARMA(1,1)-EGARCH(2,3)-model both with the explanatory variable and the skewed generalized error distribution 28
2.2 Test results ($N = 2000$ bootstrap iterations) for the goodness-of-fit of different copula models in ascending order (p-value) 34
2.3 Cross-validation Copula Information Criterion values for the remaining copula models in ascending order (CIC-value) 34
2.4 Test results ($N = 10\,000$ bootstrap iterations) for the derivatives multiplier bootstrap of different lower tail copulas in ascending order (p-value) . . . 39
2.5 Relative number (absolute number) of backtest outliers $1 - \hat{\alpha}$ for the different applied Value-at-Risk simulations with level of confidence $1 - \alpha$, weighted average error $|\hat{\alpha} - \alpha|$ and error ranking 41
2.6 Average relative error between the observed outliers and the Expected Shortfall for the different applied Expected Shortfall simulations with level of confidence $1 - \alpha$, weighted averages and error ranking 42

3.1 Simulated rejection probabilities of TDC-Test 1 under various null hypotheses H_0^Λ 64
3.2 Simulated rejection probabilities of TDC-Test 1 under various alternatives H_1^λ 65
3.3 Simulated rejection probabilities of TDC-Test 2 and the TC-Test under the null hypothesis and one alternative using the Clayton copula within the serial independence setting 66
3.4 Simulated rejection probabilities of TDC-Test 1 and the TC-Test in the serial independence setting: The parameters are chosen such that the TDC remains constant over time while the tail copula does not 66
3.5 Simulated rejection probabilities of a test for constancy of the entire copula and TDC-Test 1 in the serial independence setting in which there is a structural break in the tail but not in the center of the distribution 69

3.6 Simulated rejection probabilities for the TDC^{MB}-Test in a serially independent setting with and without a mean change in the margins 69
3.7 Maximum likelihood estimates together with their corresponding standard errors for the Dow Jones ARMA(0,0)-GARCH(1,1)-model including the *t*-distribution and the Nasdaq ARMA(1,0)-GARCH(1,1)-model with skewed *t*-distribution 73
3.8 Summary of results for TDC-Test 1 applied to the subsample before Black Monday, to the subsample after Black Monday and to the full sample . . . 75

Bibliography

Accioly, R. M. S. and Aiube, F. A. L. (2008). Analysis of crude oil and gasoline prices through copulas. *Cadernos do IME – Série Estatística*, 24, 15–28.

Alexander, C. (2004). Correlations in crude oil and natural gas markets. In Kaminsky, V., editor, *Managing energy price risk*, pages 573–606. Risk Books, London, 3rd edition.

Aloui, R., Ben Aïssa, M. S., and Nguyen, D. K. (2013). Conditional dependence structure between oil prices and exchange rates: A copula-garch approach. *Journal of International Money and Finance*, 32, 719–738.

Aue, A. and Horváth, L. (2013). Structural breaks in time series. *Journal of Time Series Analysis*, 34(1), 1–16.

Azzalini, A. and Capitano, A. (2003). Distributions generated by pertubation of symmetry with emphasis on a multivariate skew t distribution. *Journal of the Royal Statistical Society: Series B*, 65, 367–389.

Azzalini, A. and Dalla Valle, A. (1996). The multivariate skew-normal distribution. *Biometrika*, 83, 715–726.

Bai, J. (1997). Estimating multiple breaks one at a time. *Econometric Theory*, 13, 315–352.

Breymann, W., Dias, A., and Embrechts, P. (2003). Dependence structures for multivariate high-frequency data in finance. *Quantitative Finance*, 3(1), 1–14.

Bücher, A. (2014). A note on nonparametric estimation of bivariate tail dependence. *Statistics and Risk Modeling*, 31(2), 151–162.

Bücher, A. and Dette, H. (2013). Multiplier bootstrap of tail copulas – with applications. *Bernoulli*, 5(A), 1655–1687.

Bücher, A., Kojadinovic, I., Rohmer, T., and Segers, J. (2014). Detecting changes in cross-sectional dependence in multivariate time series. *Journal of Multivariate Analysis*, 132, 111–128.

Bücher, A. and Ruppert, M. (2013). Consistent testing for a constant copula under strong mixing based on the tapered block multiplier technique. *Journal of Multivariate Analysis*, 116, 208–229.

Bücher, A. and Volgushev, S. (2013). Empirical and sequential empirical copula processes under serial dependence. *Journal of Multivariate Analysis*, 119, 61–70.

Busetti, F. and Harvey, A. (2011). When is a copula constant? A test for changing relationships. *Journal of Financial Econometrics*, 9(1), 106–131.

Caillault, C. and Guégan, D. (2005). Empirical estimation of tail dependence using copulas: application to asian markets. *Quantitative Finance*, 5(5), 489–501.

Campbell, R., Forbes, C., Koedijk, K., and Kofman, P. (2008). Increasing correlations or just fat tails? *Journal of Empirical Finance*, 15(2), 287–309.

Chan, N.-H., Chen, J., Chen, X., Fan, Y., and Peng, L. (2009). Statistical inference for multivariate residual copula of GARCH models. *Statistica Sinica*, 19(1), 53–70.

Chang, C.-L., McAleer, M., and Tansuchat, R. (2010). Analyzing and forecasting volatility spillovers, asymmetries and hedging in major oil markets. *Energy Economics*, 32(6), 1445–1455.

Chen, X. and Fan, Y. (2006). Estimation and model selection of semiparametric copula-based multivariate dynamic models under copula misspecification. *Journal of Econometrics*, 135(1-2), 125–154.

Christoffersen, P. (1998). Evaluating interval forecasts. *International Economic Review*, 39, 841–862.

Claeskens, G. and Hjort, N. L. (2008). *Model selection and model averaging*. Cambridge University Press, Cambridge.

Danielsson, J., de Haan, L., Peng, L., and de Vries, C. G. (2001). Using a bootstrap method to choose the sample fraction in tail index estimation. *Journal of Multivariate Analysis*, 76(2), 226–248.

de Haan, L. and Ferreira, A. (2006). *Extreme Value Theory*. Springer Series in Operations Research and Financial Engineering. Springer, New York.

Deheuvels, P. (1979). La fonction de dépendance empirique et ses propriétés. *Académie Royale de Belgique. Bulletin de la Classe des Sciences*, 65, 274–292.

Dehling, H., Vogel, D., Wendler, M., and Wied, D. (2013). An efficient and robust test for change-points in correlation. *arXiv: abs/1203.4871v2*.

Demarta, S. and McNeil, A. J. (2005). The *t*-copula and related copulas. *International Statistical Review*, 73(1), 111–129.

Deutsch, H.-P. (2009). *Derivatives and internal models*. Palgrawe Macmillan, 4th edition.

Drees, H. and Huang, X. (1998). Best attainable rates of convergence for estimates of the stable tail dependence functions. *Journal of Multivariate Analysis*, 64, 25–47.

Drees, H. and Kaufmann, E. (1998). Selecting the optimal sample fraction in univariate extreme value estimation. *Stochastic Processes and their Applications*, 75(2), 149–172.

Dümbgen, L. (1991). The asymptotic behavior of some nonparametric changepoint estimators. *Annals of Statistics*, 19(3), 1471–1495.

Einmahl, J., Krajina, A., and Segers, J. (2012). An m-estimator for tail dependence in arbitrary dimensions. *The Annals of Statistics*, 40(3), 1764–1793.

Einmahl, J. H. J., de Haan, L., and Li, D. (2006). Weighted approximations of tail copula processes with application to testing the bivariate extreme value condition. *The Annals of Statistics*, 34(4), 1987–2014.

Embrechts, P., Klüppelberg, C., and Mikosch, T. (1997). *Modelling extremal events*, volume 33 of *Applications of Mathematics (New York)*. Springer-Verlag, Berlin. For insurance and finance.

Embrechts, P., Lindskog, F., and McNeil, A. J. (2003). Modelling dependence with copulas and applications to risk management. In Rachev, S., editor, *Handbook of Heavy Tailed Distributions in Finance*, pages 329–384. Elsevier, New York.

Embrechts, P., McNeil, A., and Straumann, D. (2002). Correlation and dependence in risk management: properties and pitfalls. In Dempster, M., editor, *Value at Riskand Beyond*, pages 176–223. Cambridge University Press, Cambridge.

Engle, R. F. (1982). Autoregressive conditional heteroscedasticity with estimates of variance of United Kingdom inflation. *Econometrica*, 50, 987–1008.

Fattouh, B. (2010). Oil market dynamics through the lens of the 2002–2009 price cycle. *Oxford Institute for Energy Studies*.

Fermanian, J.-D. (2013). An overview of the goodness-of-fit test problem for copulas. In Jaworski, P., Durante, F., and Härdle, W. K., editors, *Copulae in Mathematical and Quantitative Finance*, Lecture Notes in Statistics, pages 61–89. Springer Berlin Heidelberg.

Frahm, G., Junker, M., and Schmidt, R. (2005). Estimating the tail-dependence coefficient: Properties and pitfalls. *Insurance: Mathematics and Economics*, 37, 80–100.

Galambos, J. (1975). Order statistics of samples from multivariate distributions. *Journal of the American Statistical Association*, 70(351), 674–680.

Galeano, P. and Wied, D. (2014). Multiple break detection in the correlation structure of random variables. *Computational Statistics and Data Analysis*, 76, 262–282.

Genest, C. and Favre, A. C. (2007). Everything you always wanted to know about copula modeling but were afraid to ask. *Journal of Hydrologic Engineering*, 12(4), 347–368.

Genest, C., Ghoudi, K., and Rivest, L.-P. (1995). A semiparametric estimation procedure of dependence parameters in multivariate families of distributions. *Biometrika*, 82(3), 543–552.

Genest, C. and Rémillard, B. (2008). Validity of the parametric bootstrap for goodness-of-fit testing in semiparametric models. *Annales de l'Institut Henri Poincaré – Probabilités et Statistique*, 44(6), 1096–1127.

Genest, C., Rémillard, B., and Beaudoin, D. (2009). Goodness-of-fit tests for copulas: A review and a power study. *Insurance: Mathematics and Economics*, 44(2), 199–213.

Genest, C. and Segers, J. (2009). Rank-based inference for bivariate extreme-value copulas. *The Annals of Statistics*, 37(5B), 2990–3022.

Ghalanos, A. (2011). *rgarch: Flexible GARCH modelling in R.* R package version 1.91.

Grégoire, V., Genest, C., and Gendron, M. (2008). Using copulas to model price dependencies in energy markets. *Energy Risk*, 5(5), 58–64.

Grønneberg, S. and Hjort, N. L. (2014). The copula information criteria. *Scandinavian Journal of Statistics*, 41(2), 436–459.

Gudendorf, G. and Segers, J. (2010). Extreme-value copulas. In Jaworski, P., Durante, F., Härdle, W. K., and Rychlik, T., editors, *Copula Theory and Its Applications*, Lecture Notes in Statistics, pages 127–145. Springer Berlin Heidelberg.

Gumbel, E. J. (1960). Bivariate logistic distributions. *Journal of the American Statistical Association*, 56(294), 335–349.

Hafner, C. and Manner, H. (2012). Dynamic stochastic copula models: estimation, inference and application. *Journal of Applied Econometrics*, 27(2), 269–295.

Huang, X. (1992). *Statistics of bivariate extreme values*. PhD thesis, Thesis Publishers and Tinbergen Institute.

Hüsler, J. and Reiss, R. (1989). Maxima of normal random vectors: Between independence and complete dependence. *Statistics and Probability Letters*, 7, 283–286.

Jäschke, S. (2014). Estimation of risk measures in energy portfolios using modern copula techniques. *Computational Statistics and Data Analysis*, 76, 359–376.

Jäschke, S., Siburg, K. F., and Stoimenov, P. A. (2012). Modeling dependence of extreme events in energy markets using tail copulas. *Journal of Energy Markets*, 5(4), 60–80.

Joe, H. (1990). Families of min-stable multivariate exponential and multivariate extreme value distributions. *Statistics and Probability Letters*, 9(1), 75–81.

Joe, H. (1997). *Multivariate Models and Dependence Concepts*. Chapman & Hall, London.

Jondeau, E., Poon, S.-H., and Rockinger, M. (2007). *Financial modeling under non-Gaussian distributions*. Springer, London.

Jorion, P. (2006). *Value at Risk: The new benchmark for managing financial risk*. McGraw-Hill, 3rd edition.

Kang, A. H., Kang, S.-M., and Yoon, S.-M. (2009). Forecasting volatitlity of crude oil markets. *Energy Economics*, 31(1), 119–125.

Kemp, J. (2010). Oil inventories lose their influence on prices. *Reuters News from March 24, 2010*.

Kojadinovic, I. (2010). Modeling multivariate distributions with continuous margins using the copula R package. *Journal of Statistical Software*, 34(9), 1–20.

Kojadinovic, I. and Yan, J. (2010). Comparison of three semiparametric methods for estimating dependence parameters in copula models. *Insurance: Mathematics and Economics*, 47, 52–63.

Kosorok, M. R. (2008). *Introduction to empirical processes and semiparametric inference*. Springer, New York.

Krämer, W. and van Kampen, M. (2011). A simple nonparametric test for structural change in joint tail probabilities. *Economics Letters*, 110(3), 245–247.

Krishnan, C., Petkova, R., and Ritchken, P. (2009). Correlation risk. *Journal of Empirical Finance*, 16(3), 353–367.

Kupiec, P. (1995). Techniques for verifying the accuracy of risk measurement models. *Journal of Derivatives*, 3, 73–84.

Liu, J. (2011). *Extreme value theory and copula theory: A risk management application with energy futures*. PhD thesis, University of Victoria.

Lu, X. F., Lai, K. K., and Liang, L. (2011). Portfolio value-at-risk estimation in energy futures markets with time-varying copula-GARCH model. *Annals of Operations Research*, pages 1–25.

Malevergne, Y. and Sornette, D. (2003). Testing the gaussian copula hypothesis for financial assets dependences. *Quantitative Finance*, 3(4), 231–250.

McNeil, A. J., Frey, R., and Embrechts, P. (2005). *Quantitative risk management*. Princeton Series in Finance. Princeton University Press, Princeton, NJ. Concepts, techniques and tools.

Mohammadi, H. and Su, L. (2010). International evidence on crude oil price dynamics: Applications of arima-garch models. *Energy Economics*, 32(5), 1001–1008.

Nelsen, R. B. (2006). *An introduction to copulas*. Springer, New York, 2nd edition.

Nelson, D. B. (1991). Conditional heteroskedasticity in asset returns: A new approach. *Econometrica*, 59(2), 347–370.

Palaro, H. P. and Hotta, L. K. (2006). Using conditional copula to estimate value at risk. *Journal of Data Science*, 4, 95–113.

Patton, A. (2006). Modelling asymmetric exchange rate dependence. *International Economic Review*, 47(2), 527–556.

Perron, P. (1988). Trends and random walks in macroeconomic time series: Further evidence from a new approach. *Journal of Economic Dynamics and Control*, 12, 297–332.

Pickands, J. (1981). Multivariate extreme value distributions (with a discussion). *Bulletin de l'Institut International de Statistique*, 49(2), 859–878, 894–902.

Rank, J. and Siegl, T. (2002). Applications of copulas for the calculation of value-at-risk. In Härdle, W., Kleinow, T., and Stahl, G., editors, *Applied Quantitative Finance*, pages 35–47. Springer, Berlin–Heidelberg.

Reboredo, J. C. (2011). How do crude oil prices co-move?: A copula approach. *Energy Economics*, 33(5), 95–113.

Reboredo, J. C. (2012). Modelling oil price and exchange rate co-movements. *Journal of Policy Modeling*, 34(3), 419–440.

Rémillard, B. (2010). Goodness-of-fit tests for copulas of multivariate time series. *SSRN: http://ssrn.com/abstract=1729982 or http://dx.doi.org/10.2139/ssrn.1729982*.

Rémillard, B. and Scaillet, O. (2009). Testing for equality between two copulas. *Journal of Multivariate Analysis*, 100, 377–386.

Schmidt, R. and Stadtmüller, U. (2006). Non-parametric estimation of tail dependence. *Scandinavian Journal of Statistics*, 33(2), 307–335.

Segers, J. (2012a). Asymptotics of empirical copula processes under nonrestrictive smoothness assumptions. *Bernoulli*, 18(3), 764–782.

Segers, J. (2012b). Max-stable models for multivariate extremes. *RevStat – Statistical Journal*, 10(1), 61–82.

Sklar, A. (1959). Fonctions de répartition à n dimensions et leurs marges. *Publications de l'Institut de statistique de l'Université de Paris*, 8, 229–231.

Smith, M. S., Gan, Q., and Kohn, R. J. (2012). Modelling dependence using skew t copulas: Bayesian inference and applications. *Journal of Applied Econometrics*, 27(3), 500–522.

Stute, W., Manteiga, W. G., and Quindimil, M. P. (1993). Bootstrap based goodness-of-fit tests. *Metrika*, 40, 243–256.

Tawn, J. A. (1988). Bivariate extreme value theory: Models and estimation. *Biometrika*, 75(3), 397–415.

Van der Vaart, A. W. and Wellner, J. A. (1996). *Weak convergence and empirical processes*. Springer, New York.

Vervaat, W. (1972). Functional central limit theorems for processes with positive drift and their inverses. *Zeitschrift für Wahrscheinlichkeitstheorie und verwandte Gebiete*, 23(4), 245–253.

Vostrikova, L. (1981). Detecting disorder in multidimensional random processes. *Soviet Mathematics Doklady*, 24, 55–59.

Wen, X., Wei, Y., and Huang, D. (2012). Measuring contagion between energy market and stock market during financial crisis: A copula approach. *Energy Economics*, 34(5), 1435–1446.

Wied, D., Dehling, H., van Kampen, M., and Vogel, D. (2014). A fluctuation test for constant spearman's rho with nuisance-free limit distribution. *Computational Statistics and Data Analysis*, 76, 723–736.

Wied, D., Krämer, W., and Dehling, H. (2012). Testing for a change in correlation at an unknown point in time using an extended functional delta method. *Econometric Theory*, 68(3), 570–589.

Wu, C.-C., Chung, H., and Chang, Y.-H. (2012). The economic value of co-movement between oil price and exchange rate using copula-based GARCH models. *Energy Economics*, 34(1), 270–282.

Würtz, D., Chalabi, Y., and Luksan, L. (2006). Parameter estimation of ARMA models with GARCH/APARCH errors – an R and SPlus software implementation. unpublished.

Yan, J. (2007). Enjoy the joy of copulas: With a package copula. *Journal of Statistical Software*, 21(4), 1–21.

Erklärung

Hiermit bestätige ich, dass ich die vorliegende Arbeit selbständig und nur unter Verwendung der angegebenen Quellen und Hilfsmittel angefertigt habe. Diese Arbeit wurde in dieser oder ähnlicher Form nicht an einer anderen Hochschule als Dissertation eingereicht.

Dortmund, den 31. März 2015